Volume 54
Number 12
21 June 2025
Pages 5739–6178

Chem Soc Rev

Chemical Society Reviews

rsc.li/chem-soc-rev

ISSN 0306-0012

ROYAL SOCIETY OF CHEMISTRY

REVIEW ARTICLE

Yuwei Liu, Tianyi Wang and Weiping Wang

Photopharmacology and photoresponsive drug delivery

Chem Soc Rev

REVIEW ARTICLE

View Article Online
View Journal | View Issue

Cite this: *Chem. Soc. Rev.*, 2025, **54**, 5792

Photopharmacology and photoresponsive drug delivery

Yuwei Liu, †[abc] Tianyi Wang †[abc] and Weiping Wang *[abc]

Light serves as an excellent external stimulus due to its high spatial and temporal resolution. The use of light to regulate biological processes has evolved into a vibrant field over the past decade. Employing light on chemical substances such as bioactive molecules and drug delivery systems offers a promising therapeutic approach to achieve precise control over biological processes. In this review, we provide an overview of the advancements in optochemical technologies for controlling bioactive molecules (photopharmacology) and drug delivery systems (photoresponsive drug delivery), with an emphasis on their relationship and biomedical applications. Gaining a deeper understanding of the underlying mechanisms and emerging research will facilitate the development of optochemically controlled bioactive molecules and photoresponsive drug delivery systems, further enhancing light technologies in biomedical applications.

Received 1st February 2025

DOI: 10.1039/d5cs00125k

rsc.li/chem-soc-rev

1. Introduction

Biological processes are naturally regulated in a spatial and temporal way at both cellular and organism levels.[1,2] Over the past few decades, tremendous efforts have been made to control biological functions of various molecules to achieve specific therapeutic outcomes.[3,4] Stimuli-responsive therapeutic drugs or carriers serve as a promising toolbox by virtue of their precise regulation similar to biological systems.[5–7] Among the various stimuli, light stands out for its ability to control biological systems with unparalleled spatiotemporal resolution and adjustable irradiation power and sites.[8,9] Utilizing light to manipulate biological systems holds substantial potential for numerous applications, such as modulating biological functions, preventing and treating diseases, and more, while minimizing side effects.

Light has been investigated to treat diseases for a long time. For example, photodynamic therapy (PDT) has a rich history spanning over a century.[10,11] Early discoveries in the 1900s observed the photosensitizing effects of certain dyes, leading to the exploration of PDT for cancer treatment in the 1920s.[12] Subsequent decades saw clinical trials and the expansion of PDT applications, from skin and bladder cancers to lung,

[a] *Department of Pharmacology and Pharmacy, Li Ka Shing Faculty of Medicine, The University of Hong Kong, Hong Kong, China. E-mail: wangwp@hku.hk*
[b] *Laboratory of Molecular Engineering and Nanomedicine, Dr. Li Dak-Sum Research Centre, The University of Hong Kong, Hong Kong, China*
[c] *State Key Laboratory of Pharmaceutical Biotechnology, The University of Hong Kong, Hong Kong, China*
† Yuwei Liu and Tianyi Wang contributed equally to this work.

Yuwei Liu

Dr. Yuwei Liu received her bachelor's degree in Pharmacy from Sichuan University. She obtained her PhD degree from the University of Hong Kong, under the supervision of Prof. Weiping Wang. She is currently a postdoctoral fellow at Department of Pharmacology and Pharmacy, the University of Hong Kong. Her research interests focus on photopharmacology, photoresponsive drug delivery, and cancer stem-like cell research.

Tianyi Wang

Dr. Tianyi Wang received his bachelor's degree in medicine from Jilin University. He obtained his PhD degree from The University of Hong Kong, under the supervision of Prof. Weiping Wang. He is currently a postdoctoral fellow at Sun Yat-sen University Cancer Center. His research interests include the influence of metabolism on tumor microenvironment, nanomedicines for cancer treatment, and photopharmacology for cell signaling control.

esophageal, and head and neck cancers.[13,14] Advancements in light sources, delivery methods,[15,16] and photosensitizing agents have improved the efficacy and selectivity of PDT, allowing its use in a growing range of medical conditions, including cardiovascular diseases and infectious diseases.[17,18]

However, despite the great contributions of PDT in the field of light-based disease treatment, its limitations lie in the fact that light irradiation can only promote reactive oxygen species (ROS) generation from photosensitizers to kill cells as a therapeutic approach. As a result, there is growing interest in exploring additional modalities that leverage light for various functionalities. In recent years, the fields of photopharmacology[19,20] and photoresponsive drug delivery[21,22] have flourished, utilizing light to control the functions of various molecules for diverse therapeutic purposes. It is important to note that combining the techniques and learnings from PDT can greatly benefit the clinical translation of these emerging photopharmacology and photoresponsive drug delivery approaches. By drawing upon the wealth of knowledge and experience gained from the development of PDT, researchers can optimize the integration of light-based therapies for more effective and targeted treatment options.

The key to modulate biological activity *via* light is to realize controlled release of active species through light at desired time and site. There are mainly two strategies to achieve the objective: using light to control bioactive molecules (photopharmacology) and using light to control drug delivery systems (photoresponsive drug delivery). Two strategies share the same photochemistry techniques and pharmaceutical aims. For bioactive molecules, their active state emerges by changing chemical structures and pharmacokinetic and pharmacodynamic properties of inactive state *via* light.[23,24] The effect of light on bioactive molecules can be reversible or irreversible and both modalities can be applied in biological systems. With regard to drug delivery systems, the active species can be encapsulated into photoresponsive vehicles and be precisely released at the specific area upon light irradiation due to the dissociation of the vehicles.[25,26] Photoresponsive drug delivery typically involves photo-triggered targeting[27] and drug release. In this review, we will specifically focus on photo-triggered drug release. Photo-triggered drug release not only reduces off-target side effects but also realizes on-demand dosing. By harnessing the tool of photochemistry, the biological processes can be regulated at a high spatio-temporal resolution *via* above-mentioned modalities.

In this review, we will introduce basic photochemistry used for both strategies and summarize the development in the optochemical control of bioactive molecules (*via* designing photoresponsive prodrugs) and drug delivery systems (*via* designing photoresponsive drug delivery systems, PDDSs) (Scheme 1). The rational design and mechanism behind photoresponsiveness will be discussed to inspire the development of novel and applicable photoresponsive prodrugs and drug delivery systems. We will highlight the relationships between these two strategies. Furthermore, a variety of biomedical applications will be presented, and the clinical translation potential will be elucidated, providing guidelines for future development of light technology in controlling biological systems for therapeutic purposes.

2. Clinical considerations of light

To bring light into clinical applications, there are two major concerns, namely light penetration and phototoxicity. The penetration ability of light into deep tissues is a long-standing problem.[28] Light can be classified into several categories based on its wavelength.[29] Ultraviolet (UV) light, with a wavelength range of 100–400 nm, penetrates only the outermost 0.1–0.5 mm of skin, making it suitable for *in vitro* studies and surface-level applications such as sterilization and fluorescence imaging. Blue light, ranging from 400–490 nm, reaches 0.5–1 mm into the upper dermis and is often used for treating superficial skin conditions. Green, yellow and orange light, with a wavelength range of 500–625 nm, penetrate 1–2 mm into the mid-dermis. These types of light are typically utilized for treatments in transparent tissues due to their moderate penetration depth. Red light, ranging from 625–750 nm, penetrates 2–5 mm into the dermis and subcutaneous tissues. Near-infrared (NIR) light, with wavelengths between 750 and 1400 nm, is beneficial for deep tissue applications due to its penetration depth of 5–10 mm. This capability allows it to effectively target deep-seated tumors and is also useful for non-invasive imaging techniques.

Another consideration is phototoxicity, which is highly correlated with photon energy and energy density (irradiance and time).[30] According to the Planck–Einstein relation: $E = hc/\lambda$ (E = energy of a photon; h = Planck's constant; c = speed of light; and λ = wavelength of light), the energy of a photon is inversely proportional to its wavelength. This implies that light with a shorter wavelength possesses higher photon energy compared

Weiping Wang

Prof. Weiping Wang is an Associate Professor at Department of Pharmacology and Pharmacy & Dr. Li Dak-Sum Research Centre, The University of Hong Kong (HKU). He is a Principal Investigator at the State Key Laboratory of Pharmaceutical Biotechnology, HKU. He obtained his PhD in 2011 from The Hong Kong University of Science and Technology. He was a Research Fellow at Boston Children's Hospital, Harvard Medical School and Postdoctoral Associate at Koch Institute for Integrative Cancer Research, Massachusetts Institute of Technology. His research interests include molecular self-assembly, photopharmacology, stimuli-triggered drug delivery, and ocular drug delivery.

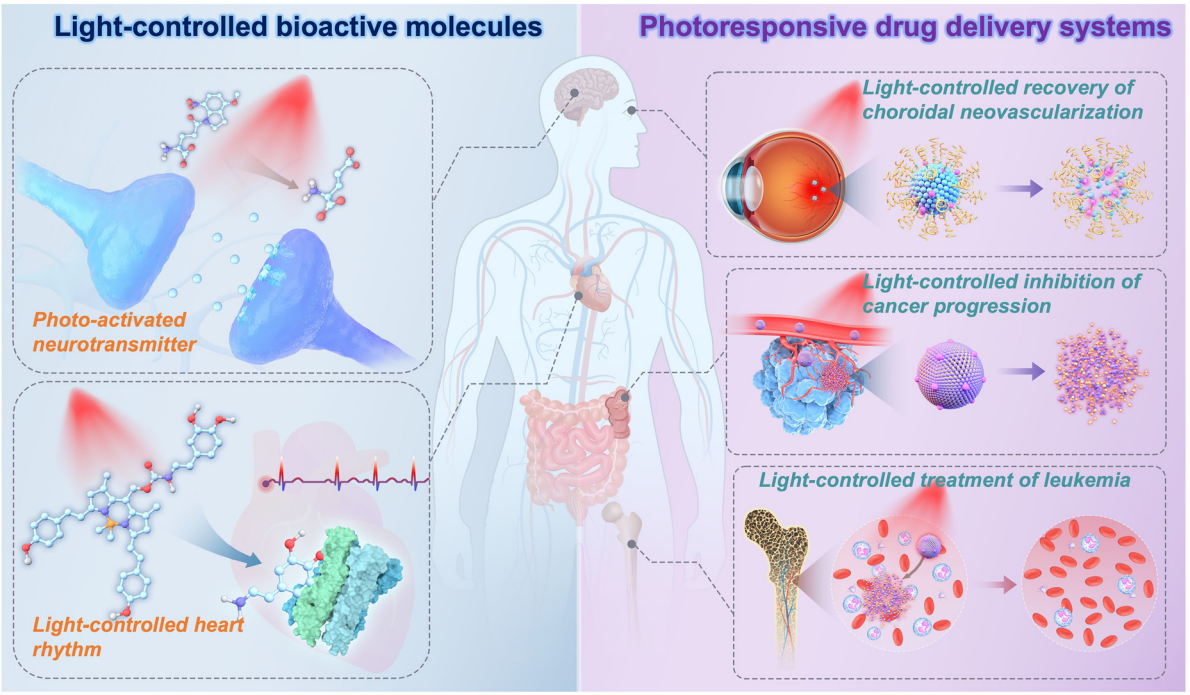

Scheme 1 Schematic illustration of strategies in light-controlled bioactive molecules and photoresponsive drug delivery systems.

to light with a longer wavelength. Higher-energy photons can interact more intensely with biological molecules, leading to greater phototoxic effects. Understanding the relationship between light wavelength and phototoxicity is crucial for developing effective treatments. Light with shorter wavelengths exhibits higher photon energy compared to light with longer wavelengths, resulting in higher phototoxicity. Therefore, developing photoresponsive molecules or drug delivery systems with the most suitable irradiation parameters is of great significance.

In addition to tissue penetration and phototoxicity, the complex physiological environments of the body must also be considered, including ordinary physiological chromophores, water, and other factors. With the development of light technology applied for biomedical purposes, the identification of the "NIR window", which exists between 600 and 900 nm, became possible after thorough characterization of the wavelength-dependent optical absorption and scattering coefficients of common chromophores.[31] Within the NIR window, ordinary physiological chromophores exhibit low light absorption, thus allowing light within this wavelength range to penetrate deeper into tissues.[32] When the wavelength is below 600 nm, it can be absorbed by major tissue chromophores, including hemoglobin, myoglobin, and melanin. Additionally, tissue penetration is also limited above 900 nm due to light absorption by water. Furthermore, light within the NIR window displays minimal phototoxicity by virtue of its relatively long wavelength. Therefore, the light within the NIR window is considered a suitable candidate for *in vivo* biomedical applications.

3. The relationship between photopharmacology and photoresponsive drug delivery

Photopharmacology, an innovative discipline combining photochemistry and pharmacology, uses light to control the biological activity of molecules. Its primary aim is to address the long-standing problem of off-target toxicity outside lesions.[33,34] The irreversible or reversible regulation of biological activity is allowed by incorporating light-responsive moieties into the structure of bioactive molecules.[35] As an irreversible regulation, the pharmacophoric features are masked when photocleavable protecting groups (PPGs) are introduced.[36] Upon light irradiation, photolabile moieties will be irreversibly removed and the potency of the parent molecule will be restored consequently. The other modality is to introduce molecular photoswitches into drug molecules, which endowed the active species with two forms.[37] Light can trigger the reversible isomerization between two isomers, which leads to different potencies against the desired target due to distinct structural and electronic features of the two isomers.

Drug delivery systems such as nano-sized particles emerge as a validated tool in treating a lot of diseases by virtue of their diverse functionalities and special characteristics.[38,39] Nanomedicine is widely applied in cancer treatment due to the well-recognized enhanced permeability and retention (EPR) effect.[40] Despite there are converse opinions towards the efficacy of the EPR effect in clinic,[41] the mechanism can be investigated in detail since there are successful applications of nanomedicine in clinical translation like Abraxane®, Doxil®, *etc.* with a total

of 100 nanomedicine products already on the market.[42] Furthermore, nanomedicine is proved to be effective in other disease models including rheumatoid arthritis (RA), taking advantage of the fact that nanocarriers can be taken up by macrophages into arthritic joints through inflamed leaky capillaries.[43,44] Besides, drug delivery systems are able to protect drugs from degradation, improve targeted drug delivery *via* functional modification, and be produced on a large and reproducible scale.[38,45] Therefore, they are good candidates to deliver drug molecules effectively. Light, as an external stimulus, is investigated to control drug delivery systems and trigger drug release at the desired area precisely. Such a kind of strategy has been widely exploited and termed as photoresponsive drug delivery. In the strategy, light-responsive molecules (such as PPGs and photoswitches) are integrated into the building blocks of nanocarriers to construct PDDSs. Light irradiation can trigger the conformation change of the drug delivery systems and initiate subsequent cargo release.

In photopharmacology, the object controlled by light is bioactive molecules, while in photoresponsive drug delivery, the object is drug delivery systems. Both photopharmacology and photoresponsive drug delivery utilize similar photochemistry techniques and share the same pharmaceutic objectives: to release active species at diseased lesions and reduce off-target effects outside these areas.

Additionally, these two strategies can converge in certain instances, sharing similarities in their photochemistry techniques and pharmaceutical objectives. In the photopharmacology approach, when photocleavable prodrugs are encapsulated in a drug delivery system, light irradiation can trigger the release of active drugs from the prodrugs. These drugs can then be further released from the delivery system due to changes in hydrophilicity. In this case, the strategy can also be considered photoresponsive drug delivery. Similarly, in the photoresponsive drug delivery approach, when drug molecules are linked to drug delivery systems *via* PPGs, the combined delivery system and PPGs can be viewed as a large PPG for the drug molecule, and this strategy can be considered photopharmacology. In summary, the objects that can be controlled by light range from bioactive molecules to drug delivery systems. The two strategies employ similar photochemistry and aim to achieve light-controlled regulation of biological activities, as well as the treatment of diverse diseases with minimized side effects.

4. Mechanism of photoresponsiveness

Photoresponsive molecules have garnered significant attention in recent years due to their intriguing properties and potential applications. These molecules possess the unique ability to undergo irreversible or reversible changes in their structure, properties, and behavior upon exposure to light, making them highly versatile and adaptable for various purposes.[46] The rational design of photoresponsive molecules involves careful consideration of molecular structures, conjugation patterns, and functional groups. Understanding the photophysical properties of photoresponsive molecules is crucial for their successful implementation.[47] This includes studying their absorption and emission behaviors, excited-state dynamics, and fluorescence modulation mechanisms. Light absorption leads to the molecules' transition to an excited state, and subsequent relaxation processes determine the observed behavior. Factors such as solvent polarity, temperature, and molecular environment can affect these properties, making them tunable. Various design strategies and related mechanisms including photocleavage, photoisomerization, photodimerization, photosensitization, photothermal effects, and photocatalytic effects are discussed in detail within this section, shedding light on the diverse approaches employed to achieve light-induced transformations.

4.1 Photocleavage

The photocleavage approach is one of the most commonly used strategies to achieve light-responsive release of active drugs. As an example in photopharmacology, the general idea of this approach is to cage an active drug with a photoremovable group or PPG at the functional moiety to block the biological activities. Under light exposure, the photoremovable group can absorb light and reach an excited state, which subsequently reacts with the solvent and undergoes photolysis. Consequently, the released free drug molecule can execute corresponding functions. Based on the absorption wavelength, different photoremovable groups are developed, including nitrobenzyl, coumarin, and BODIPY derivatives.[48]

The nitrobenzyl derivatives are among the most commonly used photocleavable groups. Upon light irradiation, the hydrogen from the *o*-alkyl substituent transfers to the nitro group, resulting in the formation of an aci-nitro tautomer as an intermediate, which is readily detected by its strong absorption around 400 nm.[48] The decay of this transient intermediate suggests the release rate of the protected compounds. Additionally, Il'ichev *et al.* identified that upon light irradiation, 2-nitrobenzyl methyl ether transferred to an aci-nitro tautomer intermediate, which further transferred to 1,3-dihydrobenzo[*c*]-isoxazole-1-ol derivatives and 2-nitrosobenzyl hemiacetals. Interestingly, the photocleavage rate was strongly attributed to the decay rate of these three intermediates in different solutions under different pH values (Scheme 2).[49]

Coumarin derivatives are another group of photocleavable molecules responsive to short-wavelength light, generally from 365 nm to 500 nm. Activated by light irradiation, the coumarin derivative, 7-(diethylamino)-4-(hydroxymethyl)-coumarin (DEACM), undergoes heterolytic cleavage of the C–O bond at the caging site, generating free carboxylic acid and the corresponding coumarinylmethyl alcohol due to the reaction of the cationic intermediate with H_2O, followed by a fast deprotonation process (Scheme 2). The coumarin chromophore, chemical properties of the leaving group, and characteristics of the bond for cleavage (ester or carbamate) play crucial roles in determining the efficiency and speed of the photocleavage reaction during the uncaging process. Interestingly, based on the different deprotection kinetics of different leaving groups, two dicyanocoumarin-caged model compounds

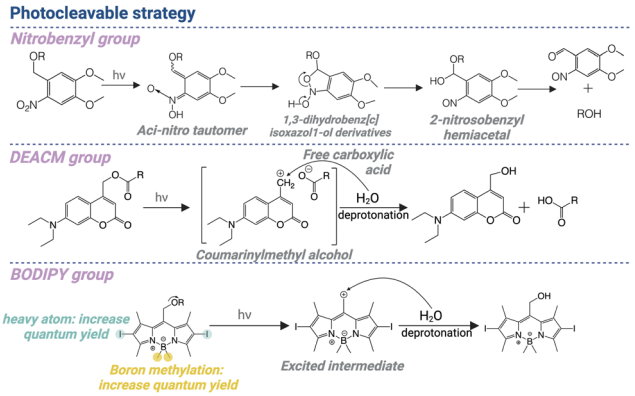

Scheme 2 Illustration of the photocleavage strategy based on nitrobenzyl groups, DEACM groups, and BODIPY groups, separately. Created with https://BioRender.com/y85u977.

(*e.g.*, benzoic acid and ethylamine) were sequentially photocleaved to generate corresponding products.[50]

To achieve photolysis with longer-wavelength light irradiation, BODIPY derivatives have been widely applied in the photocaging approach recently.[51] Similar to coumarin derivatives, *meso*-methyl BODIPY derivatives undergo a heterolysis process, followed by the reaction with a solvent molecule. Multiple modification strategies are applied to further promote the redshift and photocleavage efficiency for clinical translation. For example, 2,6-iodination improved the quantum yield by nearly 1 order of magnitude *via* facilitating intersystem crossing, based on the heavy atom effect.[52] The boron-methylation of the conventional difluoroboron unit led to more than 50-fold increase of photorelease quantum yield.[53] Additionally, the absorption wavelength can be longer by extending the conjugation with styryl groups (Scheme 2).[54]

The photolysis rate can be influenced by multiple factors of these PPGs mentioned above, including the structure, photolysis quantum yield, and stability under light excitation. The balance between the lability and stability of these PPGs controls their photolysis efficiency. Nitrobenzyl groups, in particular, are unstable under prolonged exposure to ambient light or oxygen-rich environments, with a lower quantum yield compared to DEACM or BODIPY.[55] Coumarin derivatives are more chemically stable, showing better resistance to extreme environments and higher quantum yield.[55] BODIPY-based PPGs are generally highly stable and resisted to hydrolysis under ambient light, with high quantum yield for drug release.[56] Therefore, different PPGs, with variable photolysis characteristics, can be selected for different biological applications.

4.2 Photoisomerization

Although the photocleavage approach enables spatiotemporal control of biological functions, the photolysis reaction remains irreversible. Differently, the photoisomerization strategy allows precise and reversible control of drug activity by localized light irradiation.[57–61] The drug molecule can be conjugated with a photoswitchable ligand, which undergoes *trans–cis* transformation under light irradiation. In a dark environment, the molecule is inactive due to steric hindrance or an unfavorable binding position with its target molecule. Upon light exposure, the *trans–cis* transformation reactivates the interaction between the drug and the target molecule. The drug molecule can switch back to the inactive conformation in a dark environment, enabling reversible control of drug activity.

The azobenzene group is regarded as one of the commonly used structures for the development of photoswitchable molecules. This process involves a rotation around the central azo double bond, leading to a significant change in the molecular conformation. The driving force behind this isomerization is the absorption of photons, which promote electronic excitation within the molecule. Subsequently, azobenzene at the excited state can relax through various pathways, including rotation, inversion, concerted inversion, and inversion-assisted rotation, to reach the metastable *cis*-state that reverts back to the stable *trans*-state without light irradiation (Scheme 3).[62]

The molecular structure of azobenzene plays a pivotal role in dictating its photoswitching properties. Different molecular factors such as the substitution pattern, steric hindrance, and electronic properties of the substituents profoundly impact the efficiency and kinetics of isomerization. As a result, structural modification of azobenzene enables fine-tuning of the absorption wavelength (up to 530 nm), quantum yield, and thermal stability, thereby expanding the versatility of these compounds for broad applications.[63] For example, Fang *et al.* developed a decoupling strategy by inserting a linker into the azobenzene moiety to disrupt the through-bond electronic communication.[64] 1,2,3-Triazole was directly incorporated into the azoswitch core as a decoupling spacer to construct "self-decoupling" azoswitches called (hetero)arylazo-1,2,3-triazoles. The photoisomerization properties of such azotriazole photoswitches can be manipulated by changing the substituent groups or heteroaryl rings, enabling (near-)quantitative photoswitch yields and tunable kinetic profiles. Similarly, *ortho*-fluoroazobenzene modification also significantly contributed to higher bistability.[65]

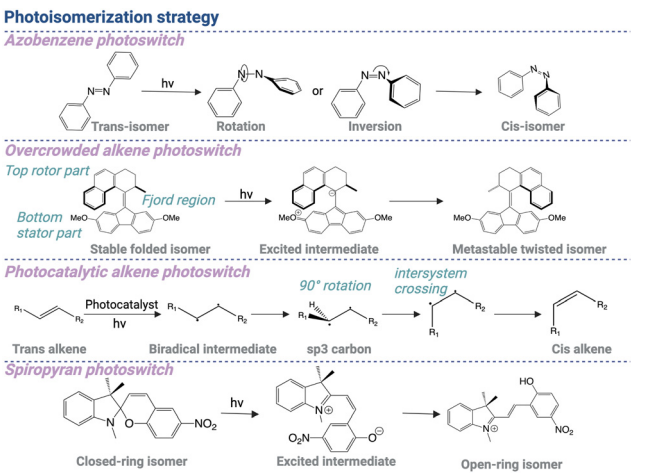

Scheme 3 Illustration of the photoisomerization strategy based on azobenzene, alkene, and spiropyran structures, separately. Created with https://BioRender.com/q41i239.

These σ-electron-withdrawing F atoms *ortho* to the N=N unit induced notable separation of the n–π* bands of *trans*- and *cis*-isomers, which greatly enhanced the thermal stability of Z isomers.

Besides controlling biological activities, *trans–cis* photoswitches are also designed as molecular rotary motors, exhibiting intrinsically dynamic behavior that can be manipulated by light. A notable example is chiral overcrowded alkene structures, which were recognized by the 2016 Nobel Prize in Chemisry.[66] This alkene-based photoswitchable scaffold constitutes a fluorene structure acting as the bottom stator part and a tetrahydrophenanthrene moiety functioning as the top rotor part, both interconnected through an alkene bond (Fjord region). Upon 365 nm light irradiation, the stable folded isomer transitions into an excited dark state as an intermediate, which subsequently converts into a metastable twisted isomer (Scheme 3).[66,67]

The overcrowded alkene photoswitch combines several advantages over the azobenzene group. This alkene-based scaffold has high thermal stability, large geometric transformation, and distinct helical chirality in the metastable state. The large spectral band separation between the two isomers also allows for precise control of the molecular motor, enabling versatile applications across different length scales. These applications include unidirectional motion at the molecular level on a surface, helical motion at the macromolecular level, and the operation of nanocars at a copper surface.[67]

The *trans–cis* transformation can also be realized in a simple alkene structure by coupling with photocatalysts, through an energy transfer mechanism. Upon light irradiation, the energy from a light-activated photoexcited catalyst results in the generation of a biradical intermediate, undergoing 90° rotation about the C–C bond to form sp^3 hybridized carbons, which subsequently change to the final product through intersystem crossing (Scheme 3).[68,69] In comparison with the azobenzene group, this photocatalytic alkene photoswitch can be more flexible in molecular design but requires more careful design of the substituents on either side to achieve desired reversibility and thermal stability. In summary, the azobenzene group exhibits superior reliability and stability compared to a photocatalytic alkene photoswitch. It demonstrates high resistance to fatigue and a quick response to light stimulus.

Another common type of photoswitchable compound for drug development and materials design is spiropyran derivatives, existing in two forms: a colorless, closed-ring form and a colored, open-ring form. The closed-ring form of spiropyran is thermally stable. However, upon exposure to ultraviolet or visible light, spiropyran molecules undergo a photochemical reaction, reaching an excited state that leads to the cleavage of the C–O bond in the spiro linkage, thereby initiating the ring-opening process. As a result, the spiropyran molecule generates a linear structure, without the two aromatic rings bounded together.[70] The open-ring form of spiropyran is not stable indefinitely and can undergo thermal and reversible conversion back to the closed-ring form. This conversion can occur spontaneously over time or can be induced by exposure to a different wavelength of light (Scheme 3).

The specific conditions and kinetics of the conversion depend on the particular spiropyran derivative and its environment. For instance, to prepare a spiropyran-based light-responsive system with a longer excitation wavelength, Gao *et al.* introduced a sulfonated spiropyran derivative, which absorbed light within the 500–600 nm region and underwent isomerization under white-light irradiation.[71] After isomerization, the proton transformation between the sulfonate and phenoxide groups stabilized the open-ring merocyanine form. As a result, this molecule demonstrated negative photochromic properties, which was indicated by the strong stability and fatigue resistance of the open form.

4.3 Photodimerization

Photodimerization, the process of light-induced formation of covalent dimers from two individual molecules, has gained considerable interest in the field of controlling biological activities. Upon light irradiation, one molecule can reach the exited state and react with another molecule in the ground state to form covalent bonds, enabling dimerization of these two molecules. This light-triggered covalent bond formation makes it a valuable tool for manipulating biological systems through regulating molecular interactions.

Coumarin derivatives are among the commonly used structures for photodimerization. Excited by 300 nm light, a coumarin molecule can reach an excited singlet state ^{1}[Coum]*, which is likely to turn to an excited triplet state ^{3}[Coum]* due to the intersystem crossing.[72,73] After combining with another coumarin molecule in the ground state, a triplet exciplex ^{3}[^{3}Coum-^{0}Coum]* can be formed. Subsequently, through the formation of a carbon–carbon bond, a triplet 1,4-diradical, ^{3}[1,4-diradical]*, can be generated, which can undergo spin inversion to a singlet diradical and subsequently result in a closure to a cyclobutane ring (Scheme 4).[74]

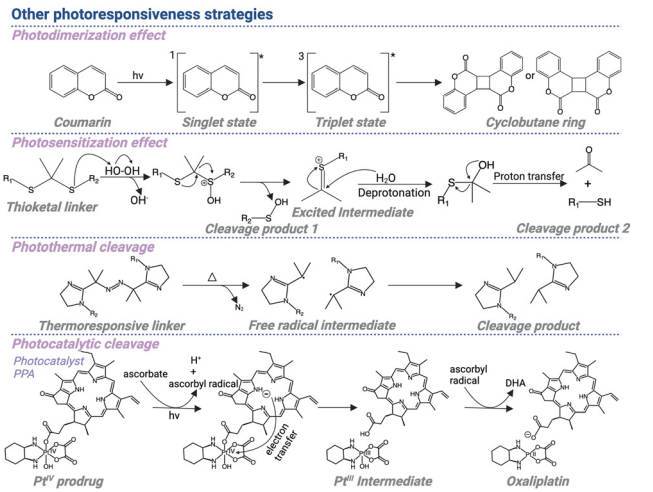

Scheme 4 Schematic illustration of other photoresponsiveness strategies based on different mechanisms including the photodimerization, photosensitization, photothermal effect, and photocatalytic effect. Created with https://BioRender.com/t57l746.

Based on the light-triggered coumarin dimerization process, a light-controlled hydrogel formation strategy has been realized for further biomedical applications. A hydrogel scaffold based on reversible photo-crosslinks was designed, allowing reprogramming of the gradient structures and 3D deformations into various configurations. The interactions between the hydrophobic coumarin monomer and hydrophilic acrylic acid resulted in the micellar polymerization, in the presence of hexadecyltrimethylammonium chloride micelles, which formed robust polyelectrolyte/surfactant complexes that served as physical crosslinks. Efficient photodimerization and photocleavage reactions of coumarins can be achieved when they are exposed to light at wavelengths of 365 nm and 254 nm, respectively. This allows for reversible adjustment of the hydrogel's network structure, enabling precise control and modification.[75]

4.4 Photosensitization

The above approaches are primarily based on direct light-triggered cleavage, isomerization, or dimerization of small molecules. The light-responsive cleavage can also be achieved in an indirect way through combining photosensitization with ROS-responsive molecules. Typically, the photosensitizer is conjugated to corresponding drugs through ROS-responsive linkers, enabling light-triggered cleavage of the linker and release of the drug molecules. Upon light irradiation, the photosensitizer reaches a triplet excited state and reacts with oxygen molecules in the ground state to generate ROS, which then cleaves the ROS-responsive linkers.

A thioketal linker is one of the most used moieties as the ROS-responsive moiety. Despite it shows broad applicability in versatile biomedical applications, the mechanism behind the ROS-induced cleavage of this structure remains unknown. Interestingly, Liu *et al.* identified that ROS induced the initial oxidation step at the thioether unit, resulting in the functional group degradation, generating a sulfenic acid intermediate and a thiocarbenium ion intermediate. After hydrolysis, the thiocarbenium ion intermediate generated corresponding thiol, which reacted with the sulfenic acid, resulting in the formation of a disulfide-based byproduct (Scheme 4).[76]

As an example, the chemotherapy drug doxorubicin was linked to a photosensitizer-based polymeric conjugate through a ROS-responsive thioketal linker. Light-induced activation of the photosensitizer resulted in ROS generation, which effectively cleaved the thioketal linker, leading to on-demand drug release.[77] Without being conjugated together through ROS-responsive linkers, photosensitizers and ROS-responsive prodrugs can also be encapsulated together in a drug delivery system. The short distance between the photosensitizers and ROS-responsive molecules allows efficient light-triggered drug release. As a proof of concept, doxorubicin was conjugated with polyphosphoester through a ROS-responsive thioketal linker, and incorporated with a photosensitizer into nanoparticles. The photosensitizer can be activated by light irradiation, inducing ROS generation, which can efficiently cleave the nearby prodrugs with thioketal linkers to release active drugs for localized cancer treatment.[78]

4.5 Photothermal effect

Like light-triggered ROS production for prodrug cleavage, light irradiation is also widely exploited to generate heat, which can also be used to activate thermo-responsive prodrugs for localized drug activation. The photothermal cleavage strategy involves the use of light-absorbing materials, generating heat upon light irradiation based on three main mechanisms, including plasmonic localized heating, non-radiative relaxation in semiconductors, and thermal vibration of molecules.[79]

In the first process, surface plasmon resonance occurs by enhancing local electric field to produce a high concentration of hot electrons. The plasmons can decay through a non-radiative process, coupling to phonon modes by electron–phonon scattering and generating heat.[80] In semiconductors, under light exposure, photons with near or higher energy than the band gap lead to the generation of electron–hole pairs. The energy of electrons can be released through non-radiative relaxation, leading to heat generation.[81] In the third mechanism, the loosely held electrons can be excited to the higher-energy orbitals from the ground state upon light exposure and relax back to the ground state through electron-vibration coupling with release of thermal energy. For some carbonaceous and polymeric materials with strong absorption, the highly conjugated π bonds can be activated to the excited state, which relax back through the thermal vibration mechanism.[82]

Based on the above mechanisms, photothermal materials are conjugated or encapsulated with prodrugs. Upon exposure to light, the generated heat triggers cleavage of specific linkers or bonds, resulting in the release and activation of the therapeutic agent at the target site. The strategy involves the use of temperature-sensitive linkers, which undergo cleavage at elevated temperatures, leading to drug release. Jiang *et al.* reported a photothermally activatable polymeric pro-nanoagonist (APNA) that was particularly controlled by second NIR (NIR-II) light.[83] An immunostimulant was covalently conjugated onto a NIR-II semiconducting transducer *via* a labile thermoresponsive linker, 2,2′-azobis[2-(2-imidazolin-2-yl)propane] (Scheme 4). In response to NIR-II light irradiation, APNA mediated the photothermal effect, which started the cleavage of the thermolabile linker to release the caged agonist for *in situ* immune activation in deep solid tumors, thereby initiating tumor ablation and driving immunogenic cell death. Such light-triggered immunostimulant activation displayed high ability to enhance systemic anti-tumor immunity and prevent tumor growth. Thus, the study provides an example of a general way of producing pro-immunostimulants *via* the spatiotemporal control of cancer nanoimmunotherapy.

4.6 Photocatalytic effect

In the above examples, photosensitization and photothermal approaches are applied by coupling photoresponsive molecules with ROS or thermal-responsive prodrugs. Similarly, photocatalysis is developed by coupling photo-redox with an electron transfer reaction. Upon light irradiation, the photocatalyst can

be activated to an excited state, generating radicals by electron transfer to or from a substrate. Subsequently, the substrate as a radical can be conjugated with other molecules through chemical reactions.

For example, photocatalytic cell tagging (PhoTag) technology was designed by conjugating photoactivatable flavin-based cofactors to single-domain antibodies.[84] Light irradiation activated the flavin cofactors, generating triplet-excited flavin. Subsequently, single-electron transfer occurred between biotin tyramide and the triplet-excited flavin, resulting in the generation of the corresponding phenoxy radicals, which react with tyrosine residues of the surrounding proteins. This approach enabled highly selective synaptic labeling across the PD-1/PD-L1 axis for investigating immune cell interactions. Through combining single-cell sequencing technology, the interactions between peripheral blood mononuclear cells and Raji PD-L1 B cells were identified.

The radicals generated by photocatalysis can also lead to the cleavage of prodrugs by promoting extrusion of leaving groups. The flavin derivatives as unconventional photocatalysts were employed to generate free radicals, which can initiate the electron transfer process. Usually, these photocatalysts can be coupled with inorganic metal molecules, which are often anti-cancer drugs, to realize photoactivated chemotherapy. Octahedral Pt^{IV} and Ru^{II}–arene piano-stool complexes are commonly used model prodrugs. These prodrugs can be more stable and less toxic in the form of a complex. The adoption of an octahedral structure by six-coordinate Pt^{IV} or Ru^{II} complexes can form a sterically crowded environment and shield the metal center, making the complexes kinetically inert and resistant to hydrolysis, thereby prolonging the half-life and promoting the drug accumulation in tumor tissues. The steric hindrance also blocks the interaction of prodrugs with DNA, making them less toxic to normal tissues where light irradiation is not applied.[85] Upon light irradiation at the tumor tissues, the bioorthogonal photocatalytic reaction induces the cleavage of the prodrugs, generating toxic Pt^{II} and Ru^{II}-OH_2 species for cancer treatment.[86] Therefore, coupling of photocatalysts and prodrugs enables unconventional design of versatile light-responsive anti-cancer prodrug systems for promising strategies in cancer treatment.

Additionally, the photocatalyst and prodrug can also be conjugated together through a linker, enabling photo-triggered release of the drug molecule. For example, a photo-absorber responding to red light, pyropheophorbide A (PPA), was employed as the photocatalyst.[87] PPA was conjugated to the axial position of the oxaliplatin to generate the PT^{IV} prodrug, phorbiplatin. The saturated coordination sphere also resulted in low reactivity and toxicity of Pt^{IV}. As a result, the toxic Pt^{II} can be caged in the dark. Upon light irradiation, PPA was activated to the triplet excited state and subsequently underwent reduction in the presence of ascorbate. With the electron transfer process at the Pt center, Pt^{IV} can be successfully reduced to toxic Pt^{II}. Phorbiplatin exhibited photocytotoxicity of up to 1786 times compared to oxaliplatin after light irradiation (Scheme 4).

5. Optochemical control of bioactive molecules (photopharmacology)

Based on the mechanisms introduced in the above section, optical regulation of different molecules can be achieved, realizing spatiotemporal control over their function and activity. This strategy can be applied to small-molecule drugs to regulate intracellular signaling pathways using light. Besides small molecules, macromolecules such as proteins and nucleotides in the cells can also be modified with light-responsive moieties, enabling direct control of these biological molecules (Scheme 5). Some examples based on optochemical control of bioactive molecules are summarized in Table 1.

5.1 Optochemical control of small molecules

Small-molecule drugs have played critical roles in the treatment of various diseases, including cancer, inflammatory diseases, neurodegenerative diseases, *etc.*[88–92] However, when intravenously injected, these compounds as therapeutic agents are distributed not only at the diseased sites but also at normal organs and tissues, thereby leading to off-target effects. By designing photocleavable or photoswitchable drugs, precise spatiotemporal control over drug release and activation can be achieved, possessing the potential to enhance therapeutic efficacy, minimize off-target effects, and reduce systemic toxicity.[93] By selectively illuminating specific subcellular regions or targeting individual molecules with light in a timely manner, their behavior, reactivity, and function can be precisely controlled,

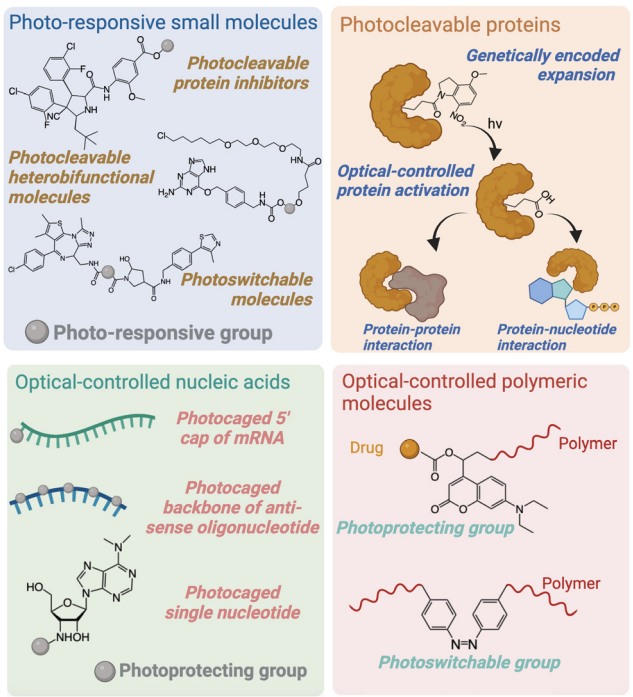

Scheme 5 Schematic illustration of general examples of photoresponsive prodrug systems, including photoresponsive small molecules, proteins, nucleic acids, and polymeric molecules. Created with https://BioRender.com/q29x232.

Table 1 A table summarizing examples of photopharmacology that are mentioned in the reivew. DEACM, 7-(diethylamino)-4-(hydroxymethyl)-coumarin; BODIPY, boron dipyrromethene; BRD4, bromodomain-containing protein 4; HCPT, hydroxycamptothecin; OGT, O-GlcNAc transferase; PEGDA, polyethylene glycol diacrylate

Types	Mechanisms	Photoresponsive groups	Drugs/proteins	Light (nm)	Applications	Ref.
Photocleavable small-molecule inhibitors	Photocleavage	DEACM	Idasanutlin	400	P53-dependent apoptosis	97
	Photosensitization	BODIPY	Carboplatin	470	G2 cell cycle arrest	102
	Photocleavage	DEACM	OSI-027	420	Autophagy	95
	Photocleavage	Naphthalimide	HCPT	470	Cancer therapy and drug distribution monitoring	107
Photocleavable heterobifunctional molecules	Photocleavage	Nitroveratryl	BRD4 PROTAC	365	BRD degradation	116
	Photocleavage	Nitrobenzyl	Halo-tag and SNAP-tag ligand	365	Cell–cell interaction	108
	Photocleavage	Nitrobenzyl	Halo-tag and TMP ligand	365	RNA translation	117
Photoswitchable small molecules	Photoisomerization	Azobenzene	Paclitaxel	415/530	Microtubule stabilization	126
	Photoisomerization	Azobenzene	BRD4 PROTAC	415/530	BRD degradation	128
	Photoisomerization	Azobenzene	Quaternary ammonium	488	Regulate HCN channels	131
	Photoisomerization	Azobenzene	Norfloxacin	365	Antibiotics	133
Optochemical control of proteins	Photocleavage	Nitrobenzyl	K842 of OGT protein	365	Glycosylation	134
	Photocleavage	Nitrobenzyl	Glu of HRV3C protein	365	HRV3C activity	141
	Photocleavage	Nitrobenzyl	K182 of biotin ligase	365	Biotinylation	142
	Photocleavage	DEACM	Lys of GTPase	405	Embryo development	144
	Photocleavage	Nitroveratryl	HwTxIV peptide	365	NaV channel	146
Optochemical control of nucleic acids	Photocleavage	Nitrobenzyl	mRNA	365	Translation of therapeutic mRNA	150
	Photocleavage	Nitroveratryl	Antisense oligonucleotide	365	RNase activation for gene silencing	151
	Photocleavage	Nitrobenzyl	Reporter peptide	365	Acquisition of HER2 distribution and level	153
	Photoisomerization	Azobenzene	Puromycin	390/520	Protein translation	156
Optochemical control of polymeric molecules	Photocleavage	DEACM	Polymeric anaesthetic conjugate	365	On-demand local anaesthesia	158
	Photocleavage	Nitrobenzyl	PEGDA	365	3D cell culture	159

enabling the study of intricate molecular processes and the design of complicated systems with fine-tuned properties. These optical control techniques can also be reversible depending on the prodrug design, allowing for the modulation of molecular states in a more controllable manner. This facilitates the ability to switch between different molecular states, providing flexibility in experimental design and applications.[94]

5.1.1 Photocleavable small-molecule inhibitors. Photocleavable small-molecule prodrugs have been widely explored to regulate biological effects considering the broad-spectrum PPGs, including nitrobenzyl-based PPGs, DEACM, BODIPY derivatives, *etc.*[36,95–101] Light-triggered activation of these small molecules enables precise control of related biological processes, allowing for spatiotemporal control with higher resolution and specificity. This facilitates the localized activation of effective small-molecule drugs for disease treatment. For example, MDM2-p53 protein–protein interaction plays an essential role in controlling cell cycle arrest and apoptotic death. Hansen *et al.* reported an optochemical control system for p53-related apoptosis.[97] An MDM2 inhibitor, idasanutlin, is photocaged directly at the reactive *m*-methoxybenzoic acid site using the DEACM photoremovable group. Upon 400 nm light irradiation, the photoremovable group was cleaved and idasanutlin was activated to bind to MDM2, thereby inhibiting its interaction with p53. The ubiquitination and degradation of p53 can be hindered, leading to its stabilization and cell cycle arrest (Fig. 1). Similarly, Pt^{IV} based opto-prodrug can also enable light-triggered cell cycle arrest for cancer treatment.

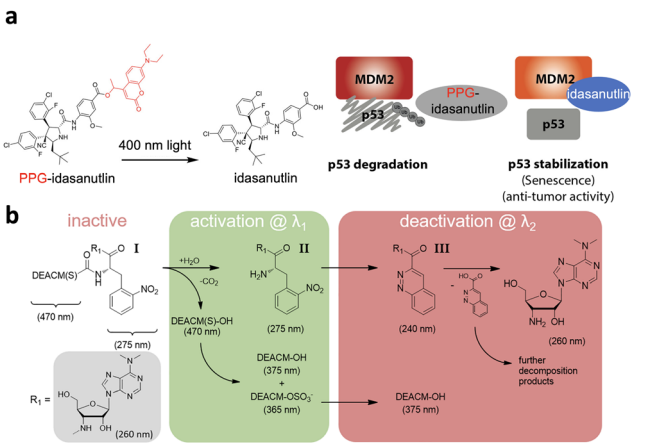

Fig. 1 (a) Schematic illustration of the photoactivatable PPG-idasanutlin prodrug, realizing spatiotemporal control of p53 stabilization (adapted from ref. 97 with permission from the © 2018 American Chemistry Society). (b) Schematic illustration of reaction mechanism of the doubly caged puromycin (thio-DEACM-nitro-puromycin I) upon sequentially light irradiation (adapted from ref. 103 with permission from the © 2021, American Chemistry Society).

The BODIPY ligand was conjugated at the axial position of carboplatin to form Pt^{IV} prodrug, called BODI-Pt, that was highly stable in the dark. Green light irradiation sensitized the BODIPY group, leading to ROS-dependent photocleavage and generation of active carboplatin for G2 cell cycle arrest and cancer treatment.[102]

Besides cellular senescence control, the optochemical strategy can also be applied for regulating other biological processes by inhibiting protein function, like autophagy. As an important process mediating cell metabolism and oxidative stress homeostasis, autophagy plays an important role in treatments for multiple diseases, including cancer and neurodegenerative diseases.[104,105] Our group previously demonstrated that an mTOR inhibitor, OSI-027, can be caged with the DEACM photoremovable group. Light irradiation can cleave the photoremovable group and activate OSI-027, which inhibited both mTORC1 and mTORC2 pathways. In addition, light can also trigger the formation of a LC3 puncta signal in cells treated with caged OSI-027, implying that this optochemical control strategy can be used for selectively inducing autophagy.[95]

The photocleavable prodrugs are not only developed based on conventional PPGs but are also derived from some PPGs that are not commonly used. For example, naphthalimide derivatives display advantages of high quantum yield and good light stability as fluorescent probes and act as anti-cancer drugs due to the ability for nucleic acid intercalation.[106] A 4-α-amino acid substituted naphthalimide derivative was designed, which can be specifically activated by blue light irradiation, leading to the photocleavage of the C–N bond between the 4-amino and the amino acid residue and resulting in the release of 4-aminonaphthalimide. Another anti-cancer drug, 10-hydroxycamptothecin (HCPT), can be conjugated to 4-α-lysine substituted naphthalimide *via* succinic acid. Due to the high fluorescence intensity, the prodrug can be used as a fluorophore to monitor drug distribution. Upon blue light irradiation, the prodrug can be efficiently cleaved, generating an active HCPT drug and naphthalimide to promote selectivity for cancer treatment.[107]

With the development of various PPGs responsive to different-wavelength light, multiple PPGs can be incorporated into one small molecule to achieve sequential photocleavage, realizing timely and reversible drug activation. For instance, an approach called two-PPGs-one-molecule (TPOM) was developed by orthogonal photolysis of two PPGs, a thiol-DEACM derivative responsive to 488 nm light and an *ortho*-nitrophenylalanine that cyclizes under 365 nm light (Fig. 1).[103] A puromycin analog was employed as the model drug and modified with these two photoresponsive moieties. Thiol-DEACM was cleaved upon the first 488 nm light irradiation, releasing the active *o*-nitropuromycin analog. Subsequently, 365 nm irradiation triggered the cyclization of *ortho*-nitrophenylalanine moiety, producing the deactivated cinnoline-puromycin analog. The two-step, activation/deactivation process inhibited protein translation in a reversible manner through a cell-free translation assay, representing a valuable approach for both mechanistic studies of gene expression regulation and clinical treatment as an antibiotic.

5.1.2 Photocleavable heterobifunctional molecules. In the photocleavable approaches mentioned above, one drug molecule with one specific protein target was masked by PPGs, making them unsuitable for mediating protein–protein interactions between two designated targets. To solve this problem, a series of photocleavable heterobifunctional molecules are designed. Generally, two warheads as targeting ligands are connected through a linker to form a backbone, with PPGs conjugated on either side of the backbone or inserted into the linker.[108] Upon light irradiation, PPGs can be cleaved to activate or deactivate the molecules, regulating protein–protein interactions.

As an example, proteolysis targeting chimera (PROTAC) and related optical-controlled PROTAC (opto-PROTAC) have been rising in recent years, mediating targeted protein ubiquitination and degradation. Conventional protein inhibitors may have to occupy the ATP-competitive binding sites to inhibit protein phosphorylation or allosterically regulate protein function. However, these processes require persistent interaction of small molecules and proteins, which may restrict the development of inhibitors of undruggable proteins.[109] In contrast, a PROTAC molecule is a dual-functional construct that comprises two functional components: a high-affinity ''warhead'' for specifically targeting the protein of interest and a ligand that interacts with an E3 ubiquitin ligase, with a short PEG linker.[110] Unlike the conventional small-molecule inhibitors, PROTAC catalyzed targeted protein degradation efficiently.[111,112] However, the high degradation efficiency of PROTAC may also lead to off-target effects in normal tissue when systemically administered for cancer therapy.

To achieve spatiotemporal control of targeted protein degradation, opto-PROTAC is developed to increase specificity for anti-cancer treatment.[113–115] For example, dBET1 was previously developed as a PROTAC to efficiently degrade bromodomain-containing protein 2 (BRD2) and BRD4. However, this significant loss of BRD2 and BRD4 proteins may reduce the therapeutic window of dBET1. Hence, a light-controlled dBET1 (opto-dBET1) was developed (Fig. 2).[116] The key hydrogen bond is formed between the glutarimide NH of the pomalidomide and the backbone carbonyl of His380 in CRBN E3 ligase during the ubiquitination process. Therefore, the NH group was caged with nitroveratryloxycarbonyl PPGs. Upon light irradiation, the PPG was photocleaved and the glutarimide group was exposed to interact with CRBN E3 ligase, leading to opto-PROTAC activation to mediate BRD protein degradation. Although less toxic than free dBET1, this opto-dBET1 could be timely triggered by light irradiation to suppress cell proliferation, which may significantly increase the specificity for this anti-cancer treatment. Opto-PROTAC was not only designed by caging the CRBN ligand but also constructed by blocking the VHL ligand[114] or by masking the warhead of the targeted protein with the nitrobenzyl group, achieving spatiotemporally controlled protein degradation in both an *in vitro* study and in a zebrafish model.[113] DEACM PPGs can also be applied, showing specific degradation of ERRα and Erα-mediated transcriptional activation.[115]

Light-controlled heterobifunctional molecules are also applied to investigate cell–cell interaction at the subcellular level. By coupling with fusion proteins including HaloTag protein and eDHFR protein, versatile design of photocleavable small molecules with the targeting ligands enables various light-controlled protein functions. Ollech *et al.* developed an

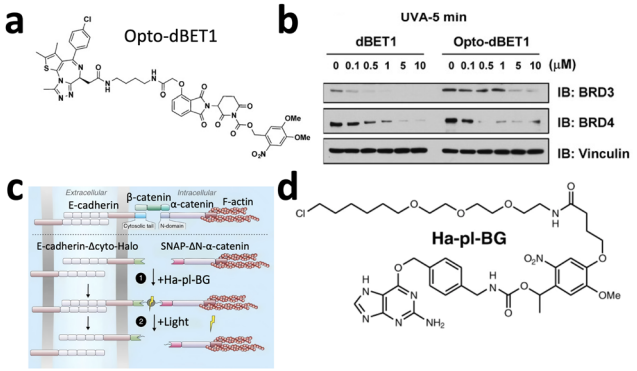

Fig. 2 (a) Chemical structure of opto-dBET1. (b) Western blot analysis of optical-controlled BRD3 and BRD4 degradation (adapted from ref. 116 with permission from © 2020, American Association for the Advancement of Science). (c) Schematic illustration of photocleavable Ha-pl-BG in spatiotemporally controlling the interactions of the E-cadherin-α-catenin heterodimer. (d) Chemical structures of Ha-pl-BG as the photocleavable group dimerizes mediating protein–protein interactions (adapted from ref. 108 with permission from the © 2020, Springer Nature Limited).

optochemical tool by connecting the Halo-tag ligand and SNAP-tag ligand with a photocleavable nitrobenzyl group (Fig. 2).[108] By utilizing this chemical tool, the mechanical coupling between cells can be turned on with prodrug treatment and turned off upon light irradiation. The highly spatiotemporal controllability enabled precise control of adhesion patterns at the irradiated cell–cell interface, which also provided a potential strategy to investigate the influence of cell–cell interactions on the integrity and internal tension of epithelium.

The photocleavable covalent chemical tags can also be employed to control translation. A caliciviral VPg-based translational activator (CaVT) was employed as the RNA binding protein to control the translation of modified nucleoside-containing mRNAs (modRNAs). The CaVT is a fusion protein constructed by the dlFG mutant of a bacteriophage MS2 coat protein (MS2CP) and a feline caliciviral VPg protein (VPg(FCV)). The MS2CP unit binds to the binding motif of target RNA, while the VPg(FCV) functions as a substitute of 50 cap of mRNA. The complete CaVT protein enables the translation of modRNA without canonical 50 cap. To achieve photoresponsiveness, the MS2CP and VPg(FCV) units were split and fused with eDHFR and HaloTag, respectively.[117] The HaloTag ligand and TMP ligand were connected through the linker and caged with a nitrobenzyl group. Upon light irradiation, the protein ligands were activated after the cleavage of the nitrobenzyl group, mediating the interaction between HaloTag-MS2CP and eDHFR-VPg(FCV), which initiated the CaVT-mediated modRNA translation.

Usually, the above-mentioned light-controlled prodrugs are further encapsulated into nanocarriers or self-assembled with stabilizers to form photoresponsive nanovehicles, allowing higher specificity for cancer treatment. Zhao *et al.* introduced 7-dioctylamino-coumarin-4-ylmethyl to Cb and encapsulated prodrugs into a yolk–shell UCNP structure coated with mesoporous silica to achieve light-triggered Cb activation for cancer therapy.[118] Instead of utilizing a two-photon excitation and upconversion strategy, longer wavelength excitation can be also achieved by a one-photon upconversion-like strategy or directly introducing a long-wavelength responsive PPG like BODIPY family.[119] Lv *et al.* modified Cb with a BODIPY group and loaded prodrugs into the hydrophobic core of PLA–PEG polymeric micelles together with PtTPBP. Light-controlled release of Cb could be achieved under red light irradiation through the TTET process.[120] Other PPG-photosensitizer pairs, such as perylen-3-ylmethyl and PdTPBP can likewise realize red light-responsive cleavage *via* TTET.[121]

Furthermore, caged prodrugs have been extensively investigated to develop carrier-free nanovehicles considering their hydrophobicity. Cyanine dyes were usually incorporated to stabilize the nanoparticles and achieve different biological functions. For example, our lab developed a nanosystem self-assembled from the BODIPY-chlorambucil prodrug and NIR dye IR783, contributing to a high prodrug loading capacity (~99%) and efficient light-triggered activation of the prodrug.[122] The IR783 dye, which was integrated into the nanoparticles, not only provided stability to the nanoparticles and enhanced tumor targeting but also served as a real-time tracker of nanoparticle disintegration upon light irradiation.

Since cyanine dyes are responsive to light and capable of executing photothermal functions, dual-wavelength light-controlled systems can be developed to enhance anti-tumor efficacy. For example, a self-assembled nanoplatform comprising a BODIPY-caged γ-secretase inhibitor MK-0752 and indocyanine green was constructed.[123] Irradiation with 656 nm light efficiently cleaves the prodrug, blocking the Notch pathway to inhibit cancer stemness. Subsequent exposure to 808 nm light triggers ICG-derived hyperthermia, enabling photothermal therapy (PTT). The inhibition of cancer stemness significantly enhances tumor sensitivity to PTT. Therefore, the sequential light-triggered system provided precise spatiotemporal control to maximize anti-tumor efficacy. Additionally, the photoresponsiveness of cyanine dyes allows them to directly serve as photocleavable scaffolds. For example, vascular-disrupting agents, such as combretastatin A-4, were conjugated with the photoresponsive IR820 to form prodrugs, which self-assembled into nanoparticles with the VEGF-R inhibitor sorafenib.[124] Upon 690 nm light irradiation, IR820 is cleaved to release both combretastatin A-4 and sorafenib, enabling combination therapy for choroidal neovascularization.

Through a photocleavable small molecule approach, drug activity can be precisely manipulated through the light-controlled caging and photocleavage process, enabling higher selectivity for the treatment of various diseases, including cancer and infective diseases. By coupling with fusion protein engineering technology, this strategy also allows spatiotemporal control of protein functions at the subcellular level for basic biomedical research.

5.1.3 Photoswitchable small molecules. Although photocleavage approaches display strong potential to enhance clinical treatment specificity and provide research tools for mechanistic

investigations with various PPGs available, a single-PPG-caged system will only allow irreversible activation of prodrugs. The persistent activation of prodrugs may lead to unwanted effects and could be unfavorable for investigating intracellular dynamic processes. Therefore, photoswitchable moieties, such as azobenzene moieties, were widely applied to realize reversible control of biological activities.[24,125] For example, a photoswitchable paclitaxel-based approach was developed to stabilize the microtubule through optical control.[126] The benzoyl group at the side chain was replaced with the azobenzamide moiety, enabling temporally reversible inhibition of microtubule polymerisation, at the single cell level or subcellular regions within individual neurites.

In addition, photoswitchable PROTACs were also developed to turn on and off the targeted protein degradation function in a timely manner, avoiding long-term unwanted effects.[127,128] Pfaff *et al.* designed a photoswitchable PROTAC by replacing the conventional PEG linker with a photoswitchable *ortho*-F4-azobenzene linker to reversibly control the topological distance between both ligands (Fig. 3).[128] With prodrug treatment, the azo-*cis*-isomer is inactive to mediate the complex formation and protein degradation. Upon 415 nm light exposure, it changed into an azo-*trans*-isomer, engaging both protein partners to form a ternary complex for protein degradation. The azo-*trans*-isomer converted back to the azo-*cis*-isomer and became inactive upon exposure to 530 nm light. Importantly, due to the bistable structure of the *ortho*-F4-azobenzene linker in this molecule, the photostationary state of this photoswitchable PROTAC is durable, with no need for continuous irradiation.

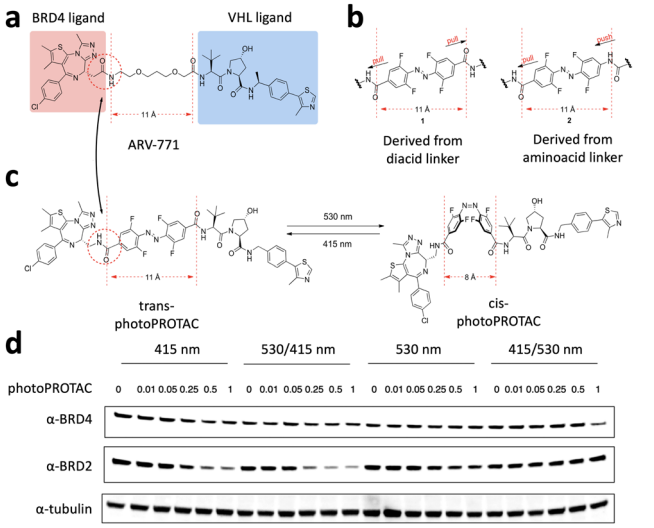

Fig. 3 (a) The molecular structure of PROTAC and ARV-771 is depicted, showing a maximal distance of 11 Å between the dual warhead components. (b) A conceptual diagram presents the "pull–pull" and "push–pull" mechanisms of action with the incorporation of an *o*-F4 azobenzene group. (c) Schematic illustration of photoisomerizing BRD-targeting photoPROTAC, showing different distances between the two moieties under light irradiation. (d) Western blot analysis showing photoPROTAC activation for BRD2 degradation in response to 530 nm and 415 nm light reversibly and dynamically (adapted from ref. 128 with permission from the © 2019, American Chemistry Society).

Similarly, in another example of photoswitchable PROTAC, different-wavelength light showed different BRD4 and BRD2 degradation efficiency, indicating the ability to reversibly control targeted proteins.[127]

The photoswitchable azobenzene group is not only widely exploited in cancer treatment, but is also highly applicable in neuroscience research, allowing spatiotemporal and reversible control of neurotransmission.[129,130] For instance, the axon initial segment (AIS) is where the generation of action potentials primarily occurs in many neurons. However, it has been challenging to distinguish the contributions of voltage-gated ion channels in the AIS from those in the soma and dendrites. A photoswitchable acrylamide azobenzene quaternary ammonium (AAQ) was designed to investigate the role of the hyperpolarization and cyclic nucleotide-gated (HCN) channel.[131] When exposed to 488 nm light, AAQ changes to its *cis* configuration, which unblocks the HCN channels. Then it spontaneously reverts back to its *trans* configuration in a dark environment, blocking those functions again. By this precisely controlled "on and off" function of the channels, Ko *et al.* found that spiking was more likely to occur when HCN channels were blocked in the AIS but not in the soma or dendrites.

The function and applicability of AAQ were further verified in other ionotropic glutamate receptors in rat brain neurons. When applied extracellularly in the absence of light, AAQ rapidly and reversibly inhibited *N*-methyl-D-aspartate (NMDA) receptor-mediated currents with an IC50 value of 10 μM. Upon light-induced transformation into the *cis* form, the IC50 values increased to 30 μM, indicating a profoundly decreased ability to block the NMDA receptors (Fig. 4).[132] Interestingly, the activity of AAQ was found to be highly dependent on pH values of the environment.

Besides direct drug–protein interactions, the photoisomerization approach is also designed to modulate the supramolecular interactions, such as self-assembly with α-cyclodextrin to regulate biological effects with a higher "on–off" ratio. Fu *et al.* developed a supramolecular photo-responsive antibiotic strategy, *trans*-Azo-Nor, by conjugating an azobenzene group to a broad-spectrum antibiotic, norfloxacin (Fig. 5).[133] Then, α cyclodextrin (αCD) was introduced into the system. Under dark conditions, the *trans*-Azo-Nor self-assembled with αCD through host–guest

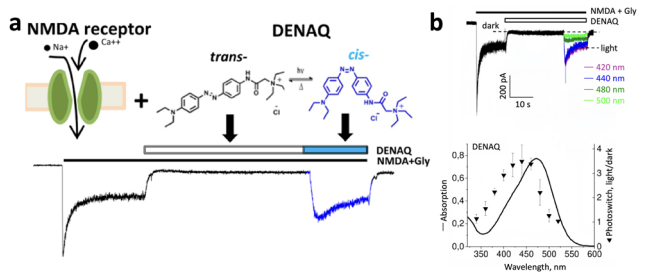

Fig. 4 (a) Schematic illustration of azobenzene-based quaternary ammonium compounds for optical control of ion channels to regulate neuronal excitability. (b) Light-controlled inhibition of NMDA receptor-mediated currents by DENAQ (adapted from ref. 132 with permission from the © 2021, American Chemistry Society).

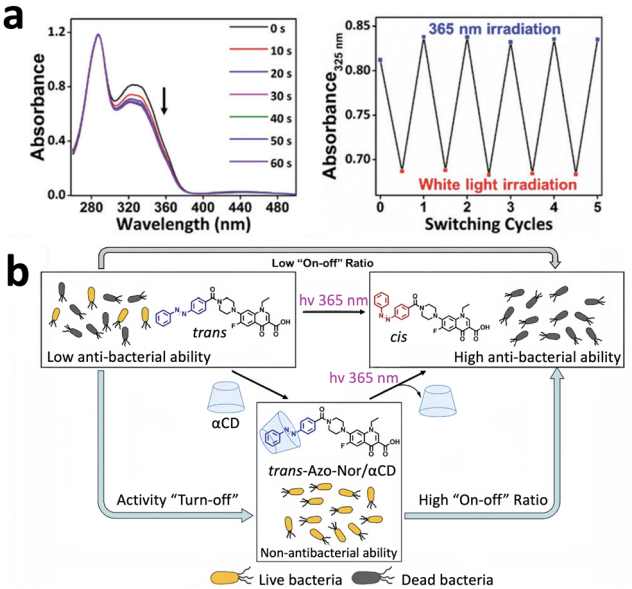

Fig. 5 (a) UV-Vis characterization of Azo-Nor upon 365 nm light and photoswitch cycles of Azo-Nor by light irradiation between 365 nm and white light alternatively. (b) Schematic illustration of the supramolecular photo-responsive antibiotic for antibacterial treatment (adapted from ref. 133 with permission from the © 2019 The Royal Society of Chemistry).

interactions, which significantly blocked the activity of norfloxacin. Under irradiation of 365 nm light, *trans*-Azo-Nor underwent a conformation change from *trans* to *cis*, leading to disassembly of *cis*-Azo-Nor and αCD because of the unmatched size of the *cis* form. The reversible disassembly process exhibited a high "on–off" ratio to control antibacterial activity in a timely manner, harboring great potential to overcome antibiotic-induced bacterial resistance.

The above-mentioned photoisomerization strategy realizes reversible control of small molecules not only for the treatment of cancers and bacterial resistance but also for basic neuroscience research. Yet, primarily based on the azobenzene photoswitch, it is highly desirable to further investigate long-wavelength photoswitches for broad basic and clinical implementation.

5.2 Optochemical control of macromolecules

Optical control of small molecules requires the introduction of prodrugs from extracellular space, which are usually unnatural components in comparison to intracellular macromolecules such as proteins and nucleotides. In the past few decades, light-controlled macromolecules have been designed to undergo conformational changes or exhibit specific functionalities in response to light stimuli, allowing researchers to finely tune and manipulate molecular behavior without introducing synthetic organic molecules. By exploiting the unique properties of light, such as wavelength, intensity, and polarization, these macromolecules enable precise spatiotemporal control over biological processes.

Light-triggered macromolecules encompass a diverse range of molecular structures, including photochromic proteins, light-activated nucleotides, and photoresponsive polymers. These macromolecules are engineered to possess specific photoresponsive units or chromophores that undergo irreversible or reversible structural or conformational changes upon exposure to light. The design and synthesis of these macromolecules involve careful consideration of the desired functionality, compatibility with biological systems, and optimization of the photophysical properties.

5.2.1 Optochemical control of proteins. Optical control of protein inhibitors or related PROTACs offers powerful approaches to realize loss-of-function control of protein activity. However, the gain-of-function control methods are much less investigated. In recent years, researchers developed a genetically encoded photocaged strategy to introduce light-responsive moieties and cage the key residues of targeted proteins to block the protein function, which can be recovered by light irradiation.[134,135] To understand the function and biological effects of O-linked *N*-acetylglucosamine as a prevalent protein modification process, He *et al.* designed a light-controlled system to control the activity of O-GlcNAc transferase (OGT).[134] The catalytically essential K842 of OGT was replaced with a light-responsive, nitrobenzene-based lysine analog, allowing light-triggered OGT activation. A broad-spectrum protein glycosylation was induced upon 365 nm light irradiation using LC-MS detection.

The genetically encoded photocage strategy was not only employed to modify lysine residues with photocleavable groups but was also widely exploited to manipulate other amino acids, including tyrosine,[134,136,137] cysteine,[138,139] and serine.[140] Interestingly, Ling *et al.* firstly developed a photocleavable protein with glutamate modification. To realize this point, the authors constructed an *Escherichia coli* LeuRS (EcLeuRS) mutant library to identify the applicable EcLeuRS/tRNA pair for genetical incorporation of photocleavable glutamate (Fig. 6).[141] Using a secreted alkaline phosphatase and a protease HRV3C as the models, the authors demonstrated that the proteins with modified glutamate displayed recovered activity upon light irradiation. As a critical addition to the photocleavable non-canonical amino-acid toolbox, this approach provides a general strategy for optical control of protein activity based on photocleavable glutamate.

Based on the genetically encoded photocaged approach, a technology known as subcellular-specific uncaging-assisted biotinylation and mapping of phosphoproteome (SubMAPP) has been established to track the phosphorylation level within living cells and animals in a spatiotemporal manner.[142] The K182 residue of TurboID, an efficient biotin ligase, was replaced with a photocleavable lysine analog. Light irradiation triggered the activation of TurboID, which mediated protein biotinylation. Subsequently, the orthogonal pull-down process generated digested phosphopeptides, which can be analyzed by quantitative mass spectrometry. Therefore, this multistep technology allowed investigation of phosphoproteome at the subcellular level with high spatial–temporal resolution.

The interactions between proteins and nucleotides can also be precisely controlled with localized light irradiation, realizing spatiotemporal manipulation of related biological functions,

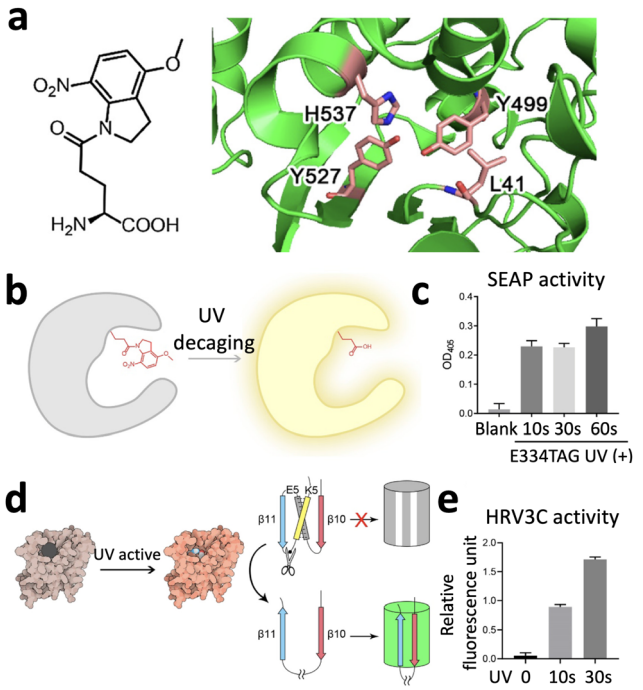

Fig. 6 (a) Chemical structure of photocaged glutamate and crystal structure of *E. coli* LeuRS (PDB code: 4cqn). (b) Scheme illustration of a light-controlled strategy for SEAP activation upon the photo-cleavage of MNI-Glu. (c) SEAP activity measurement in cells incubated with pNPP substrate after light irradiation. (d) Scheme representing the Flip-GFP reporter system to monitor the restored HRV3C activity after photo-triggered MNI-Glu activation. (e) HRV3C activity after different light irradiation times (adapted from ref. 141 with permission from the © 2023, Chinese Chemical Society).

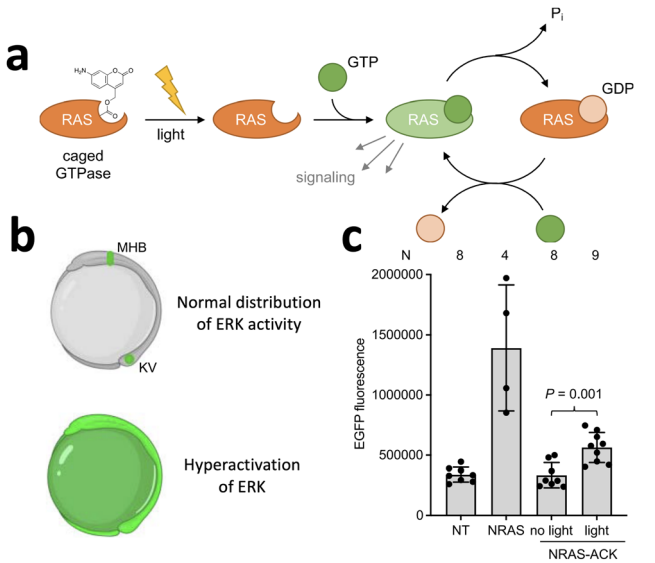

Fig. 7 (a) Schematic illustration of the photocaged GTPase offering spatiotemporal control over activation of the NRAS signaling pathway and related embryo development. (b) Schematic illustration of EGFP intensity and distribution in tg(dusp6:egfp) at the bud stage (10 hpf) as an indicator of ERK activity. (c) Light-controlled EGFP intensity as a marker of ERK activity (adapted from ref. 144 with permission from the © 2023, American Chemical Society).

for instance, embryo development. Embryo development involves a series of tightly regulated cell signaling molecules, including the conformational changes of GTPases driven by nucleotides as cofactors. In these GTPases, lysine residues in the nucleotide-binding pockets are reported to play critical roles in the nucleotide–protein interactions.[143] By utilizing the genetic code expansion method, a new photocaged lysine unnatural amino acid (UAA) was developed in both mammalian cells and zebrafish. By replacing the lysine with DEACM-conjugated lysine at specific binding sites within the protein kinase A (PKA) and NRAS proteins, control over their activity can be achieved (Fig. 7).[144] Interestingly, in the zebrafish embryo model, the photocaged NRAS protein was employed to investigate the effect of NRAS activation on heart defects. Light irradiation was found to trigger photocleavage of the caged-NRAS protein, resulting in the failure of the looping effect and leading to heart defects, which suggested the indispensable role of activated NRAS in establishing a spatial context for heart development.

The residues of peptides can also be directly caged with photocleavable moieties, using a solid phase peptide synthesis procedure.[145] Montnach *et al.* introduced a Nvoc photocaged HwTxIV peptide that can be cleaved by UV light and activated, specifically targeting voltage-gated sodium (NaV) channels.[146] The molecular docking analysis implied that the caging group would introduce van der Waals steric clashes between the peptide and important amino acids of the NaV channel significantly, reducing the peptide affinity. The researchers validated the efficacy of HwTxIV-Nvoc in various experimental settings, including *in vitro* studies using HEK293 cells, *ex vivo* experiments with brain slices, and *in vivo* investigations involving mice neuromuscular junctions. Furthermore, the researchers expanded the scope of this toxin-photoactivation technology by developing variable photoactivatable peptides, showcasing its broad applicability in various contexts.

In summary, the genetically encoded photocage strategy allows direct photocleavage modification of key residues on target proteins, which does not require introduction of exogenous molecules. Through light-triggered exposure of the key residues, we are able to further investigate the gain-of-function effect of target proteins, as a promising tool for a deeper understanding of intracellular signaling pathways.

5.2.2 Optochemical control of nucleic acids. As another type of biomacromolecules, nucleic acid serves as an essential mediator in various biological effects, including protein translation, energy transfer, signal transduction, immune response, *etc.*[147,148] Many nucleic acid-based processes are dynamic in nature, involving rapid changes and complex interactions. Spatiotemporal control enables researchers to study these dynamic processes in real time. This information is crucial for understanding how nucleic acids contribute to cellular functions and for developing targeted interventions.[149] Due to the easily modified hydroxyl group and amino group of the nucleic acid, which are often essential for protein binding, photocaged or photoswitchable nucleic acid can be developed for precise control or related biological functions.

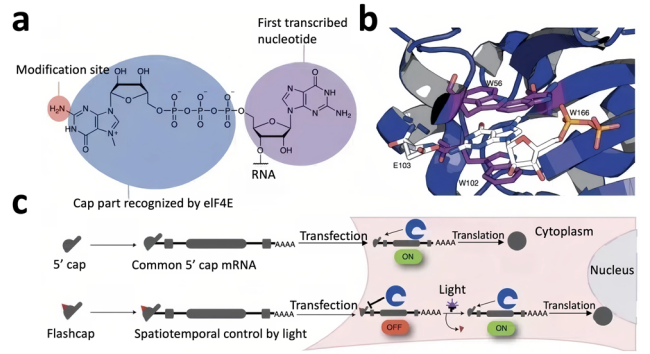

Fig. 8 (a) Eukaryotic mRNA with modification sites at the cap part recognized by eIF4E. (b) Molecular interactions of eIF4E with the cap recognition part of mRNA. (c) Schematic illustration of FlashCaps, utilizing a photoremovable group at the 5′ cap to control protein translation through light irradiation (adapted from ref. 150 with permission from the © 2022, Springer Nature Limited).

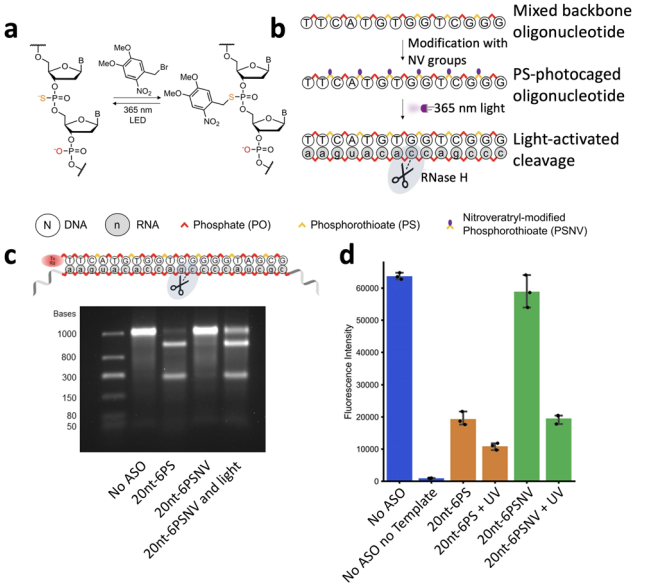

Fig. 9 (a) Chemical structure of nitrobenzyl modification in a mixed backbone oligonucleotide, which is photocleavable upon UV irradiation. (b) Caging of a mixed backbone antisense oligonucleotide to block RNase H activity, which can be activated through UV irradiation to mediate target mRNA degradation. (c) Agarose gel indicating light-controlled activation of RNase H and degradation of target mVenus mRNA. (d) Light-controlled cell-free protein synthesis of mVenus (adapted from ref. 151 with permission from the © 2023, Springer Nature Limited).

The translation of mRNA is a crucial process in gene expression, and the regulation of translation is vital for controlling protein synthesis within cells. One of the key features of eukaryotic mRNAs is the presence of a 5′ cap, which interacts with the eukaryotic translation initiation factor eIF4E and plays a crucial role in initiating translation. Klöcker *et al.* synthesized nitrobenzyl group-conjugated N7-methylated guanosine, which was linked to first transcribed nucleotide *via* a 5′-5′ triphosphate bridge, called FlashCap (Fig. 8).[150] Through *in vitro* transcription technology, a photocleavable mRNA was developed, which cannot bind to eIF4E and was resistant to cleavage by decapping enzymes. The presence of a single photocaging group in the FlashCap-mRNA prevents translation both *in vitro* and in mammalian cells, without causing an increase in immunogenicity. However, upon irradiation with light, the native cap structure is restored, leading to the efficient initiation of translation. The FlashCaps allowed precise control over the expression of a specific mRNA, with potential applications in the field of mRNA therapeutics, enabling the dosing of mRNA-based treatments with spatio-temporal precision.

Besides controlling the protein translation process, RNA degradation can also be controlled to regulate expression. A simple, one-step technique to photocage the backbone of antisense oligonucleotides at specific sites was developed (Fig. 9).[151] A commercially available halogenated photocage-precursor, 2-nitroveratryl bromide, was utilized to react with the phosphorothioate backbone. After modification, the photocages surrounding the backbone significantly diminished the ability of the antisense oligonucleotides to form a duplex. Without light irradiation, the inhibited hybridization ability and steric hindrance on the oligonucleotides dramatically blocked RNase H-mediated cutting of the targeted mRNA. Upon light irradiation, the photoremovable groups were cleaved, resulting in activation of antisense oligonucleotides and realizing cell-free knockdown with a highly spatiotemporal pattern.

Aptamers are short sequences of artificial nucleotides that are able to recognize target proteins, allowing versatile design of a light-controlled system to regulate the protein location, without influencing the natural structure and expression level. A nanoplatform modified with aptamer targeting RelA and a double-strand DNA hybrid on the surface was employed (Fig. 10).[152] One strand of the DNA hybrid (cDNA) was partially complementary to the aptamer sequence, while the other strand contained UV light-photocleavable linkers and acted as a blocking probe (bDNA) for the cDNA. Due to its stronger hybridization stability with intact bDNA, the cDNA strand has a negligible influence on the molecular recognition capability of the aptamer. After cellular uptake of the nanoplatform, the aptamer specifically captured the target RelA protein, causing it to assemble around the nanoparticles. The formation of these high-order protein clusters around the nanostructure effectively

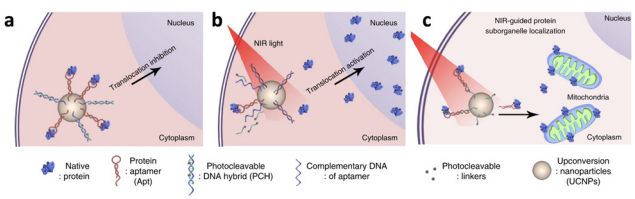

Fig. 10 (a) In a dark environment, nanoparticles functionalized with DNA hybrids and aptamers can capture target proteins and block the translocation. (b) Upon light irradiation, DNA hybrids were cleaved, exposing cDNA to compete aptamers and activate protein translocation. (c) Upon light irradiation, DNA hybrids were cleaved, exposing cDNA to compete aptamers to trigger P53 translocation to mitochondria (adapted from ref. 152 with permission from the © 2020, Springer Nature Limited).

trapped proteins and inhibited their function, thereby robustly inhibiting subcellular trafficking of RelA. Light irradiation cleaved the linker and released cDNA to compete with the aptamer for binding to RelA. As a result, the captured RelA protein was released, allowing it to restore its natural activity and transfer into the nucleus for regulating biological functions.

Multiple light-controlled biosensors can also be designed based on the aptamer structure, for example, to enhance the accuracy of HER2 detection. Based on the idea, liquid chromatography-tandem mass spectrometry (LC-MS/MS) and immunohistochemistry (IHC) were combined, which could potentially improve HER2 mapping and testing accuracy. The probe was composed of four distinct components: an HB5 aptamer for precise targeting of HER2, a fluorescent dye (FITC) for visualizing through fluorescence imaging, and a reporter peptide for quantification by mass spectrometry, connected *via* a photocleavable *o*-nitrobenzyl linker that allows for peptide release upon exposure to light.[153] Based on the interaction between the aptamer and HER2, a fluorescence image is obtained after the peptide-tagged mass probe bound to HER2. Subsequently, light-triggered photolysis was initiated to rapidly release the reporter peptide, which was then quantified using LC-MS/MS. This sequential process allowed for the acquisition of HER2 distribution and levels.

Optical control of nucleotide activity was not only realized by the photocleavage strategy but also by the photoisomerization approach, enabling reversible control of corresponding biological activity. For example, puromycin acts as an analog of aminoacyl tRNA and leads to premature termination of protein synthesis. A series of light-responsive puromycin analogs were developed, including nitrobenzyl-caged, DEACM-caged, or diazocine-conjugated puromycin, to achieve optical control of protein translation.[154–156] For example, the photoswitchable, diazocine-conjugated puromycin was designed, called puroswitch (Fig. 11).[156]

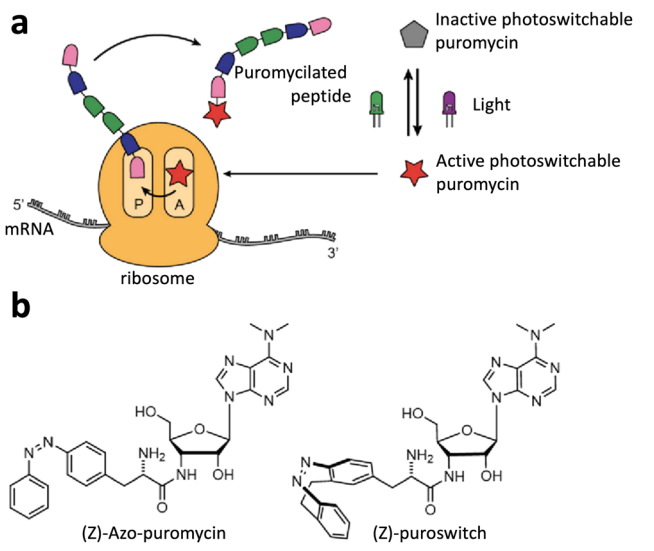

Fig. 11 (a) Schematic illustration of the photoswitchable puromycin analogs for light-controlled protein translation. (b) Chemical structures of photoswitchable puromycin (adapted from ref. 156 with permission from the © 2022, American Chemical Society).

Through a computational docking study, it was found that the *trans*-isomer of the puroswitch was more likely to occupy the binding pocket in the ribosome, resembling the binding site of puromycin. On the other hand, the *cis* isomer of the puroswitch was unable to adequately interact with this binding pocket and mimic the binding of puromycin. This suggested that the conformational change induced by the reversible isomerization of the puroswitch played a crucial role in its ability to interact with the ribosome and interfere with translation. A chromodosing analysis was employed to apply light irradiation with different wavelengths, showing that the EC50 of the puroswitch could be gradually tuned upon light irradiation between 390 and 477 nm.

Unlike photocaging on proteins, the modification of nucleic acids can be much more convenient due to the linear structure and easily modified hydroxyl and amino groups. These photoresponsive nucleic acids enable precise regulation of versatile biological activities, considering different kinds of nucleic acids. However, these photoresponsive nucleic acids are still limited by short-wavelength irradiation.

5.2.3 Optochemical control of polymeric molecules. The photocleavable strategy was not only designed to trigger the functions of biological macromolecules but was also developed to regulate biological functions using synthesized polymers.[157] Drug–polymer conjugations can have a higher "on–off" ratio because of significantly hindered drug-target interactions under dark conditions. For example, a local anesthetic drug tetracaine was attached to the polymer poloxamer 407 *via* a photocleavable coumarin linkage using a click reaction. Through pulsatile light irradiation, real-time light-controlled drug release can be achieved precisely, which was in proportion to the intensity and duration of light irradiation, realizing precisely controlled local anesthesia (Fig. 12).[158]

The polymeric structure was not only employed as the basic structure for light-controlled prodrug construction but also exploited as the functional component for optical control of biological applications, such as the seeding and encapsulation of mammalian cells. Poly(ethylene glycol) diacrylate (PEGDA) was conjugated with nitrobenzyl groups on the two terminals to construct a photodegradable 2D thin film. Localized 365 nm light irradiation induced regional photolysis, resulting in degraded and nondegraded regions with different cross-link densities. The difference in cross-link density induced different volumetric swelling and binding movement, leading to a shape change of the gel. By seeding cells on the gel, 3D cell culture and cell encapsulation can be achieved in a spatiotemporal manner through light irradiation.[159]

The light-responsive drug–polymer conjugation can also be self-assembled to form nanoparticles, which may further protect the prodrug from being degraded, as the drugs are often sheltered in the hydrophobic core of nanoparticles. For example, the chemotherapy drug doxorubicin was conjugated with pegylated biotin through the light-responsive nitrophenyl group. The amphiphilic polymers were able to self-assemble into nanoparticles. As a result, the activity of doxorubicin was profoundly blocked. Upon localized 365 nm light irradiation, the nitrophenyl group was cleaved to release active doxorubicin, which

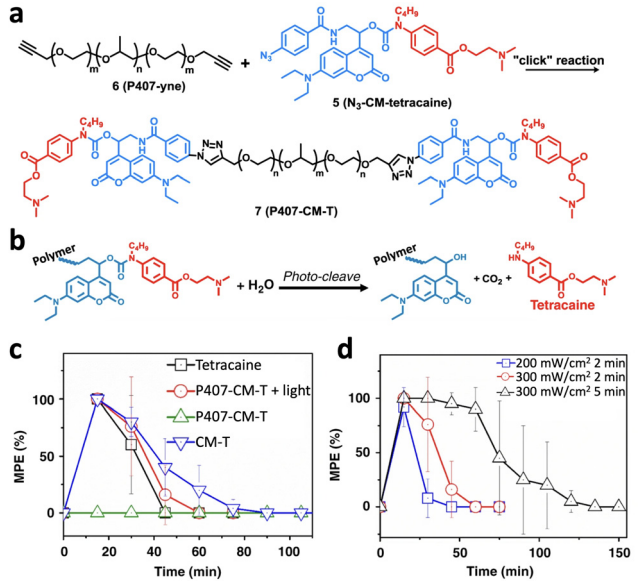

Fig. 12 (a) Synthesis of photocleavable polymer–drug conjugation, P407-CM-T, through a click reaction. (b) Photo-cleavage reaction of P407-CM-T to generate an anesthesia drug, tetracaine. (c) Time courses of nerve block after injection of polymeric prodrugs with or without light irradiation immediately after injection. (d) Nerve block after injection of prodrugs with irradiation at various irradiances and durations (adapted from ref. 158 with permission from the © 2020, Springer Nature Limited).

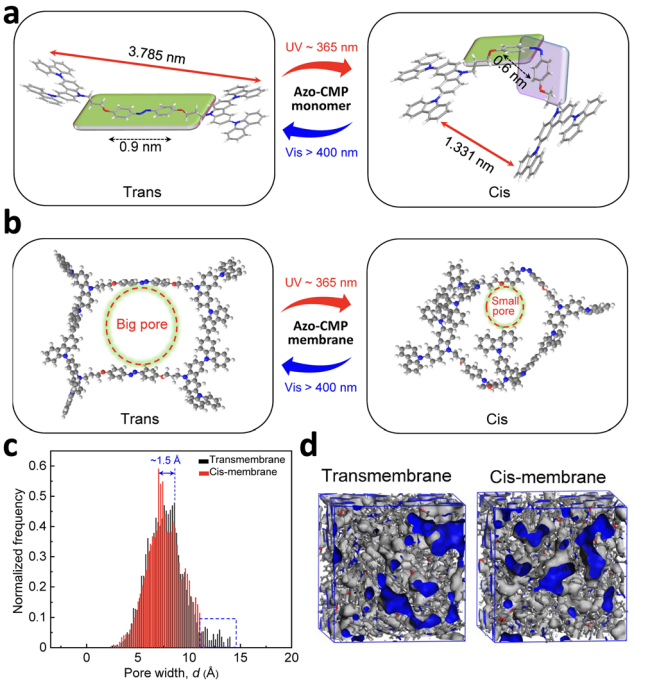

Fig. 13 (a) Schematic illustration of a "bottom-up" approach for the construction of an artificial light-gated ion channel membrane. (b) The elementary pore structure of the azo-CMP membrane under different light irradiation. (c) Simulation results of pore-size distribution of the membrane in *trans* and *cis* states. (d) 3D view of the membrane (with free volume in gray and the Connolly surface in blue) in *trans* and *cis* states (adapted from ref. 161 with permission from the © 2022 American Association for the Advancement of Science).

significantly enhanced the tumor-targeting ability and reduced adverse effects in normal tissues.[160]

The function of polymeric materials can also be reversibly controlled under light irradiation using the photoisomerization approach. Inspired by the light-gated ion channels found in cell membranes, which play crucial roles in various biological processes, Zhou *et al.* developed an artificial light-gated ion channel membrane using conjugated microporous polymers. By designing an azobenzene-containing monomer which was homo coupled to each other *via* a continuous electrochemical oxidation–reduction reaction, structurally well-defined elementary micropores can be formed (Fig. 13).[161] Through the light-responsive switching of the azobenzene moiety, precise control of the pore size and thickness of the membrane at the molecular level can be achieved. The polymer chain's ability to undergo photoisomerization facilitated the reversible manipulation of pore dimensions, thereby enabling ion transport across the membrane that could be regulated by light. This light-gated mechanism was effective for a variety of ions, such as hydrogen, potassium, sodium, lithium, calcium, magnesium, and aluminum.

5.3 Long-wavelength photopharmacology for *in vivo* application

The above-mentioned examples of optochemically controlled molecules are mainly based on UV-visible light (mainly 365–530 nm), enabling spatiotemporal control of biological activities *in vitro* or in a zebrafish model. Further validation of these approaches in advanced biological systems and clinical applications requires long-wavelength optochemical tools for deep penetration depth. In recent years, BODIPY-based PPGs with a red-shifted absorption band have been established. The π-system can be extended by adding styryl groups to the BODIPY backbone. Quantum yield was increased by replacing fluorine atoms with methyl groups on the boron. Hence, efficient photolysis can be achieved at 650 nm, achieving light-controlled dopamine release and contract rhythm of human cardiomyocytes (Fig. 14).[36] In another example, a NIR Cy7-PPG was designed by transforming Cy7 with suitable molecular orbital configurations. To the best of our knowledge, this Cy7-PPG currently stands as the most redshifted PPG (λ_{max} = 746 nm) (Fig. 14).[162] Although much effort has been made for the development of novel PPGs with long-wavelength excitation, *in vivo* applications are hardly reported, due to the high molecular weight, low water solubility, poor biodistribution, and biocompatibility of PPGs.[162] It is necessary to further modify the chemical structure of PPGs to improve water solubility and biodistribution or develop novel drug delivery systems for prodrug incorporation.

6. Optochemical control of drug delivery systems (photoresponsive drug delivery)

In Section 5.1.2, we discussed how prodrugs based on PPGs can be encapsulated into nanoparticles to improve pharmacokinetics

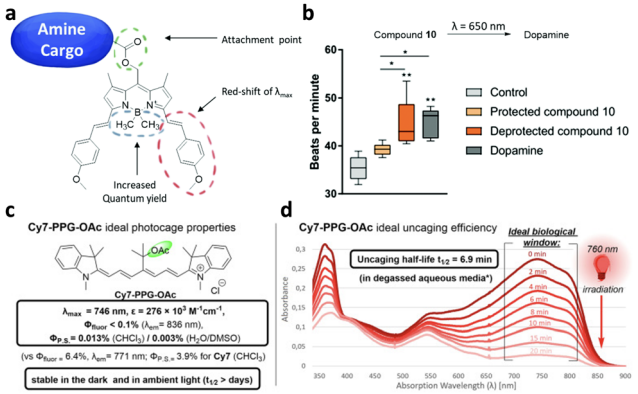

Fig. 14 (a) Chemical structure of a 650 nm light-responsive BODIPY prodrug for heart rhythm control. (b) CiPA analysis of beating frequency of cardiomyocytes treated with indicated prodrugs with or without light irradiation (adapted from ref. 36 with permission from the © 2020 The Royal Society of Chemistry). (c) Chemical structure and photolysis characteristics of Cy7-PPG-OAc. (d) Absorption change of Cy7-PPG-OAc upon 760 nm light irradiation (adapted from ref. 162 with permission from the © 2022 Wiley-VCH GmbH).

and enable targeted drug delivery. This is the first bond between photopharmacology and photoresponsive drug delivery. Besides, there are three main modalities applied in constructing PDDSs based on photocleavage, photoisomerization, and light-induced generation of ROS or heat, separately (Scheme 6).

Apart from being directly conjugated with drug molecules that are exploited in photopharmacology, PPGs and photoswitches can be inserted into the backbone or building block of drug delivery systems as well. Upon light irradiation, PPGs can be removed or photoswitches can transform, leading to instability of the backbone, dissociation of nanocarriers, and release of encapsulated drug molecules as a result. For light-induced generation of ROS and heat-based PDDSs, photosensitizers which can transfer light energy to ROS or heat are usually incorporated. The building block of such PDDSs is sensitive to ROS or heat. Therefore, light can indirectly induce the dissociation of nanocarriers *via* energy transfer of photosensitizers.

6.1 Photoresponsive drug delivery systems based on photocleavage

Photocleavage-based drug release commonly employs photo protecting groups (PPGs, also called photocages) to control the activity of photoresponsive nanocarriers. The PPGs are covalently linked with nanocarriers or drug molecules and are removed upon light irradiation, leading to the disintegration of the nanocarriers and the release of encapsulated cargos. Besides, the discussion will also cover metal-based anticancer prodrugs that undergo both photocleavage and photocatalysis to construct PDDSs. Current examples are summarized in Table 2.

6.1.1 Nanocarriers modified with PPGs. The most widely used strategy was to insert PPGs into the structure of building blocks, which can self-assemble into nanoparticles. Upon light irradiation, the removal of PPGs will lead to unstable transformation of nanoparticles due to the change of interaction forces driven for self-assembly.

To the best of our knowledge, the first photoresponsive polymeric micelle was reported by Jiang *et al.*, based on the light-induced disturbance of the balance between hydrophilicity and hydrophobicity (Fig. 15).[163] PPGs, pyrenylmethyl groups, were conjugated on the side chain of block copolymers poly(ethylene oxide) (PEO) and polymethacrylate (PMA), resulting in the formation of an amphiphilic polymer, which can self-assemble into micelles and then loaded hydrophobic mock drug molecules Nile red. UV light illumination cleaved the PPGs, exposing the hydrophilic PMA moiety, which significantly disrupted the amphiphilicity and facilitated micellar dissociation for cargo release. Based on a similar mechanism,

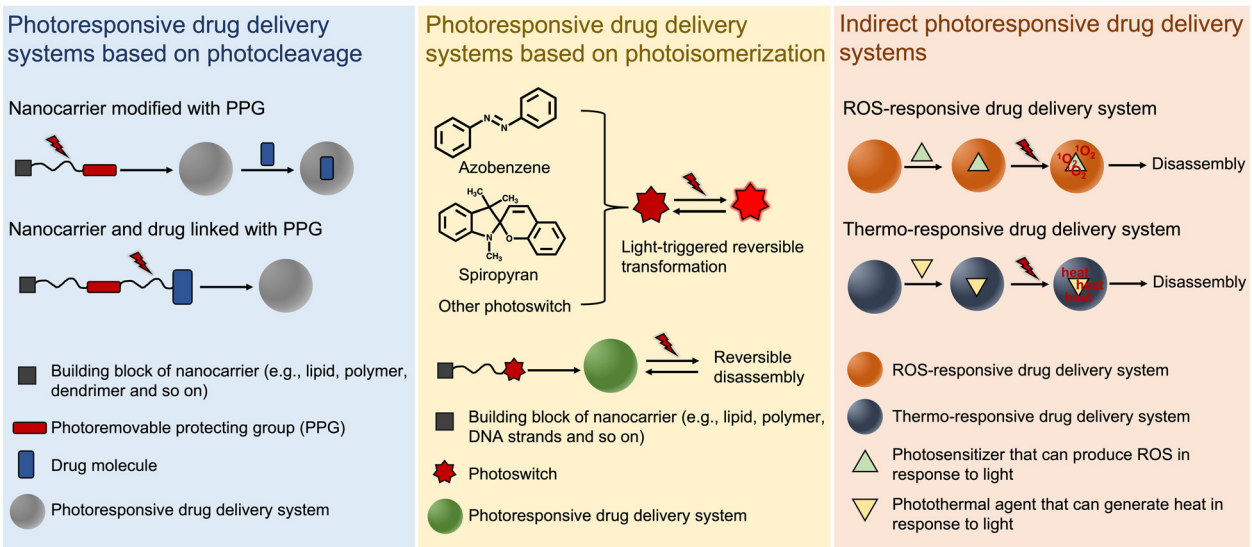

Scheme 6 Schematic illustration of three modalities applied in constructing photoresponsive drug delivery systems.

Table 2 A table summarizing strategies for photoresponsive drug delivery systems based on photocleavage that are mentioned in the review. DMNC, 4,5-dimethoxy-2-nitrobenzyl chloroformate; ONB, 5-hydroxy-2-nitro-benzyl methacrylate; UCNPs, upconversion nanoparticle; DOX, doxorubicin; DMNB, 2,3-dimethyl-2,3-dinitrobutane; and MSNs, mesoporous silica nanoparticles

Types	PPGs	Drug vehicles	Light	Drugs/dyes	Ref.
Nanocarriers modified with PPGs	Pyrenylmethyl	Polymeric micelles	365 nm	Nile red	163
	DMNC	Polymeric micelles	365 nm	Retinoic acid	164
	2-Nitrobenzyl	Polymeric micelles	410 nm	NO and formaldehyde	165
	ONB	Polymeric nanoparticles	365 nm	Nintedanib	166
	4-(Hydroxymethyl)-3-nitrobenzoic acid	Silica-coated UCNPs	980 nm (upconversion)	Intracellular icariin	167
	ONB	Silica-coated UCNPs	980 nm (upconversion)	DOX	168
	2-Nitrobenzyl	Polymeric nanoparticles	980 nm (upconversion)	Fluorescein	169
	2-Nitrobenzyl	Polymeric nanoparticles	980 nm (upconversion)	siRNA	170
	DEACM	PAMAM dendrimers	420 nm	Protein	171
	DEACM	PAMAM dendrimers	420 nm	Chloroquine	172
	BODIPY	PAMAM dendrimers	520 nm	Chlorin e6 and inhibitor of FSP1	173
	BODIPY	PAMAM dendrimers	656 nm	LY-411, 575 and paclitaxel	174
	Cobalamin derivative	Red blood cells	525 nm	Protein	175
	Cobalamin derivative	Red blood cells	650 nm	Dexamethasone	176
	Dicyanomethylene-coumarin	Small-molecule based nanoparticles	505 nm	DOX	177
	BODIPY	Small-molecule based nanoparticles	635 nm	PTX	178
Nanocarriers and drugs linked with PPGs	DMNB	PAMAM dendrimers	980 nm (upconversion)	DOX	179
	o-Nitrobenzyl	UCNPs	980 nm (upconversion)	5-Fluorouracil	180
	Perylen-3-ylmethyl	Silica-coated UCNPs	976 nm (upconversion)	Chlorambucil	181
	Ortho-nitrobenzyl	UCNPs	980 nm (upconversion)	DOX	182
	o-Nitrobenzyl	Silica-coated UCNPs	980 nm (upconversion)	siRNA	183
	DEACM	Harmonic nanoparticles	790 nm (upconversion)	Tryptophan	184
	Coumarinyl photocleavable linker	Harmonic nanoparticles	1250 nm (upconversion)	Erlotinib derivative	185
Photoresponsive drug delivery based on photoactivated therapy	Pt^{IV} complex functionalized with pyropheophorbide	Polymeric nanoparticles	808 nm	Pt^{II} and oxaliplatin	186
	Pt^{IV} prodrug	UCNPs	980 nm	Pt^{II}	187
	Pt^{IV} prodrug	UCNPs	980 nm	Pt^{II} and chlorin e6	188
	Pt^{IV} prodrug	Polymeric nanoparticles	530 nm	Pt^{II} and siRNA	189
	Ru^{II} complex	MSNs	465 nm	$[Ru(tpy)(biq)(H_2O)]^{2+}$	190
	Ru^{II} complex	MSNs	Visible light	$[Ru(tpy)(biq)(H_2O)]^{2+}$ and safranin O	191
	Ru^{II} complex	Polymeric micelles	455 nm or 535 nm	$[Ru(tpy)(biq)(H_2O)]^{2+}$	192
	Ru^{II} complex	Polymeric nanoparticles	520 nm	$[Ru(tpy)(biq)(H_2O)]^{2+}$	193
	Ru^{II} complex	Polymeric nanoparticles	656 nm	$[Ru(tpy)(biq)(H_2O)]^{2+}$	194
	Ru^{II} complex	Self-assembled nanoparticles	660 nm	DOX and $[Ru(tpy)(biq)(H_2O)]^{2+}$	195
	Ru^{II} complex	Self-assembled nanoparticles	625 nm	$[Ru(tpy)(biq)(H_2O)]^{2+}$	196
	Ru^{II} complex	Polymeric nanoparticles	760 nm	Tetrahydrocurcumin and $[Ru(tpy)(biq)(H_2O)]^{2+}$	197
	Ru^{II} complex	UCNPs	796 nm	$[Ru(tpy)(biq)(H_2O)]^{2+}$	198

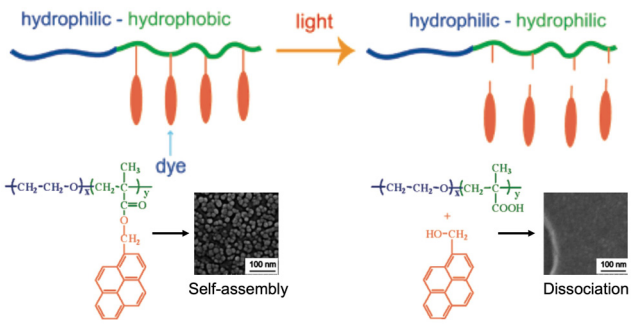

Fig. 15 Chemical structure of the designed amphiphilic diblock copolymer and light-triggered destruction of its hydrophobic and hydrophilic balance, resulting in the dissociation of self-assembled nanoparticles (adapted from ref. 163 with permission from the © 2005 American Chemical Society).

light-sensitive photochrome 4,5-dimethoxy-2-nitrobenzyl chloroformate (DMNC) conjugated with poly(ethyleneimine) was added to dextran sulfate (DS) to form nanoparticles by electrostatic and hydrophobic interactions and then loaded retinoic acid.[164] The disassembly upon UV light irradiation was likely due to the breakage in the nanoparticles' hydrophilic/hydrophobic balance after DMNC photocleavage, which leads to release of retinoic acid and efficient reduction of the clonogenicity of bone marrow cancer cells from patients with acute myeloid leukemia. Parallel design was utilized in polymersomes,[199] tubisomes[200] and nanocapsules[201] for light-triggered dissociation.

Besides treating malignancies, PDDSs based on the above-mentioned strategy were anticipated to be applied in more biomedical applications with longer-wavelength light excitation. In a recent study, nitric oxide (NO) and formaldehyde (FA) were

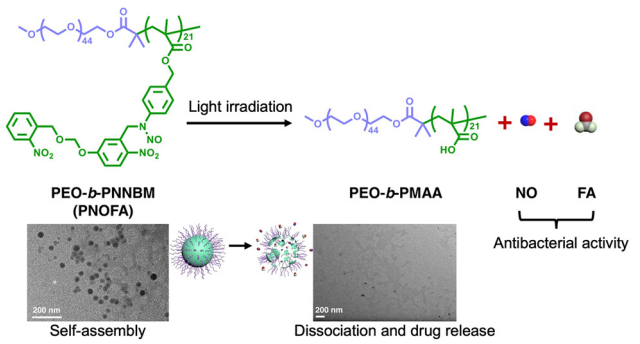

Fig. 16 Schematic illustration of light-triggered dissociation of micelles assembled from PEO-*b*-PNNBM copolymers and subsequent release of NO and FA for antibacterial activity (adapted from ref. 165 with permission from the © 2021 American Chemical Society).

loaded into a polymeric micelle self-assembled by an amphiphilic diblock copolymer of PEO-*b*-PNNBM containing PPG 2-nitrobenzyl(-poly(4-((2-nitro-5-(((2-nitrobenzyl)oxy)methoxy)benzyl)-(nitroso)amino)benzyl methacrylate)) (Fig. 16).[165] Light irradiation can lead to the disassembly of the micellar nanoparticles and release of NO and FA, which exhibit a combinational antibacterial performance against both Gram-positive and Gram-negative bacterial pathogens. The strategy provides a feasible way to develop gaseous signaling molecule-based antibacterial materials by rational molecular engineering. Another study taking advantages of PDDSs to treat retinal diseases like age-related macular degeneration by virtue of transparency of eye tissues was reported.[166] Nintedanib is a small molecular drug for treating choroidal neovascularization *via* suppressing angiogenesis. Nintedanib was loaded into light-responsive nanoparticles based on copolymers employing a 5-hydroxy-2-nitro-benzyl methacrylate (ONB) moiety as a UV-labile photocage. For the rats treated with designed nanovehicles under 365 nm light irradiation, the size of choroidal neovascularization was reduced and vessel growth was inhibited. Injection of PDDSs into intravitreal fluid enabled on-demand delivery of nintedanib to mouse eyes. The design achieved non-invasive and controlled drug delivery to the posterior segment of the eye, which can reduce possibility of repeated intravitreal injections and the risk of infection and retinal detachment, therefore holds great promise in clinical translation by improving patient compliance.

For longer-wavelength excitation, the most-widely exploited strategy is to encapsulate up-conversion nanoparticles (UCNPs) through chemical conjugation or physical absorption.[202–205] *Via* the conversion of lower-energy photons into higher-energy photons by UCNPs, a lot of light-induced processes can be achieved by 980 nm light irradiation.[206] For example, a nanoplatform was fabricated by modifying photocaged linker 4-(hydroxymethyl)-3-nitrobenzoic acid and the PEG linker to the surface of UCNPs coated with mesoporous silica nanoparticles.[167] The cap β-cyclodextrin (β-CD) and targeted peptide were conjugated subsequently and drug molecules intracellular icariin (ICA) were loaded. Upon NIR light irradiation, controlled release of ICA can be realized due to removal of the cap for efficient and precise regulation of osteogenic differentiation of mesenchymal stem cells for osteoporosis therapy. The photocages ONB, as a light crosslinking agent, can be utilized to be coated on UCNPs as well.[168] Together with methacrylic acid, they were coated on UCNPs@SiO_2 *via* distillation precipitation polymerization to synthesize well-distributed nanocomposites. DOX was encapsulated as a model drug for studying drug loading and controlled release behavior under NIR light irradiation.

Another example is constructing a polymer with a positively charged polyelectrolyte and poly(ethylene glycol) (PEG) modified with and 2-nitrobenzyl derivatives on the side chain.[169] The light-responsive polymers can self-assemble with silica-coated UCNPs into nanoparticles *via* electrostatic interaction and then loaded the negatively charged fluorescein as a model molecule. NIR light irradiation could induce dissociation of nanoparticles and promote drug release. Distinct from previous examples, the disintegration was proved to be the disruption of the electrostatic equilibrium due to the removal of positively charged moieties and formation of the negatively charged carboxyl groups.

Apart from loading small molecules, the PDDSs, which are self-assembled driven by electrostatic interactions, are able to load biomacromolecules. *Via* quaternary ammoniation of photodegradable 2-nitrobenzyl-2-bromoacetate on a *N*-functionalized polyfluorene brush, a cationic conjugated polyelectrolyte brush (CCPEB) was synthesized (Fig. 17).[170] The obtained CCPEB subsequently self-assembled with UCNPs into nanoparticles and then loaded photosensitizers and siRNA by virtue of abundant positive charges in CCPEB. Under 980 nm light irradiation, UCNP@CCPEB exhibited efficient single oxygen production for photodynamic therapy (PDT) and siRNA release. The strategy can be applied for other biomacromolecules such as DNA,[207] and proteins[208] as well.

Furthermore, longer-wavelength depolymerization can also be achieved by introducing DEACM into the main chain of poly(ester amide) through two-photon excitation,[209] utilizing PPGs with long-wavelength absorption like BODIPY into the

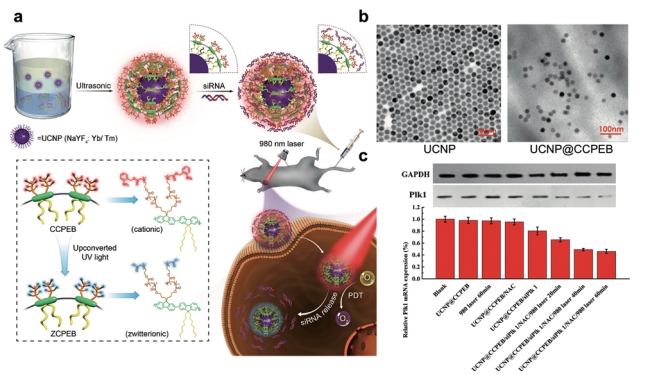

Fig. 17 (a) Schematic illustration depicting the preparation of light-responsive drug delivery system UCNP@CCPEB and its combined PDT and siRNA therapy. (b) TEM images of UCNP and UCNP@CCPEB. (c) Light-triggered Plk1 gene silencing and resulting downregulated expression of siRNA targeting protein (adapted from ref. 170 with permission from the © 2017 Wiley-VCH Verlag GmbH & Co. KGaA, Weinheim).

junction of PEG and polystyrene blocks,[210] and exploiting a one-photon upconversion-like photolysis strategy.[211]

For example, a DEACM-modified poly(amidoamine) (PAMAM) dendrimer was fabricated to form nanocomplexes with proteins through physical adsorption or small molecules through hydrophobic interactions (Fig. 18a and b).[171,172] DEACM serves as both photolabile moieties and stabilizers. Moreover, hyaluronic acid (HA) and bovine serum albumin (BSA) was utilized for surface coating to neutralize positive surface charge of the PAMAM dendrimer. Upon 420 nm light irradiation, the cleavage and removal of DEACM will lead to instability of nanocarriers, which results in the dissociation of nanocarriers and cargo release. Moreover, surface charge turning from negative to positive was observed, which explained enhanced cellular uptake of drug molecules upon light irradiation. Based on a similar strategy, the DEACM can be replaced by PPGs with long-wavelength absorption BODIPY (Fig. 18c).[173] In the design, the PDDS was self-assembled by BODIPY-modified PAMAMs, which further stably incorporated the inhibitor of FSP1 (iFSP1) and photosensitizer chlorin e6 (Ce6) for synergistic anti-tumor efficacy. The developed system promoted intracellular delivery and tumor penetration under 520 nm light irradiation with increased tumor infiltration of $CD8^+$ T cells and enhanced efficacy of anti-PD-L1 immunotherapy. The excitation wavelength of the PDDS can be further extended by conjugating a NIR light-responsive BODIPY to the PAMAM dendrimer.[174] A combinational strategy was developed to co-deliver paclitaxel and the gamma-secretase inhibitor LY-411575 to solid tumors using NIR-light-responsive PAMAM dendrimers, addressing the heterogeneity associated with cancer stemness. The developed system demonstrated excellent anti-tumor efficacy in a mouse breast cancer model, effectively targeting both differentiated cancer cells and undifferentiated cancer stem-like cells.

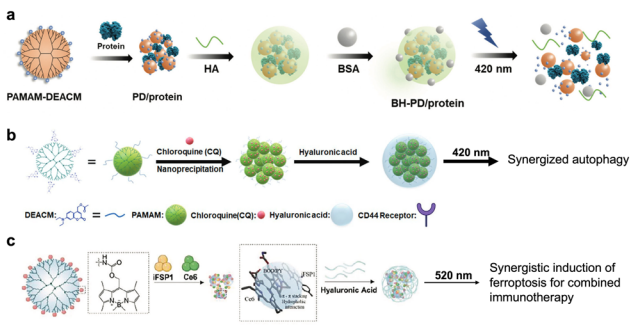

Fig. 18 (a) Schematic illustration of HA and BSA coatings and the photo-induced disassociation of the protein nanocomplex (adapted from ref. 171 with permission from the © 2021 The Royal Society of Chemistry). (b) Preparation and mechanism of the photoresponsive PAMAM (DEACM modified)-assembled nanoparticles encapsulated with chloroquine for synergistic anti-tumor therapy (adapted from ref. 172 with permission from the © 2021 Wiley-VCH GmbH). (c) Preparation of the photoresponsive PAMAM (BODIPY modified)-assembled nanoparticle co-delivered Ce6 and iFSP1 for induction of ferroptosis for combined immunotherapy (adapted from ref. 173 with permission from the © 2023 The Authors. Advanced Healthcare Materials published by Wiley-VCH GmbH).

Besides polymers, photocleavable moieties could be intergrated with lipids as well. A novel approach for light-controlled release of therapeutic proteins from engineered red blood cells (RBCs) was reported.[175] Therapeutic proteins could be loaded into the interior of RBCs by taking advantage of the pores that formed when RBCs were exposed to hypotonic conditions. Restoring isotonic conditions sealed the pores and trapped the proteins inside the RBCs. To trigger the release of the loaded proteins, the RBCs were modified with a photoactivatable system. This system consisted of melittin (Mel), a hemolytic peptide that could cause lysis of the RBC membrane, a blocking segment (BS) peptide that kept Mel inactive, and a cobalamin (Cbl) derivative that was conjugated to the BS peptide. The Cbl–Co–C bond could be photocleaved by 525 nm light irradiation, thus releasing the BS peptide from Cbl. This activated the Mel peptide, causing hemolysis of the RBC membrane and release of the entrapped therapeutic proteins. The light irradiation wavelength could be extended by introducing Cy5 into the photocleavable system. The targeted delivery of a clot-inducing enzyme was confirmed in a mouse model. Moreover, it is proposed that this light-triggered drug release strategy could be extended beyond RBCs to other membrane-based carrier systems, providing spatiotemporal control over therapeutic drug delivery. In a subsequent study, the photoresponsive RBCs were applied to treat arthritic inflammation by encapsulating dexamethasone inside.[176] The irradiation of 650 nm light successfully enabled the efficient and effective delivery of dexamethasone, making it five times more effective in suppressing inflammation than the parent drug.

Furthermore, photoresponsive small molecules can also be the building blocks for nanocarrier formation. For instance, a trigonal molecule (BTAEA) was synthesized by Long *et al.* through linking tris(2-aminoethyl) amine with a coumarin-4-ylmethyl derivative on each of the three arms (Fig. 19).[177] These photocleavable trigonal molecules can be co-assembled with DOX and stabilized with DSPE-PEG to form nanoparticles. The nanovehicles were dissociated upon 505 nm light irradiation to release DOX and the efficacy was verified in the retinoblastoma-bearing mice. Moreover, longer wavelength excitation can be achieved by incorporating a photosensitizer (PtTPBP) into nanoparticles by co-assembly *via* a one-photon process.[178] Upon red-light irradiation at 635 nm, the energy was harvested by a photosensitizer platinum(II) tetraphenyl-tetra-benzoporphyrin (PtTPBP) and transferred to BTAEA *via* triplet–triplet energy transfer (TTET),[212] resulting in BTAEA photolysis and PTX release.

To conclude, PPGs can be directly modified on or inserted into the building blocks or backbone of nanocarriers. The mechanism behind the light-triggered dissociation lies in light-induced transformation of the instable state due to the change of driven forces for self-assembly or direct degradation of the backbone. To achieve long-wavelength photoresponsiveness, UCNPs, PPGs with long-wavelength excitation, and two-photon excitation and one-photon upconversion-like photolysis strategies can be exploited. Apart from small-molecule drug molecules, biomacromolecules are capable of being encapsulated

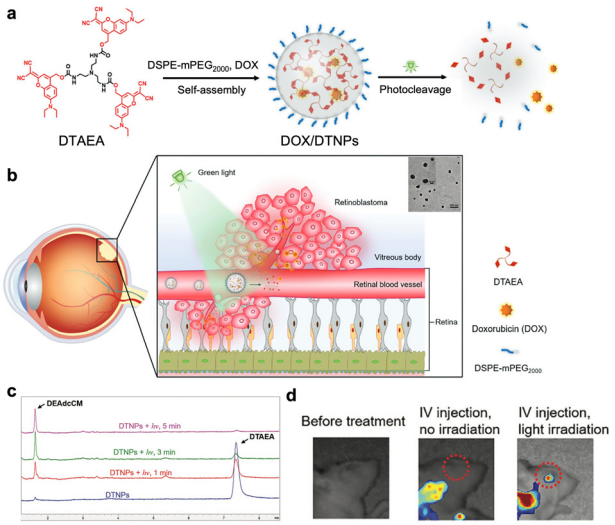

Fig. 19 Schematic illustration of photo-triggered chemotherapy of retinoblastoma. (a) Self-assembly, photodegradation, and drug release of the DOX-loaded photoresponsive nanocarrier. (b) Proposed mechanism of photo-enhanced drug accumulation in the eye. (c) Light-triggered photocleavage process monitored by HPLC. (d) Light-induced drug release in the eye of the mouse (adapted from ref. 177 with permission from the © 2021 The Authors. Advanced Science published by Wiley-VCH GmbH).

via different interaction forces, providing a promising modality for diverse biomedical applications.

6.1.2 Nanocarriers and drugs linked with PPGs. PPGs can also serve as linkers between nanocarriers and drugs likewise. Compared with directly modifying PPGs on nanocarriers, linkage between drug molecules and nanocarriers not only endows nanocarriers with photoresponsiveness but also cages the activity of drug molecules and further prevents premature release. For example, PAMAM is an ideal dendrimer by virtue of ease of modification, relatively good biocompatibility and the hydrophobic interior for loading small molecules.[213] UV-light responsive nanovehicles were synthesized by conjugating DOX with terminal amines of the PAMAM dendrimer using the DMNB-containing thioacetal linker.[179] Subsequently, UCNPs were employed to extend the wavelength of light irradiation. Upon 980 nm light illumination, DOX was successfully released from the dendrimers.

Currently, several types of drug molecules were directly linked with UCNPs to realize NIR light-controlled drug release. For example, core–shell UCNPs were coated with *o*-phosphorylethanolamine ligands and coupled to an *o*-nitrobenzyl photocaged anti-cancer drug 5-fluorouracil (5-FU).[180] 980 nm light irradiation could trigger the photocleavage process and successful release of 5-FU, resulting in light-controlled chemotherapy. The research based on such a mechanism was extended. Chlorambucil (Cb) was linked with silica-coated UCNPs *via* a perylen-3-ylmethyl group. 976 nm light irradiation can trigger photolysis and release of Cb.[181] A recent study has reported an indirect way to link chemo drugs and UCNPs *via* PPGs.[182] GC-rich DNA duplexes introduced with PPG *ortho*-nitrobenzyl moieties were modified on UCNPs. Subsequently, DOX was linked with DNA duplexes *via* specific hydrogen bonds. NIR light irradiation could induce photolysis of DNA duplexes. The destruction of the double stranded structure of DNA duplexes enabled release of DOX. The design of linking chemo drugs with nanocarriers enabled precise control of chemotherapy *via* light, providing a paradigm for precision medicine in treating a variety of malignancies.

Besides small molecules, biomacromolecules can also be designed to be delivered in the same way. For example, silica-coated UCNPs were covalently bonded with cationic photocaged linkers.[183] Subsequently, anionic siRNA could be efficiently absorbed by electrostatic attraction. The neutralization of "naked" positively charged siRNA promotes its cellular uptake since there are a lot of negatively charged peptides existing on cancer cell membranes.[214] Moreover, the system realized precise control of siRNA release in response to NIR light irradiation to minimize the side effects. The strategy will further facilitate wide application of gene therapy.

The upconversion mechanism with flexible wavelength was investigated (Fig. 20a).[184] Silica-coated harmonic nanoparticles (HNPs) were conjugated with L-tryptophan by DEACM. The system could absorb two photons and scatter one with twice the energy through second harmonic generation, realizing photocleavage and cargo release upon 790 nm femtosecond pulsed irradiation. The DEACM could also be substituted by other PPGs. For example, a photoresponsive drug delivery system was prepared utilizing lithium niobate harmonic nanoparticles to treat malignancies with epidermal growth factor receptor (EGFR) overexpressed (Fig. 20b).[185] An erlotinib derivative (ELA) was covalently conjugated to the surface of silica-coated nanoparticles through a coumarinyl photo-cleavable linker. 1250 nm laser light irradiation initiated successful imaging of nanoconjugates in DU145 cell lines (human prostate cancer cells with EGFR overexpressed), with second harmonic emission at 625 nm detected as well.

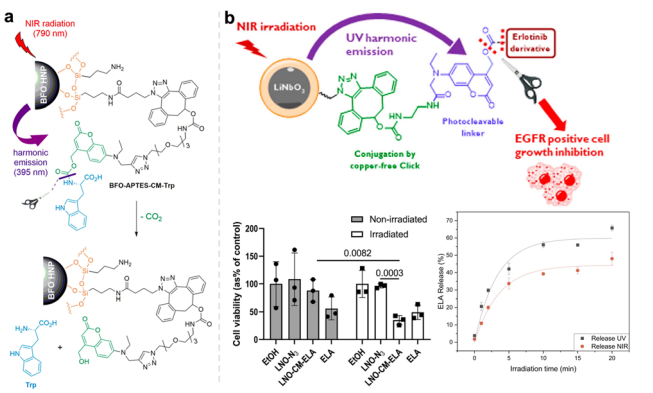

Fig. 20 (a) Chemical structure of silica-coated harmonic nanoparticles conjugated with L-tryptophan by DEACM and 790 nm light triggered cleavage and drug release (adapted from ref. 184 with permission from the © 2019 American Chemical Society). (b) Schematic illustration of fabrication of lithium niobate harmonic nanoparticles and NIR-light triggered on-demand chemotherapeutic release and cell toxicity (adapted from ref. 185 with permission from the © 2022 The Authors. Published by American Chemical Society).

In summary, PPGs serving as linkers between nanoparticles and drug molecules represent a toolbox for constructing PDDSs and achieving precise drug release in a spatiotemporal way. Small-molecule and biomacromolecule based therapeutics can both be delivered in such modality. In the near future, more light-controlled drug delivery systems with applicable-wavelength light irradiation for diverse biomedical applications were anticipated.

To promote photocleavage-based drug delivery systems for broader application, there is still room for improvement. Firstly, the development of photocages excited within the NIR window with minimized side effects and superior deep-tissue penetration is necessary. Secondly, the rational design of photocages with a modifiable chemical structure and excellent photocleavage efficiency is crucial. Since some PPGs' underlying photochemical mechanisms for photocleavage remain elusive, it is likely to generate metabolites and side products that can exert cytotoxicity or unknown biological functions.[215] It is hard to achieve 100 percent photolysis and the low photocleavage efficiency hinders further application based on current studies. The design principle, photocaging performance and photoactivation mechanism need further investigation and evaluation when being utilized in biomedical applications.

6.1.3 Photoresponsive drug delivery based on photoactivated chemotherapy. As described in Section 4.6, photocatalytic reaction-induced activation of prodrugs was extensively investigated. Metal-based anti-cancer prodrugs such as platinum(IV) (photoreduction) and ruthenium(II), rhodium(III), and iridium(III) (photosubstitution) complexes were employed to deliver the active chemotherapeutic agent to kill cells. This research is part of the emerging field of photoactivated chemotherapy (PACT).[216–219] PACT resembles the photocaging strategy, where a "caged" compound has its bioactivity concealed, hindering interaction with its target by disrupting the precise key-lock fit.

In photoreduction, the platinum(IV) (Pt^{IV}) complex is selectively reduced to a highly reactive platinum(II) (Pt^{II}) species upon light irradiation. This process essentially "cages" the toxic Pt^{II} in the dark, activating it only through photochemical reactions. The resultant platinum(II) complex exhibits heightened reactivity, forming covalent bonds with DNA that lead to DNA damage and subsequent cell death. In photosubstitution, using ruthenium(II) (Ru^{II}) as an example, light excitation triggers the replacement or "substitution" of one of the ligands in the ruthenium complex with water or other surrounding molecules. This process generates a highly reactive and cytotoxic ruthenium(II) species, ultimately resulting in cell death.

Metal complexes are increasingly being used as dual agents in PDT and PACT.[220–222] There are two types of PDT. The first involves a photosensitizer moving into a triplet excited state ($^3PS^*$) and transferring an electron (PDT type I). The second type involves the transfer of energy (PDT type II) to oxygen molecules to form singlet oxygen. PACT is similar to PDT type I, involving electron transfer from the triplet excited state of the compound. The combination of PDT and PACT presents promising potential for treating cancer and other diseases. Based on these mechanisms, prodrugs based on photocatalytic reactions were exploited in constructing PDDSs.[223]

For example, a Pt^{IV}-functionalized nanoparticle that can be excited using NIR light at 808 nm was reported (Fig. 21a).[186] Notably, the Pt^{IV} complex was functionalized with pyropheophorbide, a photosensitizer that absorbs in the red region of the spectrum, in order to extend the excitation wavelength. The nanoparticle design involved a polymeric chain with three key components: a chemotherapeutic agent oxaliplatin, a photosensitizer with properties for aggregation-induced emission photodynamic therapy, and a cancer-targeting peptide R8K to enhance accumulation in the cell nucleus. In aqueous solution, the functionalized polymer chains self-assembled into spherical nanoparticles. While the nanoparticles remained stable in the dark, upon irradiation the Pt^{IV} center was reduced to Pt^{II} and the axial ligands were released, causing rapid nanoparticle degradation. The resulting Pt^{II} complex formed adducts with DNA, and the photosensitizer catalytically generated ROS, leading to immunogenic cell death. The designed system provided a multimodal treatment approach combining chemotherapy and photodynamic immunotherapy. When selectively accumulated in tumor tissue, these multifunctional nanoparticles demonstrated the ability to eradicate triple-negative breast cancer tumors in a mouse model through this combined therapeutic strategy.

Upconversion nanoparticles (UCNPs) were also employed to extend the excitation wavelength of drug delivery systems. Platinum(IV) prodrugs were functionalized on $NaYF_4$:Yb^{3+}/Tm^{3+}@$NaYF_4$ core–shell UCNPs *via* coupling using biocompatible PEGylated phospholipid DSPE-PEG(2000)-NH_2.[187] 980 nm light irradiation could initiate photoreduction reactions and

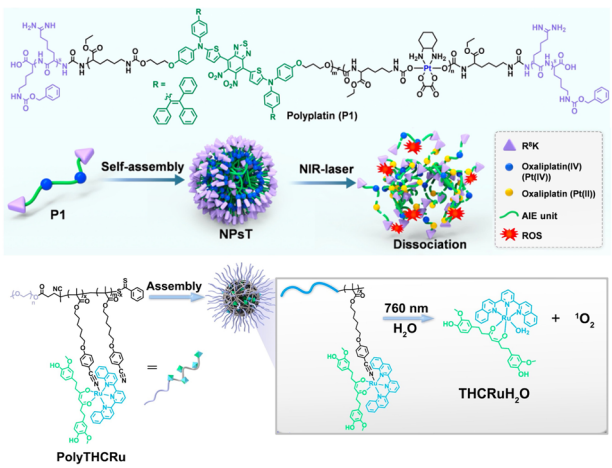

Fig. 21 (a) Chemical structure of building block P1 and its self-assembly into nanoparticles. NIR light irradiation triggered the dissociation of nanoparticles *via* photoreduction of the Pt^{IV} prodrug for combined chemotherapy and PDT (adapted from ref. 186 with permission from the © 2022 Wiley-VCH GmbH). (b) Chemical structure of building block PolyTHCRu and its self-assembly into nanoparticles. 760 nm light irradiation triggered the dissociation of nanoparticles *via* photocleavage of the ruthenium prodrug for combined chemotherapy and PDT (adapted from ref. 197 with permission from the © 2023 Wiley-VCH GmbH).

subsequent release of cytotoxic Pt^{II} for anti-cancer treatment. A similar strategy was further developed for synergistic photodynamic therapy (PDT) and chemotherapy.[188] The amphiphilic oligomer was synthesized by a conjugated platinum(IV) complex with a photosensitizer chlorin e6 (Ce6) *via* PEG, which co-assembled with UCNPs into nanoparticles. Upon 980 nm light excitation, the UCNPs can absorb the light energy and convert it into 365 nm and 660 nm emissions to trigger the release of Pt^{II} and PDT, respectively. Furthermore, the exacerbation of hypoxia induced by PDT could be alleviated by the release of oxygen from the photoreduction reactions of the Pt^{IV} complex. The NIR drug delivery system involving UCNPs has been proven to be a promising modality for cancer treatment with localized toxicity and limited side effects. The incorporation of metal complexes also provides a valuable approach for developing novel photoresponsive nanomaterials.

Apart from delivering small drug molecules, a platinum prodrug-based drug delivery system could also be fabricated to deliver macromolecules. For example, a photoactivated polyprodrug nanoparticle system (PPNPsiRNA) for light-controlled co-delivery of the Pt(IV) prodrug and siRNA for synergistic cancer therapy was designed.[189] The photosensitive Pt(IV) served as a prodrug, a light-responsive unit, and a comonomer in the backbone of the photoactivated polyprodrug. Under dark conditions, the Pt(IV) prodrug remained inactive and non-toxic, but upon 530 nm light activation, it released cytotoxic Pt(II) and generated azidyl radicals ($N3^{\bullet}$). Unlike the limited ROS generation in the hypoxic tumor environment, $N3^{\bullet}$ is oxygen-independent and can be sustainably generated from nanoparticles under mild light irradiation. This led to the disassociation of nanoparticles, controlled release of Pt(II), and unpacking of siRNA. The system is a promising light-controlled drug/gene co-delivery nanoplatform for cancer combination therapy.

A drug delivery platform was obtained by grafting the surface of mesoporous silica nanoparticles with ruthenium(II) dipyridophenazine complexes.[190] The ruthenium(II) complex and a monodentate ligand were covalently conjugated to the nanoparticles. Upon visible light irradiation at 465 nm, the ruthenium(II) complex was released from the surface of mesoporous silica nanoparticles by selective substitution of this ligand with a water molecule. Furthermore, paclitaxel as a model drug was loaded into nanoparticles and co-delivered with the ruthenium(II) complex to breast cancer cells. The developed system exhibited enhanced cellular uptake and synergistic cell killing effects, representing a promising candidate to achieve light-controlled therapeutic functions. Similarly, based on the photocleavage ability of ruthenium(II) complexes, they were modified on mesoporous silica nanoparticles as molecular gates.[191] Visible light irradiation could initiate the photocleavage of ligands and rapid release of safranin O dye.

Moreover, ruthenium(II) complexes could be directly inserted into building blocks such as polymers to construct drug delivery systems. For example, polypyridyl–ruthenium(II) complexes were utilized as cores to conjugate block copolyemrs, which were synthesized by *N*-carboxyanhydride polymerization and functionalized with aromatic nitrile-groups on the glutamic acid side chain.[192] The developed copolymers could self-assemble into polymeric micelles and exhibited good stability in human blood plasma. 455 or 535 nm light irradiation could facilitate photocleavage and successful delivery of ruthenium drugs. In another research, a green light-sensitive Ru based drug was coordinated to polymers to construct polymeric nanoparticles.[193] 520 nm light-induced cell death with A431 and A549 cancer cell lines was observed, demonstrating effective photoactivated chemotherapy by virtue of cleavage and release of cytotoxic Ru agents.

The Ru complex can also be excited by long wavelength by virtue of the metal-to-ligand charge transfer bands in the visible or NIR region. NIR light not only triggers the photocleavage of the ruthenium(II) complex but also the generation of cytotoxic singlet oxygen. For instance, the Ru complex was inserted into block copolymers, which could self-assemble into different nanostructures.[194] NIR light (656 nm) irradiation not only activates the Ru(II) prodrug to trigger the release of cytotoxic $[Ru(tpy)(biq)(H_2O)]^{2+}$ but also the generation of singlet oxygen for combined photochemotherapy and photodynamic therapy. Likewise, hydrophobic photoresponsive ruthenium complexes were conjugated with hydrophilic biodegradable hyaluronic acid (HA) to prepare the building blocks, which could self-assemble into nanoparticles and load chemotherapeutic doxorubicin (DOX).[195] HA could mediate CD44 targeting effects for improved tumor accumulation. 660 nm light irradiation facilitated the photocleavage process and dissociation of nanoparticles. Subsequent release of DOX and cytotoxic Ru agents and generation of singlet oxygen were observed, which worked synergistically to effectively kill tumors in a mouse model. The singlet oxygen generated could be utilized to cleave the Ru–S bond.[196] In a recent research study, PEG and a hydrophobic polypeptoid bearing thioether side chain were coordinated with the Ru complex *via* a Ru–S bond. 625 nm light illumination induced the generation of ROS as a result of photosensitization of the Ru complex, which oxidized hydrophobic thioether to hydrophilic sulfoxide and caused disruption of polymer micelles. The developed system protected metallodrugs and exhibited low cytotoxicity in the dark while displayed distinct anticancer effects with spatiotemporal control *via* light.

To promote a wider application of ruthenium(II) complexes, the synthesis of a ruthenium prodrug with extended irradiation wavelength is necessary. Recently, a ruthenium-based photocage containing tetrahydrocurcumin was synthesized for NIR light-controlled drug delivery (Fig. 21b).[197] Tetrahydrocurcumin is a commercially available anticancer drug. After coordinating tetrahydrocurcumin to a ruthenium(II) center, a ruthenium-based photocage was created that responds to NIR light at 760 nm. This ruthenium-based photocage also inherited the anticancer properties of tetrahydrocurcumin. The synthesized photocage was then conjugated to amphiphilic block copolymers, which can self-assemble into nanoparticles. Upon 760 nm light irradiation, the ruthenium complex-based photocages were released from the polymeric nanoparticles and effectively inhibited tumor growth *in vivo*.

Similarly, ruthenium(II) prodrugs could be conjugated to UCNPs.[198] A ruthenium(II) polypyridyl complex was synthesized

with a photocleavable bis(thioether) ligand modified. The bis(phosphonate) group in the prodrug was utilized to conjugate the complex to UCNPs, where the incorporation of a neodymium-doped shell layer allowed for the generation of blue light using low-energy, deep-penetrating 796 nm light. This strategy circumvents the disadvantage of 980 nm light irradiation, which is a high-intensity energy that results in unwanted heating. The 796 nm light irradiation could initiate the cleavage and release of the ruthenium drugs. This is the first demonstration of the photoactivation of a ruthenium thioether complex using 796 nm irradiation of a water-dispersible nanoconjugate.

To sum up, photoresponsive drug delivery based on photoactivated chemotherapy is a validated modality. By incorporating metal-based prodrugs into building blocks of drug delivery systems, light-controlled release can be achieved *via* photochemical reactions. In the future, research can be focused on developing metal-based prodrugs with longer light irradiation wavelength or UNCPs with biocompatible light excitation for potential clinical translation.

6.2 Photoresponsive drug delivery systems based on photoisomerization

The light dissociation process can be rendered as reversible by the use of photoswitchable groups, such as azobenzene, spiropyran, and dithienylethene.[224] Azobenzenes can undergo isomerization reversibly from *trans* to *cis* conversion upon UV light irradiation and from *cis* to *trans* form under visible light.[225] Spiropyrans transform reversibly the neutral spiropyran isomer into zwitterionic, positively charged merocyanine upon UV light illumination, while opened merocyanine is converted back to the closed spiropyran conformation under visible light irradiation.[226] By taking advantage of reversible conformational change of photoswitches under light irradiation, a series of drug delivery systems have been developed to achieve efficient control of the ''on/off'' drug release and avoid the multiple drug administration in clinical use (Table 3).

6.2.1 Azobenzene-based photoisomerization in drug delivery systems. Azobenzene was first discovered in 1834 and is an extensively applied light-responsive molecule with a long history.[253,254] Such molecules have been systematically explored

Table 3 A table summarizing strategies for photoresponsive drug delivery systems based on photoisomerization that are mentioned in the review. MSNs, mesoporous silica nanoparticles; DOX, doxorubicin; ATP, adenosine triphosphate; β-CD, β-cyclodextrin; MOFs, metal–organic frameworks; COFs, covalent organic frameworks; UCNPs, upconversion nanoparticles; PTX, paclitaxel; DASAs, donor–acceptor Stenhouse adducts; DTEDA, a photochromic diarylethene derivative; and TBPDI, a red fluorescence dye, 1,6,7,12-tetra(*p*-^{t}Bu-phenoxy)-3,4,9,10-di(anhydride) perylene

Types	Mechanisms	Drug vehicles	Light	Drugs/dyes	Ref.
Photoisomerization in drug delivery based on azobenzene	Azobenzene tethered DNA	MSNs	UV/visible light	DOX	227
	Azobenzene tethered DNA	Nanochannels	UV/visible light	ATP	228
	Azobenzene-modified MSNs capped *via* β-CD	MSNs	UV/visible light	Hexaconazole	229
	MOFs modified with azobenzene	MOFs	408 nm	Propidium iodide	230
	COFs modified with azobenzene	COFs	UV/visible light	Rhodamine B	231
	Azobenzene modified lipids	Liposomes	Dark/UV light	DOX	232
	Azobenzene modified polymers	Polymeric nanoparticles	UV/visible light	N/A	233
	Cationic azobenzene derivatives	Self-assembled nanoparticles	UV/visible light	Rhodamine B and DOX	234
	Azobenzene-modified MSNs capped *via* β-CD	MSNs	760 nm (two photon)	Camptothecin	235
	Lipids modified with tetra-*ortho*-chlorination azobenzene	Liposomes	465/630 nm	N/A	236
	Azobenzene tethered DNA	UCNPs	980 nm (upconversion)	DOX	237
	Azobenzene modified polymers	UCNPs	980 nm (upconversion)	DOX	238
	Azobenzene-modified UCNPs capped *via* β-CD	UCNPs	980 nm (upconversion)	D-Mannose	239
Photoisomerization in drug delivery based on spiropyran	MSNs modified with spiropyran	MSNs	UV/visible light	Camptothecin	240
	Spiropyran modified polymers	Polymer networks	UV/visible light	DOX	241
	Spiropyran modified polymers	Polymeric micelles	UV/visible light	PTX, DOX, docetaxel *etc.*	242
	Spiropyran modified copolymers	Polymeric micelles	UV/visible light	N/A	243
	Spiropyran modified copolymers	Polymersomes	UV/visible light	4′,6-Diamidino-2-phenylindole	244
	Spiropyran modified cationic copolymers	Polymeric nanoparticles	UV/visible light	Plasmid DNA	245
	Spiropyran modified cationic copolymers	Ternary polyionic nanoassemblies	UV/visible light	Rhodamine-labelled DNA	246
	Spiropyran modified polymers	Gold nanoclusters	UV/visible light	N/A	247
	Spiropyran	Hydrogel	Dark/white light	N/A	248
	UCNPs modified with spiropyran	Hollow UCNPs	980 nm (upconversion)	β-Galactosidase	249
Others	DASAs modified polymers	Polymersomes	525/630 nm	Sodium fluorescein	250
	DASAs modified polymers	Polymeric micelles	656 nm	Nile red	251
	DTEDA modified polymers	Polymeric nanoparticles	254/525 nm	TBPDI	252

in the field of photopharmacology and biomedicine based on photoisomerization in recent decades.[19,255] Extensive endeavors have been made by modification or insertion of azobenzene into diverse components such as biomacromolecules, inorganic materials and organic lipids, polymers and so on to fabricate different photoresponsive nanocarriers.

It was reported that azobenzene can be grafted on DNA strands, which allowed their reversible switching of structural changes.[256] Based on this mechanism, biomaterials can be functionalized with reversible activities by incorporating azobenzene-tethered DNA. For example, azobenzene was incorporated into DNA double strands, which were then employed to be immobilized at the pore of mesoporous silica nanoparticles (MSNs).[227] Light-triggered isomerization of azobenzene resulted in a switch of complementary DNA between dehybridization and hybridization, leading to uncapping or capping of pore gates of MSNs. In the research, DOX was employed as a model drug, which was held back under visible light while can be released upon UV light irradiation. The biocompatibility and light-triggered cytotoxicity of the developed system were further confirmed *via* MTT assay in cancer cells, which provides a widely applicable modality for potential applications in cancer therapy. Similarly, an adenosine triphosphate (ATP) transport system was established by assembling azobenzene-modified DNA into the artificial conical polyimide nanochannels.[228] The transport lines could efficiently shepherd ATP across the polymer membrane upon alternant light exposure due to the structural change of the azobenzene-modified DNA aptamer.

Besides, azobenzene can also be modified directly on bimodal MSNs. For instance, hexaconazole, a broad-spectrum systemic triazole fungicide was loaded into azobenzene-modified MSNs, in which β-cyclodextrin (β-CD) was capped onto the surface *via* host–guest interactions recognized by *trans*-Azo (Fig. 22).[229] Controlled release of hexaconazole was achieved due to the reversible removal of cap, which was initiated by the *trans* to *cis* conversion of azobenzene upon UV light irradiation. The light-controlled toxicity of nanoparticles was studied on CCC-ESF-1 cells and *E. coli*. Another study did deep research on the conditions required for stabilized silica nanoparticles with photoresponsiveness that are functionalized with azobenzene photoswitches.[257] Modifying the silica particle surfaces with alcohol-terminated azobenzene compounds provided a validated approach for controlling the density of photoswitchable groups on the particle surfaces. By adjusting the length of the carbon linker used to attach the azobenzene moieties to the particle surfaces, the hydrophobicity of the particle surfaces could be tuned. Upon UV light irradiation on the system, emulsification occurred because of conversion of the modified azobenzene molecules to their more hydrophilic *cis* state. The cycle between emulsified and demulsified states could be controlled through the switch of UV or blue light, respectively. Moreover, the emulsion system like oil utilized also plays a crucial role in constructing such a delivery system. Considering the key components (particles, photoswitches and oil), it is likely to tailor the system with light-controllable ability. Moreover, it is general to apply other photoswitches, *e.g.*, donor–acceptor Stenhouse adducts (DASAs) and spiropyrans on such a system. The investigation advanced the rational design of light-responsive drug vehicles and the methodologies employed can be applied anywhere that transient encapsulation is required.

The photo-triggered ''on/off'' of drug release can also be achieved by modifying metal–organic frameworks (MOFs) with azobenzenes.[230] Azo-IRMOF-74-III is an isoreticular expansion of MOF-74 with an analogous structure and 1-D hexagonal pores. Each organic linker within the azo-IRMOF-74-III framework contains a photoswitchable azobenzene unit. These azobenzene groups could be reversibly isomerized between their *cis* and *trans* configurations by exposing the material to light of the appropriate wavelength. Irradiation with 408 nm light triggered rapid, repetitive isomerization of the azobenzene groups, causing a wagging motion that facilitated the release of dye molecules from the pores of the drug delivery system. In another recent research, azobenzenes were modified on covalent organic frameworks (COFs).[231] The azobenzene groups appended to the framework were oriented with their long axes pointing into the pore channels of the COF. This arrangement provided adequate free space within the pores to accommodate the unhindered, dynamic motion of the azobenzene units as they underwent reversible *trans*-to-*cis* photoisomerization upon exposure to light. The synthesized COF could be effectively utilized for rhodamine B storage and on-demand release. The strategy of modification of azobenzene on porous solids such as MOFs and COFs provides a mature modality for controlled delivery of small therapeutics *via* light, heralding promising future for diverse biomedical applications.

Azobenzene is also incorporated into lipids or polymeric materials to construct organic drug delivery systems, including liposomes and polymeric nanoparticles. Photoisomerization takes place under light irradiation, destabilizes lipids or polymers and results in dissociation of nanovehicles and drug release. For example, researchers have synthesized glycolipid

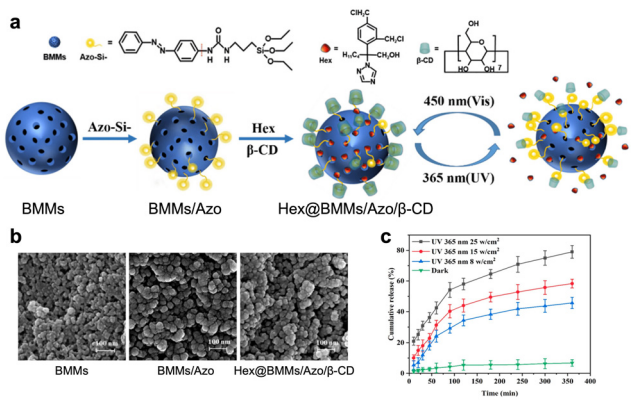

Fig. 22 (a) Schematic diagram of the preparation of azobenzene-modified MSN with β-cyclodextrin as a cap and its light-responsive release mechanism. (b) SEM images of different nanoparticles. (c) Drug release profile of Hex@BMMs/Azo/β-CD under different UV light irradiation or under the dark conditions (adapted from ref. 229 with permission from the © 2021 by the authors. Licensee MDPI, Basel, Switzerland).

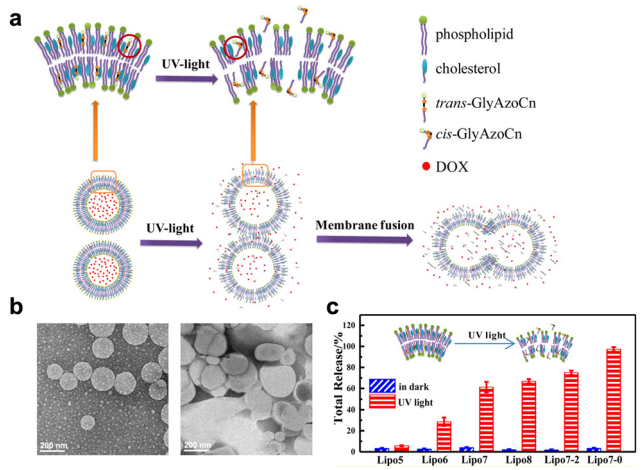

Fig. 23 (a) Diagram of photoisomerization-induced dissociation of liposomes composed of azobenzene-contained glycolipids and resulting burst cargo release. (b) TEM images of designed liposomes before (left) and after (right) UV light irradiation. (c) Total drug release amount of DOX from liposomes composed of different glycolipids (adapted from ref. 232 with permission from the © 2016 American Chemical Society).

compounds that incorporated an azobenzene unit positioned between the galactosyl and hydrocarbon chains of varying lengths (Fig. 23).[232] The reversible light-triggered isomerization was achieved in liposomal bilayers through alternating irradiation with UV and visible light. The liposome developed was able to stably retain the entrapped DOX cargo in the absence of light, with less than 10% leakage over a 10-hour period. However, upon exposure to UV irradiation, the liposome rapidly released nearly 100% of its cargo. Similarly, azobenzene can be inserted into amphiphilic polymers, which can self-assemble into vehicles and load drugs.[233] In a latest research study, amphiphilic light-responsive copolymers were synthesized by introducing azobenzene in the side chain of poly(2-oxazoline)s, which can form nanoparticles in aqueous condition.[258] Reversible photoisomerization under alternated UV light irradiation was realized to achieve effective drug release.

Apart from being incorporated into the building blocks of drug delivery systems, azobenzene itself can serve as a building block as well. As an example, researchers fabricated a self-assembled cationic drug delivery vehicle in an aqueous solution. This vehicle was constructed from a cationic azobenzene derivative, specifically 4-cholesterocarbonyl-4′-(*N*,*N*,*N*-triethylamine butyloxyl bromide)-azobenzene, in combination with the anionic surfactant sodium dodecyl sulfate.[234] Subsequently, rhodamine B was loaded inside as a model drug. The developed drug vehicle was intravitreously injected into rat retina to investigate its *in vivo* pharmacokinetic profiles and drug release behaviors. Upon UV light irradiation, enhanced release and a long duration of rhodamine was observed. Subsequently, they replaced the rhodamine B with DOX. Light-triggered cancer cell death was observed upon UV light irradiation. The simple self-assembly of azobenzene derivatives and other components provides a new modality to construct PDDSs.

However, the general requirement of utilizing UV/blue light to control the photoswitches is a bottleneck for their wider application in biomedical applications, since the short-wavelength light is unfavorable for deep penetration in tissues with high phototoxicity. To achieve NIR light responsiveness for photoisomerization based drug delivery systems, three methods can be exploited: (1) applying a NIR two-photon excitation strategy; (2) developing NIR-light responsive photoswitches; and (3) incorporating UCNPs.

Previously, gated-MSN systems based on azobenzene isomerization for drug release were fully illustrated. The two-photon excitation strategy can be combined with MSN-based drug delivery systems to achieve NIR light-controlled drug delivery. For example, MSNs modified with azobenzene and two-photon silylated fluorophores were developed.[235] Then, the cargo was loaded in the pores with β-CD as the cap, which showed efficient two-photon activated drug delivery *via* NIR light. Recently, the rational design of electronically asymmetric azobenzene molecules labeled with NIR-absorbing molecular antennas for efficient multiphoton photo-conversion was reported.[259] However, most of the azobenzene derivatives exhibit a low two-photon absorption cross section, which hinders their application for multiphoton excitation with NIR light.

The second case is to develop azobenzene-based photoswitches with visible or NIR light responsiveness. The tetra-*ortho*-substitution of the azobenzene aryl rings with halides was found to red-shift the photoisomerization properties of regular azobenzenes.[260,261] The substitution with large groups such as chlorine induces steric hindrance to the *trans*-azobenzene isomer, resulting in the two aryl rings twisted out of plane. The absorption bands and the photoisomerization properties are influenced by the nature of the substituent correspondingly. Recently, photoswitchable phospholipids (photolipids) were constructed by modification of tetra-*ortho*-chlorination azobenzene to phosphatidylcholine which undergoes photoisomerization on irradiation with tissue-penetrating red light ($\geq$630 nm) (Fig. 24).[236] Nano- and micrometer-sized liposomes were fabricated *via* incorporating photolipids, which offered great potential for application in NIR light-modulated drug delivery.

UNCPs are widely exploited for constructing PDDSs with NIR light responsiveness. In a recent study, a nanopump was constructed by assembling the azobenzene-functionalized DNA strands on UCNPs.[237] The HIV-1 TAT peptide and hyaluronic acid were grafted on the system to achieve targeted cancer cell nucleus delivery and then DOX as a model drug was loaded. The precise delivery and controlled drug release were realized under NIR light irradiation as a result from switchable hybridization and dehybridization of DNA strands. A similar strategy can be applied in constructing NIR light-responsive polymers modified with azobenzene based on UCNPs.[238] This approach could be advantageous for clinical applications, such as cancer treatment, where the unique microenvironmental conditions of tumor tissues could be leveraged to improve drug targeting and localize drug delivery. This could help prevent the non-selective destruction of normal healthy cells, which is a

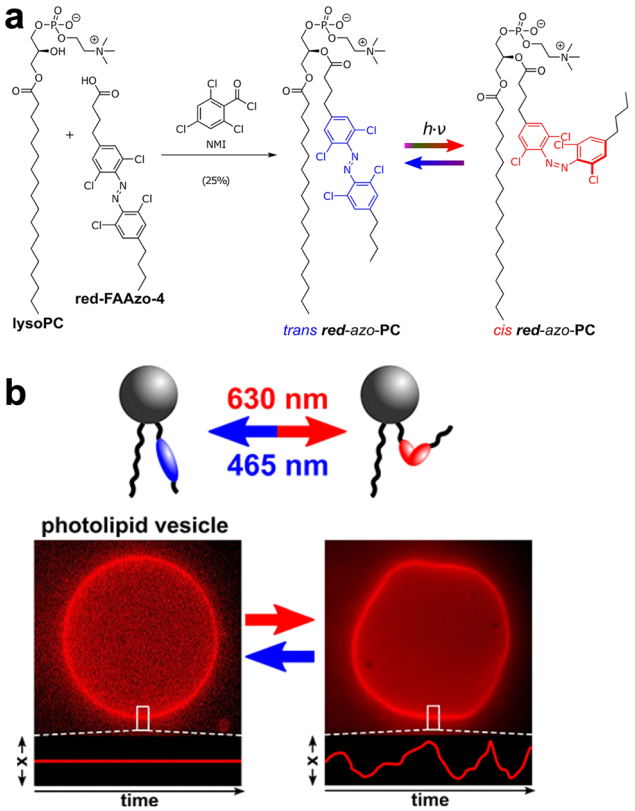

Fig. 24 (a) Chemical synthesis and photoisomerization of tetra-*ortho*-chloro azobenzene-substituted phosphatidylcholine (termed red-azo-PC). (b) Schematic diagram of the reversible change of fluidity and mechanical properties of lipid membranes due to transformation of red-azo-PC under alternate light irradiation (adapted from ref. 236 with permission from the © 2021 American Chemical Society).

major cause of the debilitating side effects typically associated with chemotherapy.

An interesting design was presented to achieve remote and reversible control of bacterial cell–cell interactions (Fig. 25).[239] A NIR light responsive drug delivery system was developed using functionalized photoisomeric azobenzene-modified glycoconjugates and β-cyclodextrin on UCNPs. Upon NIR light irradiation, reversible bacterial clustering was observed both *in vitro* and *in vivo*. By regulating cellular interactions in precise and non-invasive way, the developed platform brings new perspectives for anti-virulence therapeutics.

Azobenzene, as a widely employed photoswitch, can be modified on components varying from organic nanoparticles like polymeric micelles, liposomes, and MOFs/COFs to inorganic nanoparticles like MSNs and UCNPs. Moreover, the decoration of azobenzene on DNA strands to induce reversible dehybridization/hybridization switch of complementary DNA also enables precise control of drug release. Currently, incorporating UCNPs into PDDS based on azobenzene is the most widely used strategy to extend excitation wavelength with higher tissue penetration. In the future, more long-wavelength light-responsive azobenzene derivatives are anticipated to be synthesized and applied in building blocks of drug delivery systems to enable a wide range of biological applications.

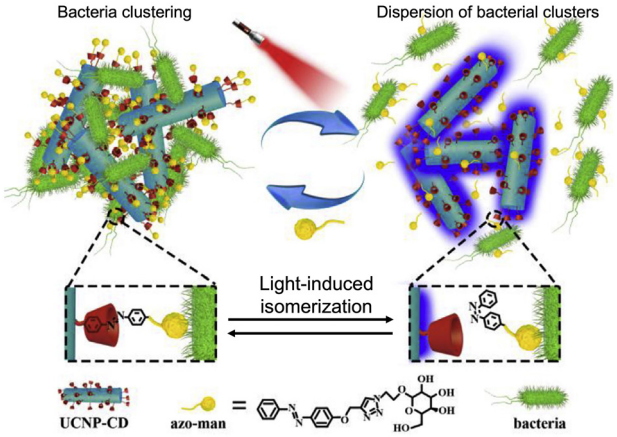

Fig. 25 Schematic illustration of NIR-driven reversible bacterial clustering (adapted from ref. 239 with permission from the © 2019 Elsevier Ltd).

6.2.2 Spiropyran-based photoisomerization in drug delivery systems. Spiropyrans were first discovered by Fischer and Hirschberg in the 1950s, and extensively investigated in the 1960s for their photochromic behavior.[262] Spiropyran transforms reversibly from the colorless and neutral spiropyran isomer to highly-colored, zwitterionic and positively charged merocyanine upon UV light illumination, while is converted back under visible light irradiation.

Similar to azobenzene, the spiropyran can be covalently attached to MSNs likewise. A light-responsive drug delivery system was synthesized by adjusting the wetting of the MSNs' surface, which exploited different hydrophobicities between the "closed" and "open" isomers of spiropyran as a photoswitchable molecular gate on the surface (Fig. 26).[240] It is found that the optimized ratio of loaded model cargo molecules fluorescein

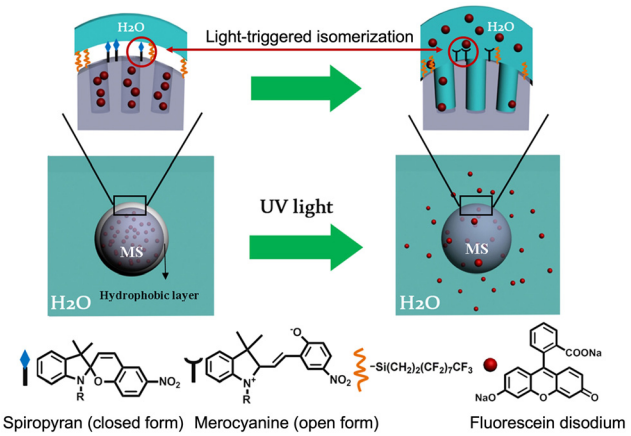

Fig. 26 The light-responsive release system involved MSNs modified with an optimal ratio of spiropyran and perfluorodecyltriethoxysilane, which rendered the particle surface hydrophobic and blocked cargo release. However, UV light at 365 nm triggered the spiropyran to convert from a "closed" to "open" form, making the surface hydrophilic and allowing the encapsulated cargo fluorescein disodium to diffuse out of the pores (adapted from ref. 240 with permission from the © 2014 American Chemical Society).

disodium (FD) to spiropyran could protect MSNs from being wet and inhibit the release of FD from pores. Subsequently, FD was replaced with anticancer drug camptothecin (CPT). 365 nm light irradiation could trigger efficient CPT release and enhanced cytotoxicity was confirmed in EA.hy926 cells and HeLa cells. A similar design was reported by functionalizing silicone-hydrogel interpenetrating polymer networks with carboxylated spiropyran.[241] On-demand light-triggered release of model drug DOX was achieved relying on controlling the wetting behavior of the surface of the developed drug delivery systems. This wettability-determined smart release platform triggered by light holds promise in the applications of drug delivery and cancer therapy.

Spiropyrans can also be incorporated into lipids and polymers. A nanoparticle self-assembled from alkyl derivatives of the chromophore spiropyran, hydrophobic drugs, and lipid-PEG chains was developed.[242] In the research, polymers incorporating spiropyrans with different carbon side chain lengths (C7, C9 and C18) were synthesized. Notably, the nanoparticles self-assembling from polymers with the spiropyrans with C9 and C18 side chains exhibited a reduction in the size while no size change was observed for that self-assembling from polymers with spiropyrans with C7 side chains. This is explained by changes in polymer hydrophilicity after photoisomerization of spiropyran to merocyanine. To enhance the stability of the nanoparticles, lipid-PEG was added. Upon UV light irradiation, hydrophobic spiropyran underwent isomerization to zwitterionic merocyanine, which induced a reversible volume change of nanoparticles from 150 to 40 nm and triggered drug release. The strategy based on reversible nanoparticle size shrinkage provides useful properties in many diseases including cancer.

The first photochromic block copolymer was developed by Kotharangannagari *et al.*[243] The block copolymer (PLGA-*b*-PEO, with side chains modified with spiropyran) can self-assemble into micelles and undergo complete reversible micellar transition under UV/visible light irradiation. Continuous studies have been carried out by developing a new amphiphilic diblock copolymer poly(ethylene oxide)-*b*-PSPA, where SPA is a spiropyran-based monomer containing a unique carbamate linkage.[244] The newly designed diblock polymer could self-assemble into polymersomes that enabled on-demand and switchable release of the cargo molecule 4′,6-diamidino-2-phenylindole within living HeLa cells, triggered by exposure to varied wavelengths of UV/visible light. Grafting copolymers with spiropyrans represents a mature toolbox for light-controlled drug delivery.

Spiropyran-incorporated cationic copolymers were developed as well (Fig. 27).[245] The electrostatic interactions enabled cationic copolymers to deliver biomacromolecules. A gene delivery system was fabricated by incorporating a small amount of spiropyran-containing cationic copolymers into the outer coating of a polyethylenimine/DNA complex, which proved to increase transgene expression.[246] Moreover, the use of spiropyran circumvents the issue of uncontrolled long-lasting photocytotoxicity in gene delivery by virtue of its reversibility.

In a recent study, a gold nanocluster engineered with a spiropyran ligand (AuNC-SP) was reported for light-controlled

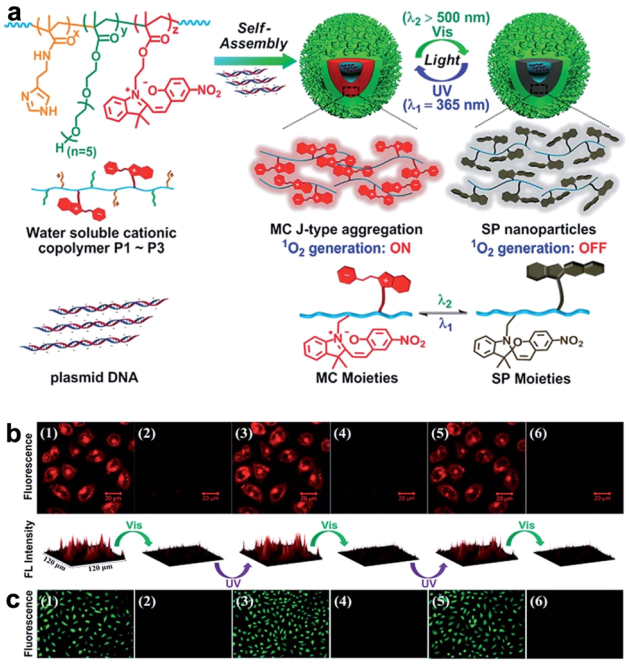

Fig. 27 (a) The self-assembly of spiropyran-containing cationic copolymers with plasmid DNA, enabling reversibly light-controlled ROS production. (b) Fluorescence images of P3 NPs taken up by the HeLa cells under altered UV and visible light irradiation. (c) Reversible ROS generation detected by DCFH-DA (ROS probe) after treatments with P3 NPs under altered light irradiation (adapted from ref. 245 with permission from the © The Royal Society of Chemistry 2018).

fluorescence bioimaging.[247] AuNC-SP was combined with chitosan to form nanoparticles with improved oxidative stability. Upon UV-vis light irradiation, the Förster resonance energy transfer from the gold nanocluster segment to the open-ring state merocyanine of spiropyran was initiated, which led to dual-color imaging. The developed system exhibited desirable cellular uptake within cancer cells and excellent and reversible dual-color fluorescence to label not only the cytoplasm but also the nucleus, showcasing a promising application in light-controlled bioimaging.

Hydrogels, with their high water content and structural similarities to the extracellular matrix, have the potential to function effectively in aqueous environments, particularly in biological microenvironments.[263] A recent study described a novel type of hydrogel inspired by origami principles, which can mimic the complex functionalities of living organisms.[248] The photoresponsive hydrogel exhibited versatile and dynamic shape transformations by leveraging a single material composition. This was achieved by incorporating spiropyran photoswitches into the hydrogel, along with the monomers *N*-isopropylacrylamide (NIPAM) and the crosslinker *N*,*N*′-methylenebisacrylamide (MBAAm). Upon exposure to localized white light irradiation, the hydrogel sheet contracted to around 80% of its original size. Remarkably, this contracted state could then be fully recovered back to the original swollen state simply by turning the light off. This reversible contraction–expansion process could be repeatedly triggered by alternating the light stimulus on and off.

The photoresponsive hydrogel system developed here provides the guidelines to aid the development of more complex structures and devices for potential biomedical applications.

In the same modality, UCNPs are incorporated into spiropyran-based drug delivery systems to realize NIR-light controlled drug delivery of different cargos like small molecular drugs and therapeutic macromolecules. For example, a DNA-mediated solvothermal method has been developed for the construction of a hollow UCNP conjugated photosensitive spiropyran dye for NIR light controlled non-invasive protein release.[249] In the research, DNA was found to play a key role in the preparation of the hollow UCNPs. The incorporation of photosensitive spiropyran molecules into the coating of the delivery system enabled a structural change from the negatively charged to the neutral form upon photoisomerization. This triggered efficient encapsulation of enzymes and allowed for sensitive NIR light-induced release of the cargo. Crucially, the transportation of enzymes into living cells and intracellular NIR triggered release of enzymes with retained biological activity in a highly spatial and temporal precision were observed. The design envisioned a promising future for advancing development of both UCNPs and light-responsive protein delivery.

To conclude, similar to azobenzene, spiropyran can be modified on building blocks of drug carriers like polymers and lipids. Spiropyran can be decorated directly on MSNs, UCNPs and other drug vehicles as well. Moreover, the difference of hydrophobicity between the "closed" and "open" isomers of spiropyran can be directly utilized as a photoswitchable molecular gate on the surface of drug delivery systems. In the future, endeavors can be focused on developing strategies to lengthen the excitation wavelength of spiropyran derivatives.

6.2.3 Photoresponsive drug delivery systems based on other photoswitchable groups. Apart from widely known azobenzene and spiropyran, there are other photoswitches that can be exploited to construct PDDSs based on photoisomerization. For example, the amphiphilic block copolymers composed of poly(pentafluorophenyl methacrylate) were developed and functionalized with donor–acceptor Stenhouse adducts (DASAs), which can isomerize upon irradiation with visible light.[250] These polymers can self-assemble into vehicles and can be loaded with hydrophilic payloads like enzymes. The permeability of polymersome membranes was enhanced upon visible light irradiation owing to switchable polarity from the nonpolar triene-enol conformation to highly polarized cyclopentenone, resulting in drug release. However, the process can be stopped as soon as the light was turned off. Furthermore, the wavelength at which the polymersomes become permeable can be adjusted as different DASAs possessing different colors can be synthesized and functionalized. The developed system enabled light-controlled wavelength-selective catalysis and provides potential application to switch reactions on and off, on demand in drug delivery. In a recent design, a novel red-light-responsive polymer with high water stability was developed by incorporating the reversible photoswitches, DASAs (Fig. 28).[251] The polymer can self-assemble into micellar nanovehicles and can be encapsulated with a hydrophobic model drug Nile red within the core.

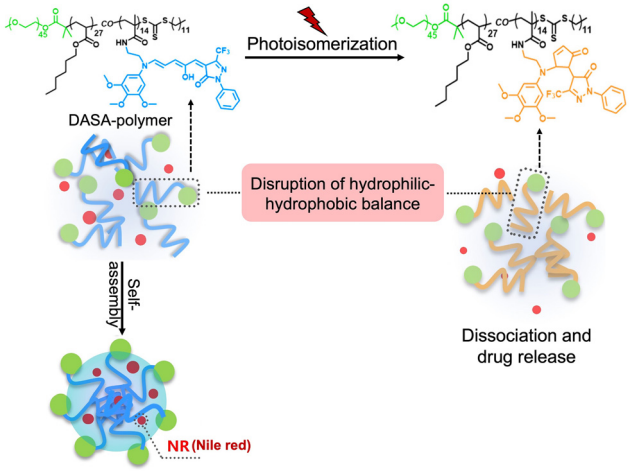

Fig. 28 A schematic illustration depicting the red light-triggered release of Nile red from a DASA-polymer nanovector, which was facilitated by the isomerization of the grafted DASA units within the nanoparticles (adapted from ref. 251 with permission from the © 2023 by the authors. Licensee MDPI, Basel, Switzerland.).

656 nm light irradiation could initiate transformation of DASAs, resulting in disruption of hydrophilic–hydrophobic balance of the nanovehicles, thereby leading to the release of cargo. DASA-incorporated nanovehicles shed light on photoresponsive polymer-based nanomedicines with broad applications.

Diarylethene molecules belong to the P-type photochromic molecules, which can change color from colorless to red reversibly in response to light.[264] However, diarylethene molecules are not thermally reversible. This suggests that the photogenerated isomers are highly stable and do not readily revert to the left-side isomers in the dark at room temperature. In latest research, a diarylethene-based nanoparticle was developed for bioimaging application.[252] A thermostable and photoswitchable red fluorescent polymeric nanoparticle was designed. It incorporated a red-emitting fluorescent dye, 1,6,7,12-tetra-(*p*-^{t}Bu-phenoxy)-3,4,9,10-di(anhydride) perylene (TBPDI), which served as the energy donor. Alongside this, the nanoparticle also contained a photochromic diarylethene derivative (DTEDA) acting as the energy acceptor. Upon exposure to UV light, the DTEDA underwent a structural transformation, transitioning from an open-ring state (DTEDA-o) to a closed-ring form (DTEDA-c). This light-induced structural change then triggered an efficient fluorescence resonance energy transfer from the TBPDI donor to the DTEDA-c acceptor species. As a result, the initial red fluorescence of the nanoparticle became effectively quenched. The developed nanoparticle was successfully utilized for reversible fluorescence bioimaging in Zebrafish.

To conclude, incorporating photoswitches into drug delivery systems can effectively achieve reversible and precise control of drug release. Despite the reversibility of photoisomerization, there are some limitations that may hinder its wide use in practice. The major concern of the photoisomerizable molecules is their safety. Certain azobenzene molecules can be irreversibly degraded by azoreductase, an enzyme produced by bacteria present in the

gastrointestinal tract.[265] This enzymatic degradation can generate byproducts such as nitrobenzene, which is considered toxic by the United States Food and Drug Administration.[266] Therefore, developing photoisomerizable molecules with better stability, less toxicity and more functionality is urgently needed.

6.3 Indirect photoresponsive drug delivery systems

Previous sections demonstrated the relationship between photopharmacology and photoresponsive drug delivery. By employing photocages and photoswitches, the "object" that light controls expand from functional molecules to polymer-based drug delivery systems for shared pharmaceutic aims. Apart from these, light-absorbing chromophores can also be exploited to construct PDDSs and achieve photoresponsive drug release in an indirect way. Upon light irradiation, light-absorbing chromophores can either generate ROS to cause photochemical reactions or transfer the energy into heat. Based on the mechanism, a variety of drug delivery systems in response to ROS or heat are developed with light-absorbing chromophores incorporated (Table 4).

6.3.1 ROS-responsive drug delivery systems with light irradiation. As light absorbers, photosensitizers (PSs) can generate a lot of strong oxidizing agents under certain wavelength light irradiation and further alter chemical shifts like disrupting the chemical structure by oxidizing substances[295] or causing cleavage of thioketal linkers.[274]

Based on light-induced oxidation, a liposome encapsulated with a photosensitizer aluminum phthalocyanine disulfonic acid (AlPcS2) was developed.[267] AlPcS2 adsorption to liposomes stabilized lipid bilayers and reduced their permeability. However, upon irradiation with tissue-penetrating red light, the AlPcS2-liposome system experienced a dramatic increase in lipid bilayer permeability. The permeability rose ten-fold compared to the baseline level. This substantial, light-triggered enhancement in permeability then facilitated the release of the liposome's payload. The release was shown to be a singlet oxygen mediated process, which could oxidize lipids containing unsaturated fatty acids in the liposomes, resulting in increased lipid bilayer permeability and release of cargo. Similar research was continued by constructing a NIR light-responsive liposome assembled from porphyrin-phospholipid and a small amount of unsaturated lipid dioleoylphosphatidylcholine (DOPC) for photo-oxidation.[268]

Table 4 A table summarizing strategies for indirect photoresponsive drug delivery systems that are mentioned in the review. AlPcS2, aluminum phthalocyanine disulfonic acid; DOX, doxorubicin; BPQDs, black phosphorus quantum dots; Ce6, chlorin e6; AIE, aggregation-induced emission; AlP, Al(III) phthalocyanine chloride disulfonic acid; ICG, indocyanine green; CCK8, a peptide derivative of the endogenous cholecystokinin ligand; and KDM3A, lysine-specific histone demethylase 3 A

Types	Photosensitizers	Drug vehicles	Light	Drugs/dyes	Ref.
ROS responsive drug delivery system	AlPcS2	Liposomes	590 nm	N/A	267
	Porphyrin	Liposomes	665 nm	DOX	268
	Selenium	Polymeric nanoparticles	785 nm	DOX	269
	BPODs	Polymeric nanoparticles	660 nm	CpG oligodeoxynucleotides	270
	Dendrimer phthalocyanine	Ternary complex	689 nm	Plasmid DNA conjugated with cationic peptide	271
	Ce6	Polymeric nanoparticles	660 nm	DOX and Ce6	272
	AIE photosensitizer	Polymeric nanoparticles	White light	Triptolide and AIE photosensitizer	273
	Ce6	Small-molecule based nanoparticles	660 nm	Cabazitaxel and Ce6	274
	AIP	Small-molecule based nanoparticles	660 nm	Camptothecin and AIP	275
	ICG	Liposomes	808 nm	DOX and ICG	276
	Verteporfin	Polymeric nanoparticles	690 nm	Dasatinib and verteporfin	277
	Ce6	Silica-coated UCNPs	980 nm	DOX and Ce6	278
Thermoresponsive drug delivery system	Gold nanocages	Gold nanocages coated with polymers	Ti: sapphire laser	DOX	279
	Gold coating	Gold coated liposomes	760 nm	CCK8	280
	Carbon nanotubes	Iron oxide nanoparticles	808 nm	DOX	281
	Gold nanorods	Nanogels	808 nm	Cisplatin and DOX	282
	Gold nanoparticles	Hydrogels	400–500 nm	Bevacizumab	283
	Gold nanorods	Hydrogels	808 nm	DC_AC50	284
	Gold nanorods	Nanofibers	808 nm	DOX and camptothecin	285
	ICG	Liposomes	800 nm	Calcein	286
	ICG	Liposomes	808 nm	ICG	287
	Gold nanoparticles	Gold nanoparticles	800 nm	ssDNA	288
	Gold–thiol bond	Gold nanoshells	800 nm	siRNA	289
	Prussian blue analogue	Gold nanoflowers	808 nm	siRNA	290
	Semiconducting polymer	Polymeric nanoparticles	1064 nm	CRISPER-Cas9	291
	Semiconducting polymer	Nanoclusters	1064 nm	KDM3A inhibitor	292
Others	Tungsten oxide nanoparticles	Tungsten oxide nanoparticles	405 nm and 808 nm	N/A	293
	Terbium-doped zinc oxide nanoparticles and polydopamine	Terbium-doped zinc oxide nanoparticles	Green light and 808 nm	Nitric oxide	294

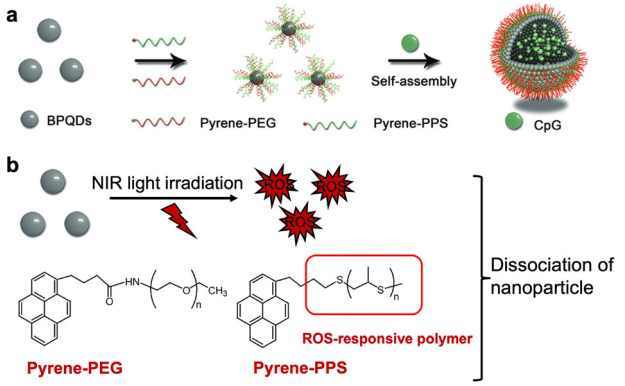

Fig. 29 (a) Preparation process of photoresponsive vehicles through self-assembly of amphiphilic BPQDs grafted with PEG and a ROS-sensitive polymer. (b) Mechasim of NIR light triggered production of ROS and the dissociation of designed vehicles for subsequent release of CpG for combined cancer imaging and immunotherapy (adapted from ref. 270 with permission from the © 2019 Wiley-VCH Verlag GmbH & Co. KGaA, Weinheim).

Likewise, polymeric nanoparticles can be designed to be responsive to photo-oxidation. For example, a NIR light-responsive polymeric nanoparticle composed of selenium-inserted copolymer and photosensitizer indocyanine green (ICG) was developed to load chemotherapeutics such as DOX.[269] NIR light irradiation oxidized the selenium-polymer, which triggered dissociation of polymeric nanoparticles and subsequent drug release. Moreover, ICG can generate hyperthermia upon light exposure, resulting in concurrent tumor ablation with chemotherapy. Recent research has produced NIR light-responsive black phosphorus quantum dot (BPQD) vehicles. These vehicles were prepared through the self-assembly of amphiphilic BPQDs that have been grafted with polyethylene glycol and a ROS-sensitive poly(propylene sulfide) (PPS) polymer (Fig. 29).[270] Moreover, immunoadjuvant CpG oligodeoxynucleotides were loaded in the cavity of the vehicles. Upon NIR laser irradiation, polymers were oxidized and transformed from hydrophobic to hydrophilic due to high levels of ROS generated, leading to disassembly of the vehicles. The developed systems exhibited concurrent PDT and immunotherapy, leading to primary tumor elimination, distant tumor growth and metastasis inhibition effectively.

Light-controlled release of therapeutics *via* oxidizable nanovehicles was implemented in developing biomacromolecule delivery. For instance, plasmid DNA has been conjugated with a cationic peptide containing a nuclear localization sequence to promote gene transfection.[271] This plasmid DNA construct was then loaded into phthalocyanine dendritic photosensitizer carriers for ocular gene delivery applications. Upon irradiation with 689 nm light, the nanovehicles were designed to destroy the endosomal membrane. This light-triggered endosomal disruption facilitated the escape of the plasmid DNA complexes, ultimately enabling their delivery to the cell nucleus. The effective gene transfection upon light irradiation was confirmed *in vitro* and *in vivo* in a Wistar rat eye model with reduced phototoxicity. The developed system achieves spatial control of gene delivery *via* light, which holds promising application in gene therapy for the treatment of a series of diseases.

In addition to photooxidation, thioketal and diselenide-containing linkers with ROS-cleavage ability can be introduced into the building blocks of drug delivery systems. A polymeric nanocarrier was constructed by self-assembly from an amphiphilic copolymer poly(ethylene glycol)-*b*-poly(ε-caprolactone) and an ROS-responsive polymer poly(thioketal phosphoester).[272] Chemotherapeutics DOX and PSs chlorin e6 (Ce6) were loaded. Upon NIR light irradiation, ROS produced by Ce6 was able to cleave thioketal linkers, which facilitated size shrinkage of nanovehicles for drug release. In the same modality, diselenide-containing crosslinked micelles and thioketal-containing amphiphilic block copolymers were constructed for NIR light-controlled drug release.[296,297] Recently, an ROS-responsive linker, a thioacetal ketone bond, was inserted into the widely employed polymer DSPE-PEG (1,2-distearoyl-*sn-glycero*-3-phosphoethanolamine-poly(ethylene glycol)), which can self-assemble into nanoparticles and then loaded Chinese medicine triptolide and an aggregation-induced emission (AIE) photosensitizer (Fig. 30).[273] Upon light irradiation, ROS generated from the AIE photosensitizer can cleave polymers, which resulted in dissociation of nanoparticles and cargo release. Triptolide is a Traditional Chinese Medicine, which can regulate autophagy homeostasis and inhibit protective autophagy of tumor cells due to the elevation of ROS. The combination of the autophagy inhibitor triptolide and PDT displays synergistic effects in a mouse breast cancer model and serves as an innovative modality in treating malignancies.

ROS-cleavable linkers can be used to link drug molecules as well, which not only act as building blocks of photoresponsive nanoplatforms, but also block the activity of the drug molecules. For example, a prodrug was synthesized by linking two

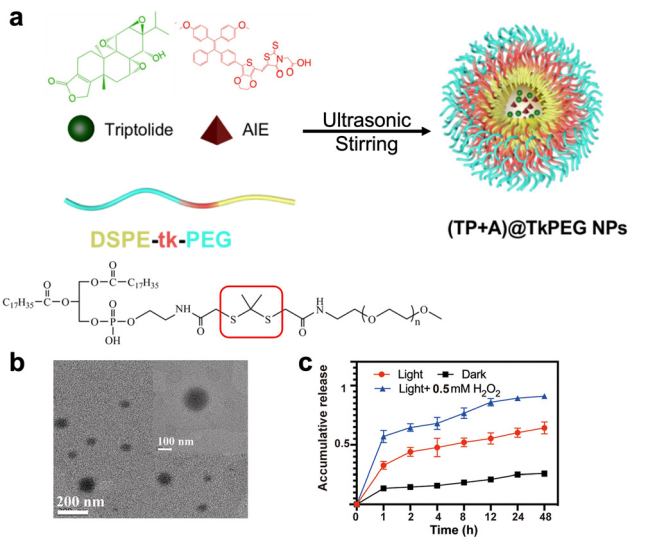

Fig. 30 (a) Schematic illustration of construction of an ROS responsive nanoherb synergistic system. (b) TEM image of the designed system and (c) drug release of the designed system in response to ROS (adapted from ref. 273 with permission from © 2023 American Chemical Society).

anticancer cabazitaxel (CTX) molecules *via* thioketal linkers.[274] The dimeric prodrug can self-assemble with Ce6 into nanoparticles. Light irradiation can not only trigger cleavage of the dimer and release of CTX, but also induce PDT for synergistic anti-tumor efficacy. A similar strategy was reported by preparing a nanoparticle using a photosensitizer Al(III) phthalocyanine chloride disulfonic acid and an ROS-activatable camptothecin prodrug.[275] The nanoparticle was able to trigger intracellular production of $^1O_2$ upon light illumination. This light-induced $^1O_2$ generation not only initiated the immediate disassembly of the nanoparticle, but also promoted the cytoplasmic delivery of the anticancer drug camptothecin, which was achieved *via* $^1O_2$-mediated rupture of the lysosomal membrane.

In a latest research study, a NIR photoactivatable microneedle-based transdermal drug delivery system with controllable drug release and effective imaging guidance was developed for treating melanoma.[276] Liposomes co-loaded with the photosensitizer ICG and ROS-activatable prodrug of DOX were contained in dissolvable polyvinylpyrrolidone microneedle arrays. The liposomes concentrated in the needle tips were released into the lesion upon applying the microneedle patch to the tumor site. Upon 808 nm light irradiation, ROS generated from ICG performed PDT and activated the ROS-activatable prodrug of DOX for combined therapy. Moreover, the fluorescence and photoacoustic imaging of ICG can be utilized to guide the treatment. The transdermal microneedle patch with photoresponsiveness curbed effective tumor growth and negligible side effects and cardiotoxicity by virtue of precise drug delivery.

Besides treating cancer, strategies that exploit ROS-activatable prodrugs and photosensitizers can be applied in treating other diseases. For example, a light-responsive drug delivery system incorporating an ROS-sensitive prodrug dasatinib and a photosensitizer verteporfin for treating choroidal neovascularization was reported (Fig. 31).[277] The prodrug was synthesized *via* linking two dasatinib molecules, as anti-angiogenic inhibitors, *via* thioketal linkers and the prodrug can self-assemble with verteporfin and amphiphilic polymers into nanoparticles. Upon 690 nm light illumination targeting the diseased eyes, an intraocular release of the anti-angiogenic drug dasatinib was observed. Concurrently, the verteporfin photosensitizer generated ROS, which selectively occluded the abnormal neovessels in the treated eyes. The developed system displays promising therapeutic efficacy against choroidal neovascularization with high biocompatibility to other tissues, providing an effective treatment modality *via* integrating a photoactivation process with combinational therapeutics into one simple nanosystem.

Apart from the NIR light-absorbing photosensitizers, visible light or UV light-absorbing photosensitizers could also be leveraged in the aforementioned strategy using an upconversion approach. For example, a NIR light-triggered, ROS-responsive upconverting nanoparticle system has been reported.[278] This system consisted of a $NaYF_4$:Yb,Er@$NaYF_4$ upconverting core, with a Ce6-doped mesoporous silica shell. A thioketal linker was coated on the outside of this core–shell structure *via* a silane coupling reaction to prevent premature release. Upon NIR light irradiation, the visible light emission upconverted by the UCNPs could then excite the Ce6 photosensitizer to produce ROS, which then promoted the cleavage of the thioketal linker. This cleavage, in turn, opened the "gate" of the mesoporous silica shell and allowed the release of the loaded cargos.

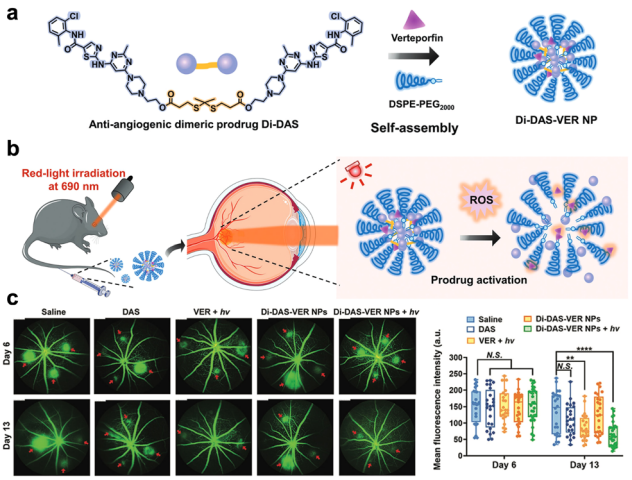

Fig. 31 (a) Schematic representation of self-assembly of nanoparticles by an anti-angiogenic dimeric ROS-sensitive prodrug dasatinib, a photosensitizer verteporfin, and amphiphilic polymers. (b) Schematic illustration showing the treatment process with the developed nanoparticles. In a laser-induced choroidal neovascularization mouse model, after intravenous administration of nanoparticles and subsequent application of 690 nm red light to the diseased eye, verteporfin-generated ROS would initiate the cleavage of the prodrug and lead the release of anti-angiogenic dasatinib intraocularly. (c) The representative fundus fluorescein angiography images and the corresponding quantitative analysis on days 6 and 13 are shown (adapted from ref. 277 with permission from © 2023 The Authors. Advanced Science published by Wiley-VCH GmbH).

In a nutshell, by incorporating photosensitizers into a drug delivery system, light-responsive drug release can be achieved either by the photooxidation or photocleavage process. ROS-sensitive substances can be encapsulated into the building blocks of nanocarriers or be employed to link the drug molecules. Such indirect PDDSs based on ROS responsiveness is a good alternative to realize precise control of drug release *via* light and combinational therapy with PDT. However, there are some limitations need to be addressed. It is well known that a tumor microenvironment is extremely complex especially featuring hypoxia.[298,299] The consumption of oxygen will further aggravate the hypoxic tumor microenvironment and facilitate tumor metastasis and progression.[300,301] Moreover, there is a competition between ROS utilization in exerting PDT and cleaving chemical bonding or oxidizing sensitive substances. It is certain that the efficacy of one part will be undermined. In the future, more endeavors are encouraged to reprogram tumor microenvironments like enhancing oxygen transport.

6.3.2 Thermo-responsive drug delivery systems with light irradiation. Carbon nanomaterials, gold nanomaterials, indocyanine green, and metallic sulfides/oxides are the commonly employed photothermal agents. By encapsulating photothermal agents into a thermo-responsive drug delivery system, light-controlled drug release can be achieved in an indirect way.

Upon light irradiation, photothermal agents can transfer the light energy into heat. The increase in temperature will enhance the drug release either by the phase change mechanism or disruption of the carrier structure. Photothermal effect-based drug delivery systems have been widely explored because of their tunable optical properties and flexible surface chemistry. The comprehensive photothermal effect-based drug delivery systems of a variety of materials have been summarized.[302] In this section, we will focus on photothermal effect-triggered dissociation systems highlighting their drug release mechanism.

Thermo-responsive polymers and lipids can be exploited together with photothermal agents to construct photothermal-responsive drug delivery systems. For example, a thermo-responsive polymer poly(*N*-isopropylacrylamide-*co*-acrylicamide) with a low critical solution temperature (LCST) of 39 °C was incorporated into gold nanocages (Fig. 32).[279] Upon light irradiation, the photothermal effects induced by gold nanocages can disrupt the hydrophilic–hydrophobic balance of thermo-responsive polymers. When the temperature increased above the lower LCST of the polymers, it rendered them hydrophobic. This hydrophobic transition caused the polymers to collapse, which, in turn, triggered the release of any encapsulated drugs or other payloads. The same modality can be applied to liposomes. A thermosensitive liposome containing dipalmi-toylphosphatidylcholine (DPPC) was fabricated.[280] DPPC is stable at physiological temperature while melts when temperature increases above its phase transition temperature 41 °C, inducing the disintegration of liposomes and facilitates cargo release. Furthermore, indocyanine green can also be incorporated into liposomes to trigger drug release by generating heat.[303]

In other works, iron oxide nanoparticles were deposited onto the surface of carbon nanotubes (CNTs), creating hybrid nanocomposite structures.[281] These hybrid nanocomposites were then coated with DSPE-PEG (1,2-distearoyl-*sn*-*glycero*-3-phosphoethanolamine-*N*-[methoxy(polyethylene glycol)]) to improve their dispersibility in various media. Subsequently, the nanocomposites were encapsulated in the matrix of 1-myristyl alcohol (1-MA) with a phase transition temperature of ~42 °C. Upon NIR light irradiation, light energy was absorbed by CNTs and converted into heat, which then melt the 1-MA and induce subsequent release of encapsulated drug and CNTs. The light-controlled drug delivery system that shares similar structures *via* combining photothermal agents and thermo-sensitive components with appropriate LCST represents a validated method for wide biomedical applications.

Recently, a biomimetic cisplatin-crosslinked DOX-loaded nanogel functionalized with photothermal gold nanorods (GNRs) was reported (Fig. 33).[282] Upon NIR light irradiation, the heat generated by GNRs destroyed the structure of the physically cross-linked nanogel, which triggered the release of cisplatin and DOX. The chemotherapeutics and light-induced hyperthermia displayed a synergistic PTT and chemotherapy against tumors. In the design, the nanogel was furthermore cloaked with a cancer cell membrane, which showed efficient accumulation by homologous tumor targeting and possessed long-term retention in a tumor microenvironment. Photothermal agents like GNRs and gold nanoparticles can be embedded

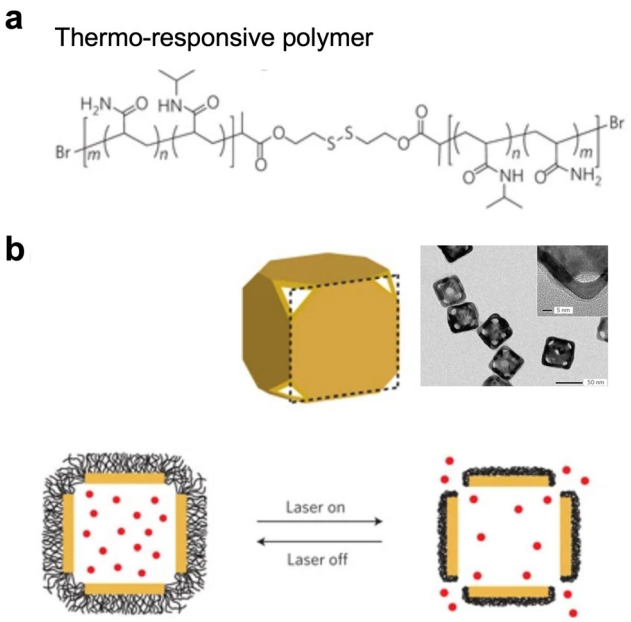

Fig. 32 (a) Chemical structure of the pNIPAAm-*co*-pAAm copolymer with an LSCT at 39 °C. (b) Schematic illustrating the working mechanism of the system. NIR light was absorbed by the nanocage and converted into heat, promoting the polymer to collapse and thus release the cargo (adapted from ref. 279 with permission from the © 2009, Springer Nature Limited).

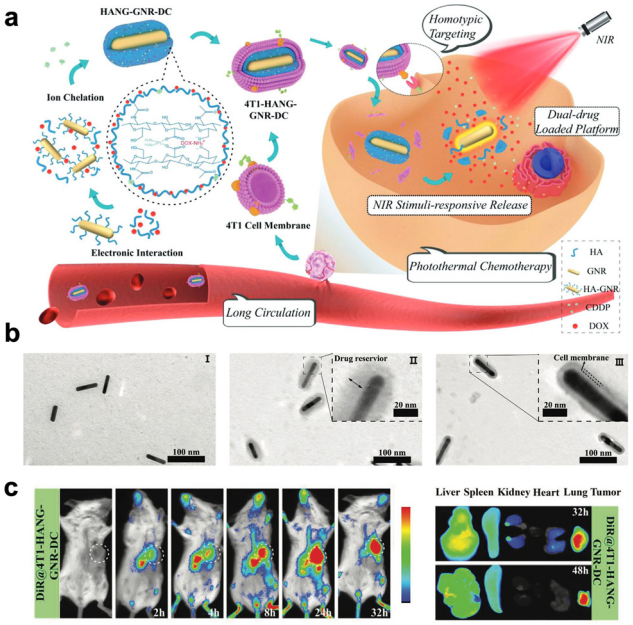

Fig. 33 (a) Schematic illustration of preparation of NIR light-responsive nanogels and their application for combined chemotherapy and homotypic targeted PTT. (b) TEM images of GNR (I), HANG-GNR-DC (II), and 4T1-HANG-GNR-DC (III). (c) Extended tumor retention of the designed system (adapted from ref. 282 with permission from the © 2020 The Authors. Published by Wiley-VCH Verlag GmbH & Co. KGaA, Weinheim).

in thermo-responsive hydrogels for other biomedical applications especially in treating eye diseases. For example, a light-responsive hydrogel for controlled delivery of bevacizumab was reported by incorporating gold nanoparticles in agarose gels for age-related macular degeneration treatment.[283] Upon visible light irradiation for successive cycles, the gold nanoparticles utilized in the drug delivery system perform photo-thermal conversion and induce local temperature rise. When temperature is higher than the melting point (45 °C) of agarose, sol–gel transition initiated, resulting in drug diffusion. In the experiments, the gold nanoparticles/hydrogel system exhibited enhanced drug release by three-fold in comparison with hydrogels without gold nanoparticles. The visible light can efficiently penetrate transparent eye tissues and the light-triggered release of the developed system was confirmed in a cadaver bovine eye model.

Similarly, GNRs were encapsulated into hydrogels as a treatment modality for uveal melanoma (UM) (Fig. 34).[284] In the design, Traditional Chinese Medicine puerarin and chitosan can spontaneously assemble into a nanofiber hydrogel under a rapid heating–cooling process. The gene-targeted anti-cancer drug DC_AC50 and GNRs were loaded inside. Upon NIR light irradiation, the photothermal conversion of GNRs regulated the mechanical strength of the hydrogel, facilitated sol–gel transformation and realizes on-demand drug release. The light-responsive hydrogel was proved to efficiently suppress tumor growth without causing damage to normal tissue. The combination of PTT using GNRs and chemotherapy offered a promising strategy for developing a multifunctional therapeutic platform against intraocular tumors. This approach exhibited great potential for clinical translation and application in the treatment of UM. In another research, a sequential drug release-based delivery system was fabricated to be potentially applied in complex diseases.[285] The research explored a layer-by-layer nanofiber platform that incorporated the anticancer drugs CPT and DOX. Linear polyethylenimine was exploited as the first layer and poly(sodium 4-styrenesulfonate) was utilized to compensate for the positive charge on the preceding layer.

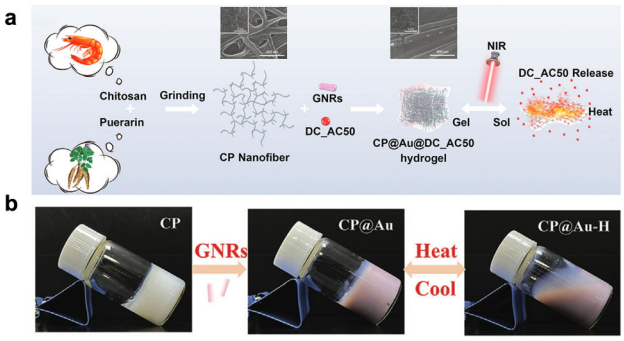

Fig. 34 (a) Schematic illustration of the preparation of the designed NIR light-responsive hydrogel. (b) Photographs of the CP hydrogel and gel–sol transition of the CP@Au hydrogel under cooling/heating conditions (adapted from ref. 284 with permission from the © 2021 The Authors. Advanced Science published by Wiley-VCH GmbH).

DOX was initially released to a lesser extent at pH 7.4, with a slightly higher release observed at pH 6. GNRs were encapsulated into the nanofibers to generate local heat *via* plasmonic resonance upon NIR light irradiation. The heat-responsive polymers in the system could undergo controlled shrinking and swelling, enabling regulated drug release. Upon exposure to NIR light, the CPT was sequentially released in a controlled manner, followed by further release of DOX. This study presented a flexible toolbox for targeted drug delivery that could be employed to treat diverse topical diseases.

As a widely exploited photothermal agent, ICG was investigated by virtue of its NIR light responsiveness, anticipated photothermal conversion efficiency and biocompatibility.[304] A light-activated liposome for controlled intravitreal delivery of calcein was reported by loading ICG as a light-sensitive moiety into hyaluronic acid (HA)-coated liposomes.[286] The HA-coated liposomes exhibited stronger binding to proteins compared to the PEG-coated liposomes when incubated with vitreous humor samples. The HA-coated liposomes also resulted in the enrichment of proteins related to collagen interactions. This enhanced protein binding and protein corona composition may explain the improved stability and reduced mobility of the HA-coated liposomes within the vitreous fluid environment. Upon 800 nm light irradiation, enhanced calcein release was observed due to detriment of stability of liposomes. In another approach, ICG was assembled in liposomes to construct a PDDS for the treatment of retinoblastoma.[287] By incorporating into liposomes, the limitations of free ICG molecules such as quenching, aggregation and instability in biological environments were overcame. Moreover, the PTT induced by ICG can be well employed for the treatment. The liposomes could achieve specific tumor tissue targeting and accumulation. 808 nm light could effectively penetrate transparent eye tissues for efficient PTT. The combination of PTT and light-activated liposomes is a promising alternative for intravenous and ocular drug delivery.

The photothermal effect-based PDDSs can also be applied in biomacromolecule delivery to achieve light-controlled gene therapy. For example, a gold nanoparticle-based complex was formulated to release single-stranded DNA (ssDNA) from its surface when illuminated with plasmon-resonant light.[288] The ssDNA was bound to complementary DNA sequences that were modified on gold nanoparticles. Local surface light illumination allows DNA thermal dehybridization and subsequent release of ssDNA. Similarly, a technique of nucleic acid delivery by conjugating siRNA to hollow gold nanoshells with covalent Au–S bonds was developed.[289] Upon NIR light irradiation, nanoparticle plasmons triggered the disassembly of the system and released the drug molecules by thermalizing the gold–thiol bond. Moreover, vapor microbubbles could form upon irradiation of plasmonic nanoparticles by virtue of photoacoustic effects, which can disrupt endosome membranes to facilitate endosomal escape as a result.

There are other novel materials which can be utilized for transferring light to heat. For example, Prussian blue analogue was exploited as a photothermal nanomaterial and was encapsulated into gold nanoflowers coated with a tumor-targeting

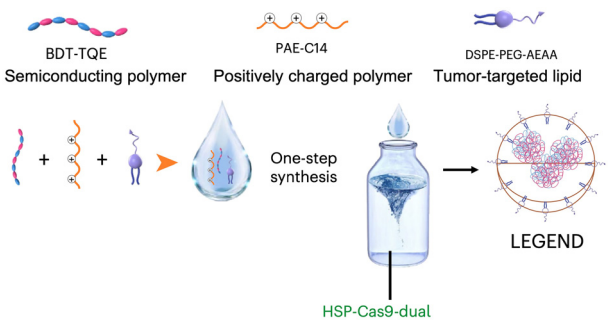

Fig. 35 Schematic illustration depicting the engineering process of LEGEND synthesis. The developed system could mediate intracellular genome editing of cancer cells and extracellular modulation of the tumor microenvironment to function synergistically and enhance the efficacy of adoptive T cells (adapted from ref. 291 with permission from the © 2023, The Author(s), under exclusive license to Springer Nature Limited).

peptide and siRNA.[290] NIR-light stimulation could activate the plasmonic theranostic system and achieve selective siRNA delivery in targeted tumors. In latest research, an intratumoral gene editing nanovehicle activated by non-invasive NIR light (LEGEND) was developed by self-assembly of a semiconducting polymer, a positively charged polymer and a tumor-targeted lipid (Fig. 35).[291] A heat-inducible CRISPER-Cas9 targeting HSP70 and BAG3 was loaded. Upon 1064 nm light irradiation, the semiconducting polymer can transfer light absorbed into heat, which initiates gene transfection. The combination of the designed system with adoptive cell therapy displays synergistic treatment efficacy in primary tumor growth and metastasis inhibition. Similarly, a semiconducting polymer nanomanipulator that can effectively manipulate intracellular protein expression with synergized PTT for thermal sensitization and tumor growth inhibition was reported.[292] The developed system included a light-absorbing semiconducting polymer core that promoted photothermal transduction. It also incorporated a lysine-specific histone demethylase 3A (KDM3A) inhibitor as a downstream effector to regulate protein expression. This dual-functional payload was loaded into a thermo-responsive lipid shell. 1064 nm light irradiation could be transferred into heat by the semiconducting polymer. The heat generated not only performed PTT but also melted the lipid shell for on-demand release of the KDM3A inhibitor, resulting in concurrent tumor growth and metastasis inhibition.

Taken together, photothermal agents and thermosensitive components are crucial for constructing PDDSs based on photothermal effects. The light absorbed by photothermal agents can be transferred into heat, which disrupts the balance of thermosensitive components, promotes dissociation of particles, and promotes drug release. The indirect PDDSs based on thermo-responsiveness are a good option for precise control of drug release with combination therapy with PTT. Furthermore, it is reported that mild hyperthermia can loosen tumor tissues and expand vasculature, which can facilitate oxygen transport and promote immune cell infiltration.[305,306] It provides an optional combination therapy potential for treating a variety of malignancies. However, it is noted that the temperature rise from heat generation should be well controlled since inevitable burning can occur if the temperature is too high, resulting in side effects. Comprehensive evaluation and investigation on parameters exploited in light irradiation should be done.

6.3.3 Orthogonal (dual) light-responsive drug delivery systems. The strategies based on light-induced ROS generation and photothermal conversion to construct PDDSs are intensively explored. Further research can be expanded to integrate these strategies together to realize multiple wavelength photoresponsiveness.

Lately, an orthogonal light-triggered photochromic nanoparticle to induce multiple effects was reported.[293] In the study, tungsten oxide (WO3) nanoparticles with photochromic characteristics were exploited, which could convert the photonic energy from visible light (405 nm) and NIR light (808 nm) into ROS and heat, respectively, for DNA cleavage, cell death induction and biofilm destruction. In another research, a dual-light-responsive nanoparticle constructed by terbium-doped zinc oxide nanoparticles conjugated with polydopamine was reported (Fig. 36).[294] Furthermore, the developed drug vehicle was modified on the surface of contact lenses to boost its bioavailability. Upon green light irradiation, lots of ROS were generated for efficient bacterial killing. Moreover, 808 nm light irradiation could be converted to heat *via* polydopamine. Subsequently, nitric oxide was produced and released to concurrently combat bacteria with a reduced inflammatory response. The platform provides a promising strategy for the prevention and treatment of bacterial keratitis and heralds promising clinical translation in global vision health improvement. Compared with single light regulation, the synergetic and complementary effects of two beams of light possess significant advantages in both improving accuracy and enhancing efficiency. The development of an orthogonal light regulation strategy to construct such an indirect PDDS is a promising new method to meet the high requirements of biomedical applications and precision medicine.

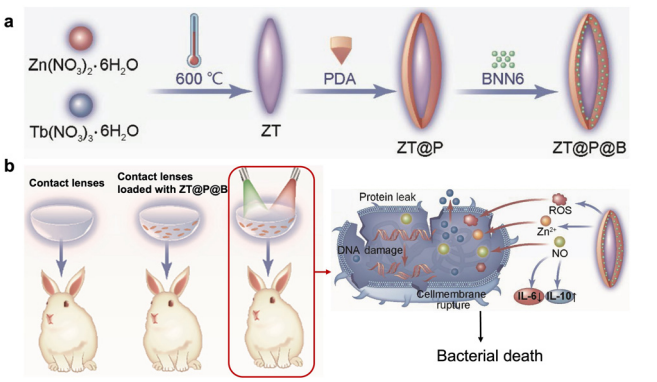

Fig. 36 Schematic illustration of (a) the synthesis of terbium-doped zinc oxide nanoparticles conjugated with polydopamine and (b) responding to dual-light to generate ROS and nitric oxide for sterilization and regulation of immunity in a rabbit model of bacterial keratitis (adapted from ref. 294 with permission from the © 2022, Tsinghua University Press).

To sum up, indirect PDDSs are introduced in the section, with an emphasis on the mechanism underlying light-triggered drug release and combination of PDT and PTT. In the future, the rational design of ROS-responsive and heat-responsive substances can be a direction to construct more novel and biocompatible building blocks. Moreover, the improvement of treatment efficacy for combination therapy can be explored. For example, the immunogenic cell death (ICD) induced by PDT and PTT can be exploited for cancer and infectious disease treatment,[307,308] which can be united with biological functions of cargo loaded in drug vehicles. In a nutshell, the development of such indirect PDDSs represents an alternative and validated toolbox to achieve precision medicine *via* light.

7. Conclusion

In this review, we summarized the development and recent advances in the design of light-activatable molecules and photoresponsive drug delivery systems, with a full illustration of mechanisms behind the photoresponsiveness and an emphasis on relationships between the two research fields. With extreme similarity to biological systems, light surpasses in its ability to control biological activity in a spatiotemporal way *via* adjusting the parameters of light irradiation (time, space, and power). The light-controlled "object" can be bioactive molecules or drug delivery systems. The common goal of both strategies is to release functional active species at the right time and right place using light. This approach enables precise regulation of biological activity, which has promising biomedical applications, such as treating various diseases.

8. Outlook

Light-activatable moieties, such as photocages and photoswitches, serve as a fundamental chemical basis for constructing a light-controlled toolbox with diverse potential applications. With the detailed electron transfer mechanisms, different chemical derivatives of conventional PPGs are demonstrated, with the emphasis on strategies of prolonging the excitation wavelength for broad biomedical applications. The photocaged small-molecule prodrugs are not only developed to inhibit protein functions but also widely exploited to control targeted protein degradation, aligning with the development of PROTAC technology in recent years. With the advancement in genetically encoded expansion strategies and nucleotide synthesis techniques, photoresponsive biological macromolecules are also developed to directly manipulate corresponding biological activities.

Light-activatable moieties can also be incorporated into drug delivery vehicles for constructing irreversible or reversible PDDSs. PPGs and photoswitches can be modified on building blocks or inserted into the backbone of drug delivery systems. The core for light-triggered drug release is based on the conformation change of drug delivery systems due to the removal of PPGs or isomerization of photoswitches. Based on the properties of drug delivery systems, the delivery cargos vary from small drug molecules to biomacromolecule therapeutics, which provides a validated toolbox for light-controlled chemotherapy, immunotherapy, gene therapy, *etc.* Furthermore, there are two types of indirect PDDSs introduced in the review based on light-induced generation of oxidized substrates or heat. ROS-responsive and thermo-responsive drug delivery systems that encapsulate light-absorbing chromophores not only greatly widen the variety of PDDSs but also offer the opportunity of combinational therapy with PDT and PTT.

However, there still are a lot of issues to be addressed to finally bring the strategy of light-controlled biological activities into clinical settings. Firstly, the penetration of light is a long-standing problem. Increased efforts are needed to develop advanced light-delivery technology to be properly applied in the human body. Secondly, the biosafety of light-activatable molecules and PDDSs is a concern. Since the metabolites of some PPGs and photoswitches exhibit toxicity, it is crucial to develop light-controlled molecules with high biocompatibility. Furthermore, the toxicity and immunogenicity of excipients that facilitate the fabrication of drug delivery systems also require delicate screening. Meanwhile, the toxicity of light irradiation itself also needs to be considered. The last but not the least, the precise control over synthesis and fabrication of light-controlled molecules and PDDSs is key to their scaled-up manufacturing at reduced cost, which is essential for clinical translation.

In the future, three aspects can be focused to advance photopharmacology and photoresponsive drug delivery: (1) developing advanced light delivery techniques. High-tech optical technologies such as optical fibers and implantable wireless LEDs with good biocompatibility are promising for treating diseases in deep tissues. Precise illumination is required to minimize side effects; (2) developing light-activatable molecules with long-wavelength light excitation and low-toxicity metabolites. The colloidal stability, toxicity, and pharmacokinetic profiles of light-activatable molecules and drug delivery systems need full evaluation; and (3) optimizing the production process. Comprehensive research on the synthesis and preparation of light-controlled molecules and drug delivery systems needs to be carried out to minimize batch-to-batch variations and promote industrial manufacturing on a large scale at a low cost.

By advancing photochemistry, more light-controlled bioactive molecules with long-wavelength light excitation and low-toxicity metabolites will be developed and applied. With the progress in nanotechnology and biomaterials, more PDDSs with excellent properties and reliable responses to light will be constructed for the treatment of a variety of relevant diseases. The emergence of new light delivery technologies is expected to broaden the applications of light-controlled molecules and drug delivery systems, facilitating their transition from bench to bedside. In general, using light to regulate bioactive molecules and drug delivery systems represents a promising strategy for controlling biological activities in pharmaceutical applications.

Author contributions

Yuwei Liu: conceptualization, writing – original draft (photoresponsive drug delivery), and writing – review and editing.

Tianyi Wang: conceptualization, writing – original draft (photopharmacology), and writing – review and editing. Weiping Wang: conceptualization, funding acquisition, supervision, and writing – review and editing.

Data availability

No primary research results, software or code have been included and no new data were generated or analysed as part of this review.

Conflicts of interest

The authors declare no conflict of interest.

Acknowledgements

This work was supported by the National Natural Science Foundation of China (Excellent Young Scientists Fund, No. 82222903).

References

1 N. Ankenbruck, T. Courtney, Y. Naro and A. Deiters, *Angew. Chem., Int. Ed.*, 2018, **57**, 2768–2798.
2 S. Jia and E. M. Sletten, *ACS Chem. Biol.*, 2021, **17**, 3255–3269.
3 S. Senapati, A. K. Mahanta, S. Kumar and P. Maiti, *Signal Transduction Targeted Ther.*, 2018, **3**, 7.
4 E. Silva and D. J. Mooney, *J. Thromb. Haemostasis*, 2007, **5**, 590–598.
5 N. Rahoui, B. Jiang, N. Taloub and Y. D. Huang, *J. Controlled Release*, 2017, **255**, 176–201.
6 S. Mura, J. Nicolas and P. Couvreur, *Nat. Mater.*, 2013, **12**, 991–1003.
7 P. Vinchhi, S. U. Rawal and M. M. Patel, *Drug Delivery Devices and Therapeutic Systems*, Elsevier, 2021, pp. 267–288.
8 Y. Li, W. Lv, L. Wang, Y. Zhang, L. Yang, T. Wang, L. Zhu, Y. Wang and W. Wang, *Nano Res.*, 2021, **14**, 2630–2636.
9 S. Voß, L. Klewer and Y.-W. Wu, *Curr. Opin. Chem. Biol.*, 2015, **28**, 194–201.
10 T. J. Dougherty, C. J. Gomer, B. W. Henderson, G. Jori, D. Kessel, M. Korbelik, J. Moan and Q. Peng, *J. Natl. Cancer Inst.*, 1998, **90**, 889–905.
11 T. J. Dougherty and S. L. Marcus, *Eur. J. Cancer*, 1992, **28**, 1734–1742.
12 A. F. dos Santos, D. Q. de Almeida, L. F. Terra, M. S. Baptista and L. Labriola, *J. Cancer Metastasis Treat.*, 2019, **5**, 10.20517.
13 Y.-G. Qiang, X.-P. Zhang, L. Jian and Z. Huang, *Chin. Med. J.*, 2006, **119**, 845–857.
14 S. L. Marcus, *Photodynamic therapy*, CRC Press, 2020, pp. 219–268.
15 J. Feather, I. Driver, P. King, C. Lowdell and B. Dixon, *Lasers Med. Sci.*, 1990, **5**, 345–350.
16 A. Premasiri, Development of an efficient, smart, and portable photonic light delivery system for use in photodynamic therapy of esophageal carcinoma, Southern Methodist University, 2008.
17 M. R. Hamblin and T. Hasan, *Photochem. Photobiol. Sci.*, 2004, **3**, 436–450.
18 M. F. Isaac-Lam and T. Nguyen, *TTU J. Biomed. Sci.*, 2023, **2**, 9–28.
19 K. Hüll, J. Morstein and D. Trauner, *Chem. Rev.*, 2018, **118**, 10710–10747.
20 W. A. Velema, W. Szymanski and B. L. Feringa, *J. Am. Chem. Soc.*, 2014, **136**, 2178–2191.
21 Y. Zhou, H. Ye, Y. Chen, R. Zhu and L. Yin, *Biomacromolecules*, 2018, **19**, 1840–1857.
22 A. Y. Rwei, W. Wang and D. S. Kohane, *Nano Today*, 2015, **10**, 451–467.
23 Y. Zhang, K. Long and W. Wang, *JoVE*, 2023, e64677.
24 D. Kolarski, W. Szymanski and B. L. Feringa, *Med. Res. Rev.*, 2025, **45**, 968–984.
25 J. Liu, W. Kang and W. Wang, *Photochem. Photobiol.*, 2022, **98**, 288–302.
26 Y. Yang, K. Long, Y. Chu, H. Lu, W. Wang and C. Zhan, *Adv. Funct. Mater.*, 2024, **34**, 2402975.
27 Y. Li, Y. Zhang and W. Wang, *Nano Res.*, 2018, **11**, 5424–5438.
28 D. F. Costa, L. P. Mendes and V. P. Torchilin, *Adv. Drug Delivery Rev.*, 2019, **138**, 105–116.
29 L. V. M. de Assis, P. N. Tonolli, M. N. Moraes, M. S. Baptista and A. M. de Lauro Castrucci, *J. Photochem. Photobiol., C*, 2021, **47**, 100403.
30 K. Kim, H. Park and K.-M. Lim, *Toxicol. Res.*, 2015, **31**, 97–104.
31 S. Mallidi, S. Anbil, A. L. Bulin, G. Obaid, M. Ichikawa and T. Hasan, *Theranostics*, 2016, **6**, 2458–2487.
32 R. Weissleder, *Nat. Biotechnol.*, 2001, **19**, 316–317.
33 P. Kobauri, F. J. Dekker, W. Szymanski and B. L. Feringa, *Angew. Chem.*, 2023, e202300681.
34 F. Iseppon and M. Arcangeletti, *STEMedicine*, 2020, **1**, e43.
35 I. M. Welleman, M. W. Hoorens, B. L. Feringa, H. H. Boersma and W. Szymański, *Chem. Sci.*, 2020, **11**, 11672–11691.
36 K. Sitkowska, M. F. Hoes, M. M. Lerch, L. N. Lameijer, P. van der Meer, W. Szymański and B. L. Feringa, *Chem. Commun.*, 2020, **56**, 5480–5483.
37 W. R. Browne and B. L. Feringa, *Mol. Switches*, 2011, **1**, 121–179.
38 E. Beltrán-Gracia, A. López-Camacho, I. Higuera-Ciapara, J. B. Velázquez-Fernández and A. A. Vallejo-Cardona, *Cancer Nanotechnol.*, 2019, **10**, 1–40.
39 B. Y. Kim, J. T. Rutka and W. C. Chan, *N. Engl. J. Med.*, 2010, **363**, 2434–2443.
40 K. Greish, *Cancer Nanotechnol.: Methods Protoc.*, 2010, 25–37.
41 F. Danhier, *J. Controlled Release*, 2016, **244**, 108–121.
42 R. K. Thapa and J. O. Kim, *J. Pharm. Invest.*, 2023, **53**, 19–33.

43 S. Dolati, S. Sadreddini, D. Rostamzadeh, M. Ahmadi, F. Jadidi-Niaragh and M. Yousefi, *Biomed. Pharmacother.*, 2016, **80**, 30–41.
44 S. Li, J. Su, W. Cai and J.-X. Liu, *Front. Pharmacol.*, 2021, **12**, 699245.
45 A. C. Anselmo and S. Mitragotri, *J. Controlled Release*, 2014, **190**, 531–541.
46 M. Di Martino, L. Sessa, R. Diana, S. Piotto and S. Concilio, *Molecules*, 2023, **28**, 3712.
47 A. Xie, S. Hanif, J. Ouyang, Z. Tang, N. Kong, N. Y. Kim, B. Qi, D. Patel, B. Shi and W. Tao, *EBioMedicine*, 2020, **56**, 102821.
48 P. Klán, T. Šolomek, C. G. Bochet, A. Blanc, R. Givens, M. Rubina, V. Popik, A. Kostikov and J. Wirz, *Chem. Rev.*, 2013, **113**, 119–191.
49 Y. V. Il'ichev, M. A. Schwörer and J. Wirz, *J. Am. Chem. Soc.*, 2004, **126**, 4581–4595.
50 A. Gandioso, M. Palau, A. Nin-Hill, I. Melnyk, C. Rovira, S. Nonell, D. Velasco, J. García-Amorós and V. Marchán, *ChemistryOpen*, 2017, **6**, 375–384.
51 Y. Zheng, M. Gao, M. Wijtmans, H. F. Vischer and R. Leurs, *Pharmaceuticals*, 2024, **17**, 536.
52 P. P. Goswami, A. Syed, C. L. Beck, T. R. Albright, K. M. Mahoney, R. Unash, E. A. Smith and A. H. Winter, *J. Am. Chem. Soc.*, 2015, **137**, 3783–3786.
53 P. Shrestha, D. Kand, R. Weinstain and A. H. Winter, *J. Am. Chem. Soc.*, 2023, **145**, 17497–17514.
54 J. A. Peterson, C. Wijesooriya, E. J. Gehrmann, K. M. Mahoney, P. P. Goswami, T. R. Albright, A. Syed, A. S. Dutton, E. A. Smith and A. H. Winter, *J. Am. Chem. Soc.*, 2018, **140**, 7343–7346.
55 C. Brieke, F. Rohrbach, A. Gottschalk, G. Mayer and A. Heckel, *Angew. Chem., Int. Ed.*, 2012, **51**, 8446–8476.
56 H. Wu, Y. S. Chua, V. Krungleviciute, M. Tyagi, P. Chen, T. Yildirim and W. Zhou, *J. Am. Chem. Soc.*, 2013, **135**, 10525–10532.
57 N. Yasuike, C. Kachi-Terajima, A. Karin, T. Mino and G. A. Woolley, *Org. Biomol. Chem.*, 2022, **20**, 8649–8656.
58 D. Prischich, N. Camarero, J. Encinar Del Dedo, M. Cambra-Pellejà, J. Prat, L. Nevola, A. Martín-Quirós, E. Rebollo, L. Pastor, E. Giralt, M. I. Geli and P. Gorostiza, *iScience*, 2023, **26**, 107899.
59 X. Gómez-Santacana, S. Panarello, X. Rovira and A. Llebaria, *Curr. Opin. Pharmacol.*, 2022, **66**, 102266.
60 Y. Norikane and N. Tamaoki, *Org. Lett.*, 2004, **6**, 2595–2598.
61 S. Sahu, A. S. Amrutha and N. Tamaoki, *Med. Res. Rev.*, 2025, DOI: **10.1002/med.22106**.
62 H. M. D. Bandara and S. C. Burdette, *Chem. Soc. Rev.*, 2012, **41**, 1809–1825.
63 P. Pfaff, K. T. G. Samarasinghe, C. M. Crews and E. M. Carreira, *ACS Cent. Sci.*, 2019, **5**, 1682–1690.
64 D. Fang, Z.-Y. Zhang, Z. Shangguan, Y. He, C. Yu and T. Li, *J. Am. Chem. Soc.*, 2021, **143**, 14502–14510.
65 C. Knie, M. Utecht, F. Zhao, H. Kulla, S. Kovalenko, A. M. Brouwer, P. Saalfrank, S. Hecht and D. Bléger, *Chem. – Eur. J.*, 2014, **20**, 16492–16501.
66 B. L. Feringa, *Angew. Chem., Int. Ed.*, 2017, **56**, 11060–11078.
67 J. Sheng, W. Danowski, S. Crespi, A. Guinart, X. Chen, C. Stahler and B. L. Feringa, *Chem. Sci.*, 2023, **14**, 4328–4336.
68 K. Singh, S. J. Staig and J. D. Weaver, *J. Am. Chem. Soc.*, 2014, **136**, 5275–5278.
69 T. Neveselý, M. Wienhold, J. J. Molloy and R. Gilmour, *Chem. Rev.*, 2022, **122**, 2650–2694.
70 J. Keyvan Rad, Z. Balzade and A. R. Mahdavian, *J. Photochem. Photobiol., C*, 2022, **51**, 100487.
71 H. Gao, T. Guo, Y. Chen, Y. Kong and Z. Peng, *J. Mol. Struct.*, 2016, **1123**, 426–432.
72 G. W. Goodall and W. Hayes, *Chem. Soc. Rev.*, 2006, **35**, 280–312.
73 R. B. Woodward and R. Hoffmann, *Angew. Chem., Int. Ed. Engl.*, 1969, **8**, 781–853.
74 I. Cazin, E. Rossegger, G. Guedes de la Cruz, T. Griesser and S. Schlögl, 2021, **13**.
75 C. N. Zhu, C. Y. Li, H. Wang, W. Hong, F. Huang, Q. Zheng and Z. L. Wu, *Adv. Mater.*, 2021, **33**, 2008057.
76 B. Liu and S. Thayumanavan, *Cell Rep. Phys. Sci.*, 2020, **1**, 100271.
77 Y. Yuan, J. Liu and B. Liu, *Angew. Chem., Int. Ed.*, 2014, **53**, 7163–7168.
78 P. Pei, C. Sun, W. Tao, J. Li, X. Yang and J. Wang, *Biomaterials*, 2019, **188**, 74–82.
79 C. Song, Z. Wang, Z. Yin, D. Xiao and D. Ma, *Chem Catal.*, 2022, **2**, 52–83.
80 M. L. Brongersma, N. J. Halas and P. Nordlander, *Nat. Nanotechnol.*, 2015, **10**, 25–34.
81 J. Wang, Y. Li, L. Deng, N. Wei, Y. Weng, S. Dong, D. Qi, J. Qiu, X. Chen and T. Wu, *Adv. Mater.*, 2017, **29**, 1603730.
82 Q. Fan, L. Wu, Y. Liang, Z. Xu, Y. Li, J. Wang, P. D. Lund, M. Zeng and W. Wang, *Appl. Energy*, 2021, **292**, 116871.
83 Y. Jiang, J. Huang, C. Xu and K. Pu, *Nat. Commun.*, 2021, **12**, 742.
84 R. C. Oslund, T. Reyes-Robles, C. H. White, J. H. Tomlinson, K. A. Crotty, E. P. Bowman, D. Chang, V. M. Peterson, L. Li, S. Frutos, M. Vila-Perelló, D. Vlerick, K. Cromie, D. H. Perlman, S. Ingale, S. D. O. Hara, L. R. Roberts, G. Piizzi, E. C. Hett, D. J. Hazuda and O. O. Fadeyi, *Nat. Chem. Biol.*, 2022, **18**, 850–858.
85 D. Spector, K. Pavlov, E. Beloglazkina and O. Krasnovskaya, *Int. J. Mol. Sci.*, 2022, **23**, 14511.
86 S. Alonso-de Castro, A. L. Cortajarena, F. López-Gallego and L. Salassa, *Angew. Chem., Int. Ed.*, 2018, **57**, 3143–3147.
87 Z. Wang, N. Wang, S.-C. Cheng, K. Xu, Z. Deng, S. Chen, Z. Xu, K. Xie, M.-K. Tse, P. Shi, H. Hirao, C.-C. Ko and G. Zhu, *Chem*, 2019, **5**, 3151–3165.
88 M. Bian, Q. Q. Ma, Y. Wu, H. H. Du and G. Guo-Hua, *J. Enzyme Inhib. Med. Chem.*, 2021, **36**, 2139–2159.
89 G. H. Liu, T. Chen, X. Zhang, X. L. Ma and H. S. Shi, *MedComm*, 2022, **3**, e181.
90 W. Liu, G. Wang, Z. Wang, G. Wang, J. Huang and B. Liu, *Drug Discovery Today*, 2022, **27**, 1994–2007.

91 R. Perez-Arancibia, M. Cisternas-Olmedo, D. Sepulveda, P. Troncoso-Escudero and R. L. Vidal, *Front. Neurosci.*, 2022, **16**, 1084493.
92 Y. Wu, Z. Yang, K. Cheng, H. Bi and J. Chen, *Acta Pharm. Sin. B*, 2022, **12**, 4287–4308.
93 B. M. Vickerman, E. M. Zywot, T. K. Tarrant and D. S. Lawrence, *Nat. Rev. Chem.*, 2021, **5**, 816–834.
94 Y. Naro, K. Darrah and A. Deiters, *J. Am. Chem. Soc.*, 2020, **142**, 2193–2197.
95 T. Wang, K. Long, Y. Zhou, X. Jiang, J. Liu, J. H. C. Fong, A. S. L. Wong, W.-L. Ng and W. Wang, *ACS Pharmacol. Transl. Sci.*, 2022, **5**, 149–155.
96 S. Chakrabarty and S. H. L. Verhelst, *Cell Chem. Biol.*, 2020, **27**, 1434–1440.e1410.
97 M. J. Hansen, F. M. Feringa, P. Kobauri, W. Szymanski, R. H. Medema and B. L. Feringa, *J. Am. Chem. Soc.*, 2018, **140**, 13136–13141.
98 M. J. Hansen, J. I. C. Hille, W. Szymanski, A. J. M. Driessen and B. L. Feringa, *Chem*, 2019, **5**, 1293–1301.
99 A. Müller-Deku, J. C. M. Meiring, K. Loy, Y. Kraus, C. Heise, R. Bingham, K. I. Jansen, X. Qu, F. Bartolini, L. C. Kapitein, A. Akhmanova, J. Ahlfeld, D. Trauner and O. Thorn-Seshold, *Nat. Commun.*, 2020, **11**, 4640.
100 N. Umeda, T. Ueno, C. Pohlmeyer, T. Nagano and T. Inoue, *J. Am. Chem. Soc.*, 2011, **133**, 12–14.
101 S. Xu, K. Long, T. Wang, Y. Zhu, Y. Zhang and W. Wang, *J. Med. Chem.*, 2025, **68**, 4373–4381.
102 H. Yao, S. Chen, Z. Deng, M. K. Tse, Y. Matsuda and G. Zhu, *Inorg. Chem.*, 2020, **59**, 11823–11833.
103 I. Elamri, C. Abdellaoui, J. K. Bains, K. F. Hohmann, S. L. Gande, E. Stirnal, J. Wachtveitl and H. Schwalbe, *J. Am. Chem. Soc.*, 2021, **143**, 10596–10603.
104 R. K. Amaravadi, J. Lippincott-Schwartz, X. M. Yin, W. A. Weiss, N. Takebe, W. Timmer, R. S. DiPaola, M. T. Lotze and E. White, *Clin. Cancer Res.*, 2011, **17**, 654–666.
105 J. Nah, J. Yuan and Y. K. Jung, *Mol. Cells*, 2015, **38**, 381–389.
106 Z. Chen, Y. Xu and X. Qian, *Chin. Chem. Lett.*, 2018, **29**, 1741–1756.
107 J. Liu, S. Zhong, L. Zhang, M. Yi, X. Liu, T. Bing, N. Zhang and D. Shangguan, *Chem. Commun.*, 2021, **57**, 6558–6561.
108 D. Ollech, T. Pflästerer, A. Shellard, C. Zambarda, J. P. Spatz, P. Marcq, R. Mayor, R. Wombacher and E. A. Cavalcanti-Adam, *Nat. Commun.*, 2020, **11**, 472.
109 C. V. Dang, E. P. Reddy, K. M. Shokat and L. Soucek, *Nat. Rev. Cancer*, 2017, **17**, 502–508.
110 D. P. Bondeson, B. E. Smith, G. M. Burslem, A. D. Buhimschi, J. Hines, S. Jaime-Figueroa, J. Wang, B. D. Hamman, A. Ishchenko and C. M. Crews, *Cell Chem. Biol.*, 2018, **25**, 78–87.e75.
111 S. L. Paiva and C. M. Crews, *Curr. Opin. Chem. Biol.*, 2019, **50**, 111–119.
112 M. Pettersson and C. M. Crews, *Drug Discovery Today:Technol.*, 2019, **31**, 15–27.
113 G. Xue, K. Wang, D. Zhou, H. Zhong and Z. Pan, *J. Am. Chem. Soc.*, 2019, **141**, 18370–18374.
114 C. S. Kounde, M. M. Shchepinova, C. N. Saunders, M. Muelbaier, M. D. Rackham, J. D. Harling and E. W. Tate, *Chem. Commun.*, 2020, **56**, 5532–5535.
115 Y. Naro, K. Darrah and A. Deiters, *J. Am. Chem. Soc.*, 2020, **142**, 2193–2197.
116 J. Liu, H. Chen, L. Ma, Z. He, D. Wang, Y. Liu, Q. Lin, T. Zhang, N. Gray, H. Kaniskan, J. Jin and W. Wei, *Sci. Adv.*, 2020, **6**, eaay5154.
117 H. Nakanishi, T. Yoshii, S. Kawasaki, K. Hayashi, K. Tsutsui, C. Oki, S. Tsukiji and H. Saito, *Cell Chem. Biol.*, 2021, **28**, 662–674.e665.
118 L. Zhao, J. Peng, Q. Huang, C. Li, M. Chen, Y. Sun, Q. Lin, L. Zhu and F. Li, *Adv. Funct. Mater.*, 2014, **24**, 363–371.
119 W. Lv and W. Wang, *Synlett*, 2020, **31**, 1129–1134.
120 W. Lv, K. Long, Y. Yang, S. Chen, C. Zhan and W. Wang, *Adv. Healthcare Mater.*, 2020, **9**, e2001118.
121 L. Huang, L. Zeng, Y. Chen, N. Yu, L. Wang, K. Huang, Y. Zhao and G. Han, *Nat. Commun.*, 2021, **12**, 122.
122 K. Long, Y. Wang, W. Lv, Y. Yang, S. Xu, C. Zhan and W. Wang, *Bioeng. Transl. Med.*, 2022, **7**, e10311.
123 Y. Liu, K. Long, T. Wang, Y. Zhang, J. Lei and W. Wang, *Nano Today*, 2024, **57**, 102342.
124 S. Xu, J. Li, K. Long, X. Liang and W. Wang, *Adv. Sci.*, 2024, **11**, 2404218.
125 J. Zhang, L. K. Herzog, D. P. Corkery, T.-C. Lin, L. Klewer, X. Chen, X. Xin, Y. Li and Y.-W. Wu, *Angew. Chem., Int. Ed.*, 2025, **64**, e202416456.
126 A. Müller-Deku, J. C. M. Meiring, K. Loy, Y. Kraus, C. Heise, R. Bingham, K. I. Jansen, X. Qu, F. Bartolini, L. C. Kapitein, A. Akhmanova, J. Ahlfeld, D. Trauner and O. Thorn-Seshold, *Nat. Commun.*, 2020, **11**, 4640.
127 M. Reynders, B. S. Matsuura, M. Bérouti, D. Simoneschi, A. Marzio, M. Pagano and D. Trauner, *Sci. Adv.*, 2020, **6**, eaay5064.
128 P. Pfaff, K. T. G. Samarasinghe, C. M. Crews and E. M. Carreira, *ACS Cent. Sci.*, 2019, **5**, 1682–1690.
129 A. Dumazer, X. Gómez-Santacana, F. Malhaire, C. Jopling, D. Maurel, G. Lebon, A. Llebaria and C. Goudet, *ACS Chem. Neurosci.*, 2024, **15**, 645–655.
130 X. Yang, G. Ma, S. Zheng, X. Qin, X. Li, L. Du, Y. Wang, Y. Zhou and M. Li, *J. Am. Chem. Soc.*, 2020, **142**, 9460–9470.
131 K. W. Ko, M. N. Rasband, V. Meseguer, R. H. Kramer and N. L. Golding, *Nat. Neurosci.*, 2016, **19**, 826–834.
132 M. V. Nikolaev, D. M. Strashkov, M. N. Ryazantsev and D. B. Tikhonov, *ACS Chem. Neurosci.*, 2021, **12**, 3347–3357.
133 X. Fu, H. Bai, R. Qi, H. Zhao, K. Peng, F. Lv, L. Liu and S. Wang, *Chem. Commun.*, 2019, **55**, 14466–14469.
134 J. He, Z. Fan, Y. Tian, W. Yang, Y. Zhou, Q. Zhu, W. Zhang, W. Qin and W. Yi, *J. Am. Chem. Soc.*, 2022, **144**, 4289–4293.
135 J. Volarić, N. J. van der Heide, N. L. Mutter, D. F. Samplonius, W. Helfrich, G. Maglia, W. Szymanski and B. L. Feringa, *ACS Chem. Biol.*, 2024, **19**, 451–461.
136 E. Arbely, J. Torres-Kolbus, A. Deiters and J. W. Chin, *J. Am. Chem. Soc.*, 2012, **134**, 11912–11915.
137 J. Luo, J. Torres-Kolbus, J. Liu and A. Deiters, *ChemBioChem*, 2017, **18**, 1442–1447.

138 W. Ren, A. Ji and H.-W. Ai, *J. Am. Chem. Soc.*, 2015, **137**, 2155–2158.
139 N. Wu, A. Deiters, T. A. Cropp, D. King and P. G. Schultz, *J. Am. Chem. Soc.*, 2004, **126**, 14306–14307.
140 E. A. Lemke, D. Summerer, B. H. Geierstanger, S. M. Brittain and P. G. Schultz, *Nat. Chem. Biol.*, 2007, **3**, 769–772.
141 X. Ling, Y. Zuo, H. Chen, D. Ji, J. Wang, L. Chang and T. Liu, *CCS Chem.*, 2023, **5**, 1301–1307.
142 Y. Liu, R. Zeng, R. Wang, Y. Weng, R. Wang, P. Zou and P. R. Chen, *Proc. Natl. Acad. Sci. U. S. A.*, 2021, **118**, e2025299118.
143 J. D. R. Knight, B. Qian, D. Baker and R. Kothary, *PLoS One*, 2007, **2**, e982.
144 W. Brown, J. Wesalo, S. Samanta, J. Luo, S. E. Caldwell, M. Tsang and A. Deiters, *ACS Chem. Biol.*, 2023, **18**, 1305–1314.
145 R. Parlato, J. Volarić, A. Lasorsa, M. Bagherpoor Helabad, P. Kobauri, G. Jain, M. S. Miettinen, B. L. Feringa, W. Szymanski and P. C. A. van der Wel, *J. Am. Chem. Soc.*, 2024, **146**, 2062–2071.
146 J. Montnach, L. A. Blömer, L. Lopez, L. Filipis, H. Meudal, A. Lafoux, S. Nicolas, D. Chu, C. Caumes, R. Béroud, C. Jopling, F. Bosmans, C. Huchet, C. Landon, M. Canepari and M. De Waard, *Nat. Commun.*, 2022, **13**, 417.
147 X. Guo and M. Su, *Int. J. Mol. Sci.*, 2023, **24**, 197.
148 N. S. Chandel, *Cold Spring Harbor Perspect. Biol.*, 2021, **13**, a040592.
149 B. Y. Michel, D. Dziuba, R. Benhida, A. P. Demchenko and A. Burger, *Front. Chem.*, 2020, **8**, 112.
150 N. Klöcker, F. P. Weissenboeck, M. van Dülmen, P. Špaček, S. Hüwel and A. Rentmeister, *Nat. Chem.*, 2022, **14**, 905–913.
151 D. Hartmann and M. J. Booth, *Commun. Chem.*, 2023, **6**, 59.
152 S. Xie, Y. Du, Y. Zhang, Z. Wang, D. Zhang, L. He, L. Qiu, J. Jiang and W. Tan, *Nat. Commun.*, 2020, **11**, 1347.
153 L. Liu, Y. Kuang, Z. Wang and Y. Chen, *Chem. Sci.*, 2020, **11**, 11298–11306.
154 F. Buhr, J. Kohl-Landgraf, S. tom Dieck, C. Hanus, D. Chatterjee, A. Hegelein, E. M. Schuman, J. Wachtveitl and H. Schwalbe, *Angew. Chem., Int. Ed.*, 2015, **54**, 3717–3721.
155 I. Elamri, M. Heumüller, L.-M. Herzig, E. Stirnal, J. Wachtveitl, E. M. Schuman and H. Schwalbe, *ChemBioChem*, 2018, **19**, 2458–2464.
156 T. Ko, M. M. Oliveira, J. M. Alapin, J. Morstein, E. Klann and D. Trauner, *J. Am. Chem. Soc.*, 2022, **144**, 21494–21501.
157 P. Strasser, M. Russo, P. Stadler, P. Breiteneder, G. Redhammer, M. Himmelsbach, O. Brüggemann, U. Monkowius, P. Klán and I. Teasdale, *Polym. Chem.*, 2021, **12**, 6927–6936.
158 W. Zhang, T. Ji, Y. Li, Y. Zheng, M. Mehta, C. Zhao, A. Liu and D. S. Kohane, *Nat. Commun.*, 2020, **11**, 2323.
159 E. Käpylä, S. M. Delgado and A. M. Kasko, *ACS Appl. Mater. Interfaces*, 2016, **8**, 17885–17893.
160 C. Schutt, S. Ibsen, E. Zahavy, S. Aryal, S. Kuo, S. Esener, M. Berns and S. Esener, *Pharm. Res.*, 2017, **34**, 2025–2035.
161 Z. Zhou, I. C. Chen, L. M. Rehman, A. M. Aboalsaud, D. B. Shinde, L. Cao, Y. Zhang and Z. Lai, *Sci. Adv.*, 2022, **8**, eabo2929.
162 G. Alachouzos, A. M. Schulte, A. Mondal, W. Szymanski and B. L. Feringa, *Angew. Chem., Int. Ed.*, 2022, **61**, e202201308.
163 J. Jiang, X. Tong and Y. Zhao, *J. Am. Chem. Soc.*, 2005, **127**, 8290–8291.
164 C. Boto, E. Quartin, Y. Cai, A. Martín-Lorenzo, M. B. G. Cenador, S. Pinto, R. Gupta, T. Enver, I. Sánchez-García and D. Hong, *Nat. Commun.*, 2017, **8**, 15204.
165 Y. Duan, K. He, G. Zhang and J. Hu, *Biomacromolecules*, 2021, **22**, 2160–2170.
166 V. A. Huu, J. Luo, J. Zhu, J. Zhu, S. Patel, A. Boone, E. Mahmoud, C. McFearin, J. Olejniczak, C. de Gracia Lux, J. Lux, N. Fomina, M. Huynh, K. Zhang and A. Almutairi, *J. Controlled Release*, 2015, **200**, 71–77.
167 R. Yan, Y. Guo, X. Wang, G. Liang, A. Yang and J. Li, *ACS Nano*, 2022, **16**, 8399–8418.
168 X. Wang, W. Hu, Y. Yang, Y. Liao, W.-C. Law and C.-Y. Tang, *Eur. Polym. J.*, 2023, **182**, 111715.
169 J. Xiang, F. Ge, B. Yu, Q. Yan, F. Shi and Y. Zhao, *ACS Appl. Mater. Interfaces*, 2018, **10**, 20790–20800.
170 H. Zhao, W. Hu, H. Ma, R. Jiang, Y. Tang, Y. Ji, X. Lu, B. Hou, W. Deng and W. Huang, *Adv. Funct. Mater.*, 2017, **27**, 1702592.
171 Y. Li, Y. Zhou, T. Wang, K. Long, Y. Zhang and W. Wang, *Nanoscale*, 2021, **13**, 17784–17792.
172 M. Jing, Y. Li, M. Wang, H. Zhang, P. Wei, Y. Zhou, N. Ishimwe, X. Huang, L. Wang, L. Wen, W. Wang and Y. Zhang, *Small*, 2021, **17**, e2102295.
173 Y. Zhou, K. Chen, W. K. Lin, J. Liu, W. Kang, Y. Zhang, R. Yang, L. Jin, Y. Cheng and A. Xu, *Adv. Healthcare Mater.*, 2023, 2300994.
174 Y. Liu, Y. Zhou, Y. Li, W. Kang, Y. Zhang, X. Xia and W. Wang, *ACS Appl. Mater. Interfaces*, 2025, **17**, 430–444.
175 B. M. Vickerman, C. P. O'Banion, X. Tan and D. S. Lawrence, *ACS Cent. Sci.*, 2020, **7**, 93–103.
176 E. M. Zywot, N. Orlova, S. Ding, R. R. Rampersad, E. M. Rabjohns, V. A. Wickenheisser, Q. Wang, J. G. Welfare, L. Haar and A. M. Eudy, *Adv. Ther.*, 2022, **5**, 2100159.
177 K. Long, Y. Yang, W. Lv, K. Jiang, Y. Li, A. C. Y. Lo, W. C. Lam, C. Zhan and W. Wang, *Adv. Sci.*, 2021, **8**, 2101754.
178 K. Long, H. Han, W. Kang, W. Lv, L. Wang, Y. Wang, L. Ge and W. Wang, *J. Nanobiotechnol.*, 2021, **19**, 357.
179 P. T. Wong, S. Tang, J. Cannon, D. Chen, R. Sun, J. Lee, J. Phan, K. Tao, K. Sun, B. Chen, J. R. Baker, Jr. and S. K. Choi, *Bioconjugate Chem.*, 2017, **28**, 3016–3028.
180 L. L. Fedoryshin, A. J. Tavares, E. Petryayeva, S. Doughan and U. J. Krull, *ACS Appl. Mater. Interfaces*, 2014, **6**, 13600–13606.
181 J. Xiang, S. Zhou, J. Lin, J. Wen, Y. Xie, B. Yan, Q. Yan, Y. Zhao, F. Shi and H. Fan, *ACS Appl. Mater. Interfaces*, 2021, **13**, 7094–7101.
182 Q. Liu, H.-B. Cheng, R. Ma, M. Yu, Y. Huang, L. Li and J. Zhao, *Nano Today*, 2023, **48**, 101747.

183 Y. Yang, F. Liu, X. Liu and B. Xing, *Nanoscale*, 2013, **5**, 231–238.
184 J. Vuilleumier, G. Gaulier, R. De Matos, D. Ortiz, L. Menin, G. Campargue, C. Mas, S. Constant, R. Le Dantec, Y. Mugnier, L. Bonacina and S. Gerber-Lemaire, *ACS Appl. Mater. Interfaces*, 2019, **11**, 27443–27452.
185 A. Gheata, G. Gaulier, G. Campargue, J. Vuilleumier, S. Kaiser, I. Gautschi, F. Riporto, S. Beauquis, D. Staedler, D. Diviani, B. Bonacina and S. Gerber-Lemaire, *ACS Nanosci. Au*, 2022, **2**, 355–366.
186 D. Wei, Y. Huang, B. Wang, L. Ma, J. Karges and H. Xiao, *Angew. Chem., Int. Ed.*, 2022, **61**, e202201486.
187 E. Ruggiero, J. Hernández-Gil, J. C. Mareque-Rivas and L. Salassa, *Chem. Commun.*, 2015, **51**, 2091–2094.
188 S. Xu, X. Zhu, C. Zhang, W. Huang, Y. Zhou and D. Yan, *Nat. Commun.*, 2018, **9**, 2053.
189 Q. Zhang, G. Kuang, D. Zhou, Y. Qi, M. Wang, X. Li and Y. Huang, *J. Mater. Chem. B*, 2020, **8**, 5903–5911.
190 M. Frasconi, Z. Liu, J. Lei, Y. Wu, E. Strekalova, D. Malin, M. W. Ambrogio, X. Chen, Y. Y. Botros and V. L. Cryns, *J. Am. Chem. Soc.*, 2013, **135**, 11603–11613.
191 Y. Salinas, O. Brüggemann, U. Monkowius and I. Teasdale, *Nanomaterials*, 2020, **10**, 1030.
192 T. A. Bauer, J. Eckrich, N. Wiesmann, F. Kuczelinis, W. Sun, X. Zeng, B. Weber, S. Wu, N. H. Bings and S. Strieth, *J. Mater. Chem. B*, 2021, **9**, 8211–8223.
193 J. Zhang, V. Ramu, X.-Q. Zhou, C. Frias, D. Ruiz-Molina, S. Bonnet, C. Roscini and F. Novio, *Nanomaterials*, 2021, **11**, 3089.
194 W. Sun, M. Parowatkin, W. Steffen, H. J. Butt, V. Mailänder and S. Wu, *Adv. Healthcare Mater.*, 2016, **5**, 467–473.
195 J.-S. Lan, R.-F. Zeng, Z. Li, Y. Wu, L. Liu, L.-X. Chen, Y. Liu, Y.-T. He, T. Zhang and Y. Ding, *ACS Appl. Mater. Interfaces*, 2023, **15**, 34554–34569.
196 Y. Ma, Z. Zhang, F. Sun, P. Mesdom, X. Ji, P. Burckel, G. Gasser and M.-H. Li, *Biomacromolecules*, 2023, **24**, 5940–5950.
197 G. He, M. He, R. Wang, X. Li, H. Hu, D. Wang, Z. Wang, Y. Lu, N. Xu and J. Du, *Angew. Chem., Int. Ed.*, 2023, **62**, e202218768.
198 M. S. Meijer, M. M. Natile and S. Bonnet, *Inorg. Chem.*, 2020, **59**, 14807–14818.
199 Y. Song, Y. Chen, P. Li and C. M. Dong, *Biomacromolecules*, 2020, **21**, 5345–5357.
200 J. Yang, J. I. Song, Q. Song, J. Y. Rho, E. D. H. Mansfield, S. C. L. Hall, M. Sambrook, F. Huang and S. Perrier, *Angew. Chem., Int. Ed.*, 2020, **59**, 8860–8863.
201 X. Wang, Y. Yang, C. Liu, H. Guo, Z. Chen, J. Xia, Y. Liao, C.-Y. Tang and W.-C. Law, *Polymer*, 2021, **229**, 123961.
202 B. Yan, J. C. Boyer, N. R. Branda and Y. Zhao, *J. Am. Chem. Soc.*, 2011, **133**, 19714–19717.
203 G. Chen, R. Jaskula-Sztul, C. R. Esquibel, I. Lou, Q. Zheng, A. Dammalapati, A. Harrison, K. W. Eliceiri, W. Tang, H. Chen and S. Gong, *Adv. Funct. Mater.*, 2017, **27**, 1604671.
204 J. Xiang, X. Tong, F. Shi, Q. Yan, B. Yu and Y. Zhao, *J. Mater. Chem. B*, 2018, **6**, 3531–3540.
205 H. Wen, H. Zhu, X. Chen, T. F. Hung, B. Wang, G. Zhu, S. F. Yu and F. Wang, *Angew. Chem., Int. Ed.*, 2013, **52**, 13419–13423.
206 B. Chen and F. Wang, *Trends Chem.*, 2020, **2**, 427–439.
207 L. Yin, H. Tang, K. H. Kim, N. Zheng, Z. Song, N. P. Gabrielson, H. Lu and J. Cheng, *Angew. Chem., Int. Ed.*, 2013, **52**, 9182–9186.
208 Q. Jin, T. Cai, Y. Wang, H. Wang and J. Ji, *ACS Macro Lett.*, 2014, **3**, 679–683.
209 L. Li, Y. Wu, F. S. Du and Z. C. Li, *J. Polym. Sci., Part A: Polym. Chem.*, 2019, **57**, 334–341.
210 N. G. Patil, N. B. Basutkar and A. V. Ambade, *Chem. Commun.*, 2015, **51**, 17708–17711.
211 W. Lv, Y. Li, F. Li, X. Lan, Y. Zhang, L. Du, Q. Zhao, D. L. Phillips and W. Wang, *J. Am. Chem. Soc.*, 2019, **141**, 17482–17486.
212 S. H. Askes, A. Bahreman and S. Bonnet, *Angew. Chem.*, 2014, **126**, 1047–1051.
213 R. V. D. Araújo, S. D. S. Santos, E. Igne Ferreira and J. Giarolla, *Molecules*, 2018, **23**, 2849.
214 S. R. Dennison, F. Harris and D. A. Phoenix, *Biophys. Chem.*, 2007, **127**, 78–83.
215 H. Xiong, Y. Xu, B. Kim, H. Rha, B. Zhang, M. Li, G.-F. Yang and J. S. Kim, *Chem*, 2023, **9**, 29–64.
216 S. Bonnet, *Dalton Trans.*, 2018, **47**, 10330–10343.
217 S. Bonnet, *J. Am. Chem. Soc.*, 2023, **145**, 23397–23415.
218 J. D. Knoll and C. Turro, *Coord. Chem. Rev.*, 2015, **282–283**, 110–126.
219 L. Ma, L. Li and G. Zhu, *Inorg. Chem. Front.*, 2022, **9**, 2424–2453.
220 D. Havrylyuk, A. Hachey and E. Glazer, *Targeted Metallo-Drugs*, CRC Press, 2023, pp. 39–65.
221 K. M. Kuznetsov, K. Cariou and G. Gasser, *Chem. Sci.*, 2024, **15**, 17760–17780.
222 A. C. Jung, F. Moinard-Butot, C. Thibaudeau, G. Gasser and C. Gaiddon, *Pharmaceutics*, 2021, **13**, 1788.
223 Z. Deng, N. Wang, F. Ai, Z. Wang and G. Zhu, *View*, 2021, **2**, 20200030.
224 G. Liu, W. Liu and C.-M. Dong, *Polym. Chem.*, 2013, **4**, 3431–3443.
225 S. K. Nalluri, J. Voskuhl, J. B. Bultema, E. J. Boekema and B. J. Ravoo, *Angew. Chem., Int. Ed.*, 2011, **50**, 9747–9751.
226 Y. Li, Y. Duan, J. Li, J. Zheng, H. Yu and R. Yang, *Anal. Chem.*, 2012, **84**, 4732–4738.
227 Q. Yuan, Y. Zhang, T. Chen, D. Lu, Z. Zhao, X. Zhang, Z. Li, C. H. Yan and W. Tan, *ACS Nano*, 2012, **6**, 6337–6344.
228 P. Li, G. Xie, P. Liu, X. Y. Kong, Y. Song, L. Wen and L. Jiang, *J. Am. Chem. Soc.*, 2018, **140**, 16048–16052.
229 H. Pan, W. Li, L. Wu, W. Huang and F. Zhang, *Coatings*, 2021, **11**, 1489.
230 J. W. Brown, B. L. Henderson, M. D. Kiesz, A. C. Whalley, W. Morris, S. Grunder, H. Deng, H. Furukawa, J. I. Zink and J. F. Stoddart, *Chem. Sci.*, 2013, **4**, 2858–2864.
231 G. Das, T. Prakasam, M. A. Addicoat, S. K. Sharma, F. Ravaux, R. Mathew, M. Baias, R. Jagannathan, M. A. Olson and A. Trabolsi, *J. Am. Chem. Soc.*, 2019, **141**, 19078–19087.

232 D. Liu, S. Wang, S. Xu and H. Liu, *Langmuir*, 2017, **33**, 1004–1012.
233 X. Wang, Y. Yang, P. Gao, F. Yang, H. Shen, H. Guo and D. Wu, *ACS Macro Lett.*, 2015, **4**, 1321–1326.
234 S. Geng, Y. Wang, L. Wang, T. Kouyama, T. Gotoh, S. Wada and J.-Y. Wang, *Sci. Rep.*, 2017, **7**, 39202.
235 J. Croissant, A. Chaix, O. Mongin, M. Wang, S. Clément, L. Raehm, J. O. Durand, V. Hugues, M. Blanchard-Desce and M. Maynadier, *Small*, 2014, **10**, 1752–1755.
236 S. D. Pritzl, D. B. Konrad, M. F. Ober, A. F. Richter, J. A. Frank, B. Nickel, D. Trauner and T. Lohmüller, *Langmuir*, 2022, **38**, 385–393.
237 Y. Zhang, Y. Zhang, G. Song, Y. He, X. Zhang, Y. Liu and H. Ju, *Angew. Chem., Int. Ed.*, 2019, **58**, 18207–18211.
238 T. Zhao, P. Wang, Q. Li, A. A. Al-Khalaf, W. N. Hozzein, F. Zhang, X. Li and D. Zhao, *Angew. Chem., Int. Ed.*, 2018, **57**, 2611–2615.
239 W. Li, K. Dong, H. Wang, P. Zhang, Y. Sang, J. Ren and X. Qu, *Biomaterials*, 2019, **217**, 119310.
240 L. Chen, W. Wang, B. Su, Y. Wen, C. Li, Y. Zhou, M. Li, X. Shi, H. Du, Y. Song and L. Jiang, *ACS Nano*, 2014, **8**, 744–751.
241 M. Ghani, A. Heiskanen, P. Thomsen, M. Alm and J. Emnéus, *ACS Appl. Bio Mater.*, 2021, **4**, 1624–1631.
242 R. Tong, H. D. Hemmati, R. Langer and D. S. Kohane, *J. Am. Chem. Soc.*, 2012, **134**, 8848–8855.
243 V. K. Kotharangannagari, A. Sánchez-Ferrer, J. Ruokolainen and R. Mezzenga, *Macromolecules*, 2011, **44**, 4569–4573.
244 X. Wang, J. Hu, G. Liu, J. Tian, H. Wang, M. Gong and S. Liu, *J. Am. Chem. Soc.*, 2015, **137**, 15262–15275.
245 J. Ji, X. Li, T. Wu and F. Feng, *Chem. Sci.*, 2018, **9**, 5816–5821.
246 J. Ji, T. Wu, Y. Zhang and F. Feng, *ACS Appl. Mater. Interfaces*, 2019, **11**, 15222–15232.
247 Y. Cong, X. Wang, S. Zhu, L. Liu and L. Li, *ACS Appl. Bio Mater.*, 2021, **4**, 2790–2797.
248 A. Aggarwal, C. Li, S. I. Stupp and M. O. de la Cruz, *Soft Matter*, 2022, **18**, 2193–2202.
249 L. Zhou, Z. Chen, K. Dong, M. Yin, J. Ren and X. Qu, *Adv. Mater.*, 2014, **26**, 2424–2430.
250 O. Rifaie-Graham, S. Ulrich, N. F. B. Galensowske, S. Balog, M. Chami, D. Rentsch, J. R. Hemmer, J. Read de Alaniz, L. F. Boesel and N. Bruns, *J. Am. Chem. Soc.*, 2018, **140**, 8027–8036.
251 H. Ma, W. Li, H. Fan and J. Xiang, *Polymers*, 2023, **15**, 2489.
252 Y. Tian, Y. Li, X. Li, Z. Lin, C. Zhang, Q. Kuang, P. Zhang, R. Zeng and J. Chen, *Eur. Polym. J.*, 2023, **183**, 111771.
253 H. B. Cheng, S. Zhang, J. Qi, X. J. Liang and J. Yoon, *Adv. Mater.*, 2021, **33**, 2007290.
254 G. S. Hartley, *Nature*, 1937, **140**, 281.
255 A. A. Beharry and G. A. Woolley, *Chem. Soc. Rev.*, 2011, **40**, 4422–4437.
256 Y. Chen, G. Ke, Y. Ma, Z. Zhu, M. Liu, Y. Liu, H. Yan and C. J. Yang, *J. Am. Chem. Soc.*, 2018, **140**, 8990–8996.
257 K. D. Richards and R. C. Evans, *Soft Matter*, 2022, **18**, 5770–5781.
258 S. Wang, P. Poudel, F. H. Schacher and L. I. Kaberov, *Polym. Chem.*, 2023, **14**, 3381–3391.
259 G. Cabré, A. Garrido-Charles, M. Moreno, M. Bosch, M. Porta-de-la-Riva, M. Krieg, M. Gascón-Moya, N. Camarero, R. Gelabert and J. M. Lluch, *Nat. Commun.*, 2019, **10**, 907.
260 S. Samanta, A. A. Beharry, O. Sadovski, T. M. McCormick, A. Babalhavaeji, V. Tropepe and G. A. Woolley, *J. Am. Chem. Soc.*, 2013, **135**, 9777–9784.
261 D. Wang and S. Wu, *Langmuir*, 2016, **32**, 632–636.
262 R. Heiligman-Rim, Y. Hirshberg and E. Fischer, *J. Chem. Soc.*, 1961, 156–163.
263 H. Cao, L. Duan, Y. Zhang, J. Cao and K. Zhang, *Signal Transduction Targeted Ther.*, 2021, **6**, 426.
264 M. Irie, *Chem. Rev.*, 2000, **100**, 1685–1716.
265 J. Rao and A. Khan, *J. Am. Chem. Soc.*, 2013, **135**, 14056–14059.
266 C. Alvarez-Lorenzo, L. Bromberg and A. Concheiro, *Photochem. Photobiol.*, 2009, **85**, 848–860.
267 E. G. Randles and P. R. Bergethon, *Langmuir*, 2013, **29**, 1490–1497.
268 D. Luo, N. Li, K. A. Carter, C. Lin, J. Geng, S. Shao, W. C. Huang, Y. Qin, G. E. Atilla-Gokcumen and J. F. Lovell, *Small*, 2016, **12**, 3039–3047.
269 Y. Wang, Y. Deng, H. Luo, A. Zhu, H. Ke, H. Yang and H. Chen, *ACS Nano*, 2017, **11**, 12134–12144.
270 Z. Li, Y. Hu, Q. Fu, Y. Liu, J. Wang, J. Song and H. Yang, *Adv. Funct. Mater.*, 2020, **30**, 1905758.
271 N. Nishiyama, A. Iriyama, W.-D. Jang, K. Miyata, K. Itaka, Y. Inoue, H. Takahashi, Y. Yanagi, Y. Tamaki and H. Koyama, *Nat. Mater.*, 2005, **4**, 934–941.
272 Z. Cao, Y. Ma, C. Sun, Z. Lu, Z. Yao, J. Wang, D. Li, Y. Yuan and X. Yang, *Chem. Mater.*, 2018, **30**, 517–525.
273 X. Zhang, H. Gao, D. Wei, X. Pei, Y. Zhang, J. Wang, D. Ding, J. Chang and X. Wu, *ACS Appl. Mater. Interfaces*, 2023, **15**, 29827–29840.
274 L. Huang, X. Chen, Q. Bian, F. Zhang, H. Wu, H. Wang and J. Gao, *J. Controlled Release*, 2020, **328**, 325–338.
275 J. Jiao, H. Lu and S. Wang, *Acta Biomater.*, 2021, **126**, 421–432.
276 F. Liu, Z. Cheng and H. Yi, *J. Nanobiotechnol.*, 2023, **21**, 1–15.
277 S. Xu, K. Cui, K. Long, J. Li, N. Fan, W. C. Lam, X. Liang and W. Wang, *Adv. Sci.*, 2023, **10**, 2301985.
278 T. Zhang, H. Lin, L. Cui, N. An, R. Tong, Y. Chen, C. Yang, X. Li, J. Liu and F. Qu, *Eur. J. Inorg. Chem.*, 2016, 1206–1213.
279 M. S. Yavuz, Y. Cheng, J. Chen, C. M. Cobley, Q. Zhang, M. Rycenga, J. Xie, C. Kim, K. H. Song, A. G. Schwartz, L. V. Wang and Y. Xia, *Nat. Mater.*, 2009, **8**, 935–939.
280 S. J. Leung and M. Romanowski, *ACS Nano*, 2012, **6**, 9383–9391.
281 X. Fu, X. Wang, S. Zhou and Y. Zhang, *Int. J. Nanomed.*, 2017, **12**, 3751–3766.
282 J. Gao, F. Wang, S. Wang, L. Liu, K. Liu, Y. Ye, Z. Wang, H. Wang, B. Chen, J. Jiang, J. Ou, J. C. M. van Hest, F. Peng and Y. Tu, *Adv. Sci.*, 2020, **7**, 1903642.

283 J. S. Basuki, F. Qie, X. Mulet, R. Suryadinata, A. V. Vashi, Y. Y. Peng, L. Li, X. Hao, T. Tan and T. C. Hughes, *Angew. Chem.*, 2017, **129**, 986–991.
284 S. Wang, B. Chen, L. Ouyang, D. Wang, J. Tan, Y. Qiao, S. Ge, J. Ruan, A. Zhuang and X. Liu, *Adv. Sci.*, 2021, **8**, 2004721.
285 B. Singh, S. Yun and M.-H. Park, *J. Drug Delivery Sci. Technol.*, 2023, **88**, 104910.
286 O. K. Kari, S. Tavakoli, P. Parkkila, S. Baan, R. Savolainen, T. Ruoslahti, N. G. Johansson, J. Ndika, H. Alenius and T. Viitala, *Pharmaceutics*, 2020, **12**, 763.
287 Y. Liu, Y. Han, S. Chen, J. Liu, D. Wang and Y. Huang, *Acta Pharm. Sin. B*, 2022, **12**, 2731–2739.
288 A. Barhoumi, R. Huschka, R. Bardhan, M. W. Knight and N. J. Halas, *Chem. Phys. Lett.*, 2009, **482**, 171–179.
289 X. Huang, A. Pallaoro, G. B. Braun, D. P. Morales, M. O. Ogunyankin, J. Zasadzinski and N. O. Reich, *Nano Lett.*, 2014, **14**, 2046–2051.
290 X. Jia, M. Lv, Y. Fei, Q. Dong, H. Wang, Q. Liu, D. Li, J. Wang and E. Wang, *Biomaterials*, 2022, **282**, 121404.
291 X. Chen, S. Wang, Y. Chen, H. Xin, S. Zhang, D. Wu, Y. Xue, M. Zha, H. Li and K. Li, *Nat. Nanotechnol.*, 2023, 1–12.
292 M. Wu, R. Qu, H. Li, L. Chen, X. Zhang, Y. Yuan, W. Chen, X. Jiang and X. Zhen, *Nano Today*, 2023, **48**, 101691.
293 L. Jiao, Q. Li, C. Li, J. Gu, X. Liu, S. He and Z. Zhang, *J. Mater. Chem. B*, 2023, **11**, 2367–2376.
294 Y. Sun, W. Zhang, M. Wang, H. Liu, Q. Li, J. Luo, M. Zhao, S. Liu and X. Wang, *Nano Res.*, 2023, **16**, 849–857.
295 N. Fomina, J. Sankaranarayanan and A. Almutairi, *Adv. Drug Delivery Rev.*, 2012, **64**, 1005–1020.
296 S. A. Salma, M. P. Patil, D. W. Kim, C. M. Q. Le, B.-H. Ahn, G.-D. Kim and K. T. Lim, *Polym. Chem.*, 2018, **9**, 4813–4823.
297 C. Wang, B. Huang, G. Yang, Y. Ouyang, J. Tian and W. Zhang, *Biomacromolecules*, 2019, **20**, 4218–4229.
298 J. Wu, Y. T. Chan, Y. Lu, N. Wang and Y. Feng, *Med. Res. Rev.*, 2023, **43**, 1946–1973.
299 X. Jing, F. Yang, C. Shao, K. Wei, M. Xie, H. Shen and Y. Shu, *Mol. Cancer*, 2019, **18**, 1–15.
300 Y. Li, L. Zhao and X.-F. Li, *Technol. Cancer Res. Treat.*, 2021, **20**, 15330338211036304.
301 J. Wu, Y. Long, M. Li and Q. He, *Acta Pharm. Sin. B*, 2021, **11**, 2286–2305.
302 A. Raza, U. Hayat, T. Rasheed, M. Bilal and H. M. Iqbal, *J. Mater. Res. Technol.*, 2019, **8**, 1497–1509.
303 T. Lajunen, L.-S. Kontturi, L. Viitala, M. Manna, O. Cramariuc, T. Rog, A. Bunker, T. Laaksonen, T. Viitala and L. Murtomaki, *Mol. Pharmaceutics*, 2016, **13**, 2095–2107.
304 X. Jiang, B. Du, Y. Huang, M. Yu and J. Zheng, *Bioconjugate Chem.*, 2020, **31**, 1522–1528.
305 X. He, S. Zhang, Y. Tian, W. Cheng and H. Jing, *Int. J. Nanomed.*, 2023, 1433–1468.
306 Q. Chen, Q. Hu, E. Dukhovlinova, G. Chen, S. Ahn, C. Wang, E. A. Ogunnaike, F. S. Ligler, G. Dotti and Z. Gu, *Adv. Mater.*, 2019, **31**, e1900192.
307 L. Galluzzi, A. Buqué, O. Kepp, L. Zitvogel and G. Kroemer, *Nat. Rev. Immunol.*, 2017, **17**, 97–111.
308 W. Kang, Y. Liu and W. Wang, *Acta Pharm. Sin. B*, 2023, **13**, 2346–2368.